การผสานซิลิกาเข้าไปในอาร์เอฟเจลเพื่อการสังเคราะห์ซิลิคอนไนไตรด์/ซิลิคอนคาร์ไบด์
คอมพอสิตพรุนด้วยปฏิกิริยาคาร์โบเทอร์มอลรีดักชันและไนไตรเดชัน

นางสาว ชรินทร์ญา เผ่าเมือง

INCORPORATION OF SILICA INTO RF GEL FOR THE SYNTHESIS OF POROUS Si$_3$N$_4$/SiC COMPOSITE VIA THE CARBOTHERMAL REDUCTION AND NITRIDATION

Miss Charinya Poumuang

A Thesis Submitted in Partial Fulfillment of the Requirements

for the Degree of Master of Engineering Program in Chemical

Engineering

Department of Chemical Engineering

Faculty of Engineering

Chulalongkorn University

Academic Year 2008

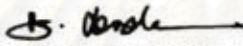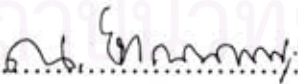|	
Thesis Title	INCORPORATION OF SILICA INTO RF GEL FOR THE SYNTHESIS OF POROUS Si_3N_4/SiC COMPOSITE VIA THE CARBOTHERMAL REDUCTION AND NITRIDATION
By	Miss Charinya Poumuang
Field of study	Chemical Engineering
Advisor	Assistant Professor Varong Pavarajarn, Ph.D.
Co-Advisor	Assistant Professor Nattaporn Tonanon, Ph.D.

Accepted by the Faculty of Engineering, Chulalongkorn University in Partial Fulfillment of the Requirements for the Master's Degree

.... Dean of the Faculty of Engineering

(Associate Professor Boonsom Lerdhirunwong, Dr.Ing.)

THESIS COMMITTEE

.... Chairman

(Professor Piyasan Praserthdam, Dr.Ing.)

.... Advisor

(Assistant Professor Varong Pavarajarn, Ph.D)

.... Co-Advisor

(Assistant Professor Nattaporn Tonanon, Ph.D)

.... Examiner

(Assistant Professor Joongjai Panpranot, Ph.D.)

.... External Examiner

(Chanchana Thanachayanont, Ph.D.)

ชรินทร์ญา เผ่าเมือง : การผสานซิลิกาเข้าไปในอาร์เอฟเจลเพื่อการสังเคราะห์ซิลิคอน
ไนไตรด์/ซิลิคอนคาร์ไบด์คอมพอสิตพรุนด้วยปฏิกิริยาคาร์โบเทอร์มอลรีดักชันและไน
ไตรเดชัน. (INCORPORATION OF SILICA INTO RF GEL FOR THE
SYNTHESIS OF POROUS Si₃N₄/SiC COMPOSITE VIA THE
CARBOTHERMAL REDUCTION AND NITRIDATION)
อ. ที่ปรึกษาวิทยานิพนธ์หลัก: ผศ.ดร.วรงค์ ปวราจารย์, อ. ที่ปรึกษาวิทยานิพนธ์ร่วม:
ผศ.ดร.ฉัฐพร โทณานนท์ 98 หน้า.

งานวิจัยนี้ศึกษาการผสานซิลิกาเข้าไปในอาร์เอฟเจลซึ่งเตรียมด้วยเทคนิคโซล-เจล โพลี
คอนเดนเซชันของรีโซซินอลกับฟอร์มัลดีไฮด์ โดยใช้โซเดียมคาร์บอเนตเป็นตัวเร่งปฏิกิริยา ซึ่ง
ปฏิกิริยาระหว่างสารตั้งต้นของซิลิกากับสารละลายอาร์เอฟนั้นเกิดขึ้นค่อนข้างรุนแรง เพราะคาย
ความร้อนอย่างมาก เมื่อเติมกรดอะซิติกลงไปในสารละลายอาร์เอฟกรดอะซิติกจะไปทำลายพันธะ
เชื่อมต่อชนิดเมทิลลีน และเมทิลลีนอีเทอร์ของอาร์เอฟคลัสเตอร์ ซึ่งทำให้สามารถทำปฏิกิริยา
กับซิลิกาได้มากขึ้น จากผลการทดลองพบว่า สารตั้งต้นของซิลิกา เช่น 3-อะมิโนโพรพิล
ไตรเมททอกซีไซเลน และ3-เมอร์แคปโตโพรพิลไตรเมททอกซีไซเลน ผสานเข้าไปในอาร์เอฟคลัส
เตอร์ที่ตำแหน่งไฮครอกซิลกรุป จากนั้นเมื่อนำซิลิกา/อาร์เอฟเจลไปสังเคราะห์เป็นซิลิกา/คาร์บอน
คอมพอสิตด้วยปฏิกิริยาไพโรไลสิสเพื่อนำไปทำปฏิกิริยาคาร์โบเทอร์มอลรีดักชันและไนไตรเดชัน
เพื่อสังเคราะห์ซิลิคอนไนไตรด์/ซิลิคอนคาร์ไบด์ พบว่าอุณหภูมิและความพรุนของการสังเคราะห์
ซิลิกา/คาร์บอนคอมพอสิตไม่มีผลต่อการเกิดซิลิคอนไนไตรด์หรือซิลิคอนคาร์ไบด์ แต่ขึ้นอยู่กับ
โครงสร้างทางเคมีของซิลิกา/อาร์เอฟเจล ในปฏิกิริยาโพลีคอนเดนเซชัน

ภาควิชา..........วิศวกรรมเคมี...................... ลายมือชื่อนิสิต..........ชรินทร์ญา เผ่าเมือง
สาขาวิชา..........วิศวกรรมเคมี...................... ลายมือชื่อ อ. ที่ปรึกษาวิทยานิพนธ์หลัก..........
ปีการศึกษา............2551.......................... ลายมือชื่อ อ. ที่ปรึกษาวิทยานิพนธ์ร่วม..........

5070256221 : MAJOR CHEMICAL ENGINEERING

KEYWORDS: POROUS / SILICON NITRIDE / SILICON CARBIDE / RF GEL / CARBOTHERMAL REDUCTION / NITRIDATION

CHARINYA POUMUANG: INCORPORATION OF SILICA INTO RF GEL FOR THE SYNTHESIS OF POROUS Si_3N_4/SiC COMPOSITE VIA THE CARBOTHERMAL REDUCTION AND NITRIDATION.
ADVISOR: ASST. PROF. VARONG PAVARAJARN, Ph.D.,
CO-ADVISOR: ASST. PROF. NATTAPORN TONANON, Ph.D., 98 pp.

Incorporation of silica into RF solution, which was prepared via the sol-gel polycondensation of resorcinol and formaldehyde with sodium carbonate as catalyst was investigated. The reaction between silica precursor and RF solution is quite violent and strongly exothermic. The addition of acetic acid into RF solution damages methylene and methylene ether bridges of the RF clusters, which enables the incorporation of increased amount of silica into the RF clusters. According to the experimental results, silica precursor (APTMS, MPTMS) incorporates into RF clusters at positions of hydroxyl group. Then, the silica/RF gel was converted into silica/carbon composite by pyrolysis before subjected to the carbothermal reduction and nitridation to synthesize silicon nitride/silicon carbide. The results indicated that temperature and porosity of silica/carbon composite does not affect the formation of silicon nitride or silicon carbide. Phase of the product depends upon chemical structure of silica/RF gel formed by polycondensation.

Department :....Chemical Engineering.... Student's Signature :...Charinya Poumuang..

Field of Study :..Chemical Engineering... Advisor's Signature :........................

Academic Year :..........2008.............. Co-advisor's Signature :........................

ACKNOWLEDGMENTS

CONTENTS

LIST OF TABLES

LIST OF FIGURES

CHAPTER I

INTRODUCTION

Porous ceramics are essential for many industries where high permeability, high surface area, and insulating characteristics are required. They can be used as filters for diesel emission, filters for molten metals, membrane reactors, and catalyst carriers. With the expansion of applications for porous ceramics, high porosity as well as high strength are required at the same time [Zhang et al., 2005].

Silicon nitride (Si_3N_4) is one of the most promising ceramic materials. Low density of Si_3N_4 of 3.2 g/cm^3 (about 40% of the density of high-temperature superalloys) may offer light-weighted components. It is, therefore, an important advantage over other high-temperature materials. Potential applications of Si_3N_4 include the all-ceramic gas turbine or the replacement for metallic components in an internal combustion engine. Moreover, other engineering applications, such as energy conversion systems, industrial heat exchangers, the use as wear-resistant material in metals processing and as material for ball and roller bearings are also under consideration [Ziegler et al., 1987].

Silicon carbide (SiC) is an important structural material because of its unique combination of properties, such as low density, high thermal shock resistance, high specific strength, and excellent corrosion resistance at high temperature. These materials are correspondingly used in a broad range of applications such as filters for molten metals, diesel particulate filters, gas burner media, and membrane supports for hydrogen separation [Matovic et al., 2007 and Kim et al., 2008].

Porous silicon nitride/silicon carbide has attracted great interest for engineering applications, such as gas filter, separation membranes and catalyst supports because of high strength at high temperature, good thermal stress resistance due to the low coefficient of thermal expansion, relatively good resistance to

oxidation compared to other high-temperature and corrosion resistance structural materials.

A well-known technique for Si_3N_4/SiC synthesis is the carbothermal reduction and nitridation of silica, i.e. reaction of silica with a source of carbon under flowing nitrogen atmosphere at temperature in range from 1200 up to 1450°C. This method requires high reactivity and good distribution of raw materials, i.e. silica and carbon to achieve satisfactory extent of the reaction.

Synthesis of Si_3N_4/SiC nanocomposite via the carbothermal reaction of silica is attractive because it can easily be integrated into the industrial production. The carbothermal reaction of silica has been a major industrial route for the production of both Si_3N_4 and SiC powders. The SiC nanoparticles can also be produced in-situ in the Si_3N_4 matrix during the carbothermal reaction, and can thus be inherently well distributed. The Si_3N_4/SiC nanocomposite ceramics sintered from the carbothermally prepared Si_3N_4/SiC nanocomposite powders have shown a dramatic improvement in the high-temperature strength and creep resistance over the components prepared from mechanically mixed Si_3N_4/SiC powders [Jinwang, 2007].

In this work, resorcinol-formaldehyde (RF) gel is used as source for carbon for the carbothermal reduction with silica. RF gel can be prepared by the sol-gel polycondensation of resorcinol (R) and formaldehyde (F) with sodium carbonate (C) as basic catalyst [Pekala, 1989 and Tamon et al., 1998]. Pyrolysis of dried RF gel results in porous carbon with high specific surface area and large mesopore volume. Then, porous Si_3N_4/SiC is synthesized via the carbothermal reduction and nitridation of the carbonized composite of silica and RF gel. This work focuses on the effective incorporation of silica into the RF gel, as well as the study on the effect of silica precursor on the subsequent formation of Si_3N_4/SiC. Effects of various factors, such as aging time for RF solution, reaction temperature during the sol-gel polycondensation of silica/RF gel, acetic acid addition to the RF solution, amount acetic acid, type of silica precursor are investigated.

This thesis is divided into five chapters. The first three chapters describe general information about the study, while the following two chapters emphasize on the results and discussion from the present study. Chapter I is the introduction of this work. Chapter II describes basic theory about silicon nitride and silicon carbide properties, the carbothermal reduction and nitridation process, sol-gel process and resorcinol–formaldehyde (RF) gel. Chapter III shows materials and experimental systems. Chapter IV presents the experimental results and discussion. In the last chapter, the overall conclusion from the results and recommendation for future work are presented.

CHAPTER II

THEORY AND LITERATURE SURVEY

2.1 Silicon Nitride

Silicon nitride (Si_3N_4) ceramics have been regarded as one of the promising engineering ceramic materials because of high-temperature strength, superior thermal shock resistance, good oxidation resistance and damage tolerance. However, silicon nitride does not exist in nature. It has to be synthesized, but it is not easy to obtain the Si_3N_4 powder with high purity, fine grain size and narrow size distribution. Those characteristics are very important for the fabrication of Si_3N_4 sintered bodies.

Si_3N_4 commonly occurs in two phases, i.e. α and β. The α-phase powder is the generally preferred as raw material for manufacturing compacted bodies because of the favourable microstructural characteristics obtained during the phase transformation into β-phase at high temperature. The following techniques are usually applied to synthesize Si_3N_4 powders: (1) nitridation of metallic silicon powder, (2) gas-phase reaction of $SiCl_4$, (3) carbothermal reduction of SiO_2 in nitrogen atmosphere, and (4) precipitation and thermal decomposition of silicon diimide [Yang et al., 2005]. There are differences in the type and amount of impurities, in the size and morphology of the powder and in the phase composition of powders obtained from these techniques. By varying the processing conditions, however, properties of the powders produced by any of these techniques may be changed, particularly the phase composition, degree of crystallinity and particle morphology. Typical properties of powders produced by different techniques are listed in Table 2.1 [Ziegler et al., 1987].

Table 2.1 Typical properties of silicon nitride powders produced by various processing techniques.

Properties	Direct nitridation of silicon	Vapor phase synthesis	Carbothermal nitridation	Diimide synthesis
Specific surface area (m^2/g)	8-25	3.7	4.8	10
Oxygen content (wt %)	1.0-2.0	1	1.6	1.4
Carbon content (wt %)	0.1-0.4	-	0.9-1.1	0.1
Metallic impurities (wt %) Σ Fe, Al, Ca	0.07-0.15	0.03	0.06	0.005
Crystallinity (%)	100	60	100	100
$\alpha/(\alpha+\beta)$ (%)	95	95	95	85

2.1.1 Crystal Structure of Silicon Nitride

Silicon nitride crystallizes in two known phases. Detailed X-ray diffractometry (XRD) examinations in the mid-1950s have proved that the crystal structure of both α and β polymorphs are hexagonal [Turkdogan et al., 1958]. In the α and β form, the basic building unit is the Si–N tetrahedron, in which silicon atom lies in the centre of a tetrahedron with nitrogen atom at each corner [Ghanem et al., 2007]. However, their respective structural dimensions are different. The structures of α-phase and β-phase are shown in Figure 2.1 and Figure 2.2 respectively [Turkdogan et al., 1958].
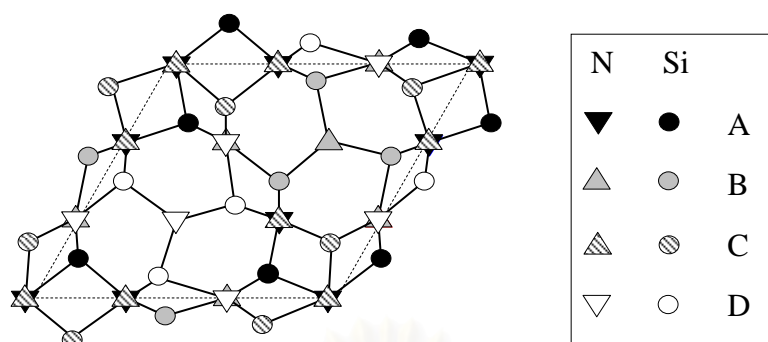
Figure 2.1 α-Si$_3$N$_4$ unit cell: the structure of α-Si$_3$N$_4$ can be described as a stacking of Si-N layers in …ABCDABCD… sequence.
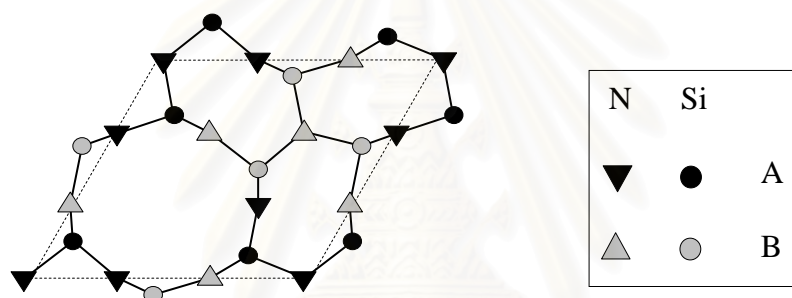
Figure 2.2 β-Si$_3$N$_4$ unit cell: the structure of β-Si$_3$N$_4$ can be described as a stacking of Si-N layers in …ABAB… sequence.

2.1.2 Properties of Silicon Nitride Ceramics

Technological investigations have mainly been concentrated during this time on two types of Si$_3$N$_4$: (a) dense Si$_3$N$_4$, which can be produced by hot-pressing, sintering or hot-isostatic pressing, and (b) porous Si$_3$N$_4$ produced by reaction-bonding of silicon powder compacts. As a consequence of processing, the two forms of Si$_3$N$_4$ are different in density, and in resulting mechanical, thermal and thermo-mechanical properties as listed in Table 2.2 [Ziegler et al., 1987].

Table 2.2 Properties of Silicon Nitride Ceramics.

Theoretical density (g cm^{-3}) :	
α-phase	3.168-3.188
β-phase	3.19-3.202
Density (g cm^{-3}) :	
dense Si_3N_4	90-100% th.d.*
reaction- bonded Si_3N_4	70-88% th.d.
Coefficient of thermal expansion	
(20-1500°C) (10^{-6}°C^{-1})	2.9-3.6
Thermal conductivity (RT) (W m^{-1}K^{-1}) :	
dense Si_3N_4	15-50
reaction- bonded Si_3N_4	4-30
Thermal diffusivity (RT) (cm^2 sec^{-1}) :	
dense Si_3N_4	0.08-0.29
reaction- bonded Si_3N_4	0.02-0.22
Specific heat (J kg^{-1}°C^{-1})	700
Electrical resistivity (RT) (Ω cm)	~ 1013
Microhardness (Vickers, MN m^{-2})	1600-2200
Young's modulus, (RT) (GN m^{-2}) :	
dense Si_3N_4	300-330
reaction- bonded Si_3N_4	120-220
Flexural strength (RT) (MN/m^2) :	
dense Si_3N_4	400-95
reaction- bonded Si_3N_4	150-350
Fracture toughness (MN m$^{-3/2}$) :	
dense Si_3N_4	3.4-8.2
reaction- bonded Si_3N_4	1.5-2.8
Thermal stress resistance	
parameter R = $\sigma_F(1 - \nu)/\alpha E$ (°C)	
and R' = Rλ (10^3W m^{-1}) :	
dense Si_3N_4	R = 300-780 R' = 7-32
reaction- bonded Si_3N_4	R = 220-580 R' = 0.5-10

th.d.* = Theoretical density is dependent on the type and composition of consolidation aids (th.d. = Theoretical density of pure Si_3N_4 = 3.2 g cm^{-3}).

2.2 Silicon Carbide

Silicon carbide (SiC) has been a focus of attention in the field of porous ceramics because of superior properties, such as low thermal expansion coefficient, high thermal conductivity and excellent mechanical strength [Ding et al., 2008]. The following techniques are usually applied to synthesize SiC powder: (1) the carbothermal reduction of silica (SiO_2), (2) the thermal decomposition of organo silicon polymer, (3) the gas phase synthesis, and (4) the direct reaction between Si metal and C.

2.2.1 Crystal Structure of Silicon Carbide

The crystal structure of SiC has a one dimensional polymorphism referred to as polytypism. The result is a unique aspect of this material where by it can exist in infinite number of possible crystallographic structures called polytypes. Nearly 200 polytypes have been identified at present. These structures fall into two phases referred to as α and β polymorphs. The α category contains primarily hexagonal, rhombohedral and trigonal structures while the β category contains one cubic or zincblende structure [Shields].
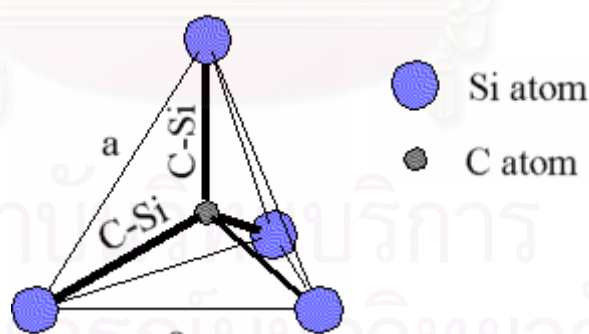
Figure 2.3   The tetragonal bonding of a carbon atom with the four nearest silicon neighbours. The distances a and C-Si are approximately 3.08Å and 1.89Å respectively.
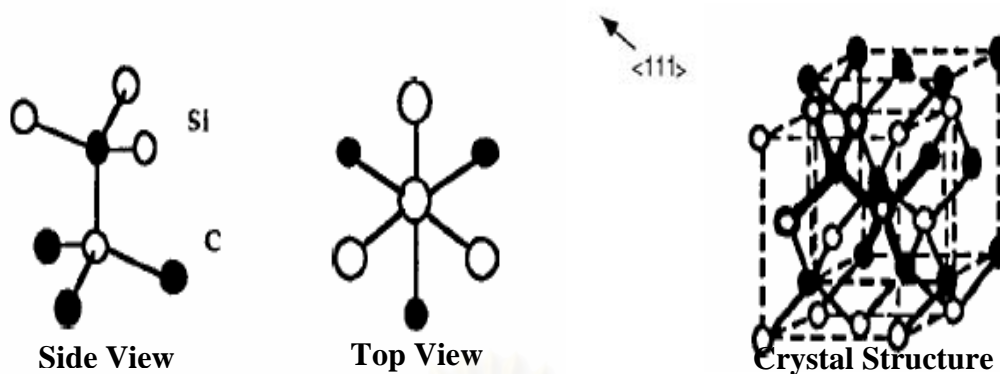
Figure 2.4   β-SiC: Crystal structure of silicon carbide tetrahedral structures.
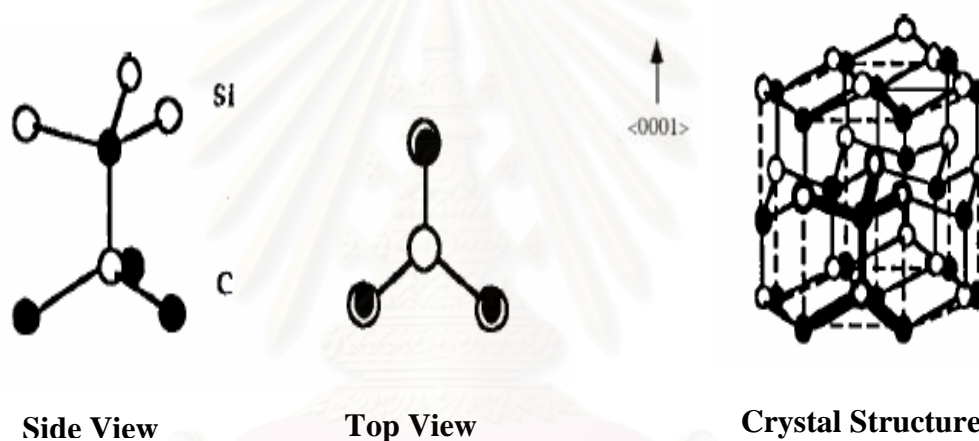
Figure 2.5   α-SiC: Crystal structure of silicon carbide tetrahedral structures.

2.2.2 Properties of Silicon Carbide Ceramics

As a consequence of the difference in crystal structure, the two forms of SiC are different in density, as well as mechanical, thermal and thermo-mechanical properties. Nevertheless, general properties of silicon carbide are listed in Table 2.3 [Shields].

Table 2.3 Properties of silicon carbide ceramics.

Properties	β-SiC (α-SiC)
Bandgap (cV) at 300 K	2.3 (>2.9)
Maximum operating temperature (℃)	873 (1240)
Melting point (℃)	Sublime >1800
Electron mobility (cm^2/V-s)	100 (600)
Hole mobility (cm^2/V-s)	40
Breakdown field, E_b (10^6V/cm)	4
Thermal conductivity σ_T (W/cm-℃) :	5
Saturated electron drift velocity, v_{sat} (107 cm/s)	2.5
Dielectron constant, ε	9.7

2.3 Carbothermal Reduction and Nitridation of Silica

The carbothermal reduction and nitridation of silica powder under nitrogen is the earliest method to product silicon nitride and silicon carbide. This reaction starts from a mixture of SiO_2 and carbon, of which the reaction with nitrogen at high temperature can produce either α-Si_3N_4 or β-Si_3N_4 [Yang et al., 2005]. These overall reactions can be written as:

$$3\ SiO_2\ (s)\ +\ 6\ C\ (s)\ +\ 2\ N_2\ (g)\ \leftrightarrow\ \alpha\text{-}Si_3N_4\ (s)\ +\ 6\ CO\ (g) \qquad (2.1)$$

$$3\ SiO_2\ (s)\ +\ 6\ C\ (s)\ +\ 2\ N_2\ (g)\ \leftrightarrow\ \beta\text{-}Si_3N_4\ (s)\ +\ 6\ CO\ (g) \qquad (2.2)$$

$$SiO_2\ (s)\ +\ 3\ C\ (s)\ \leftrightarrow\ SiC\ (s)\ +\ 2\ CO\ (g) \qquad (2.3)$$
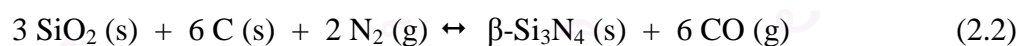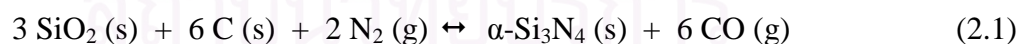
In some reports for the synthesis of α-Si_3N_4 via the carbothermal reduction method, β-Si_3N_4 and SiC were by-products when the reaction conditions were changed. Phase transformation from α-Si_3N_4 to β-Si_3N_4 occurs at temperature higher than 1600°C. Although there is a possibility of formation of SiC at relatively high temperature, the content of SiC can be control by controlling pressure of nitrogen gas.

High nitrogen pressure can promote the Si_3N_4 formation, and prevent SiC formation [Yang et al., 2005].

The carbothermal reduction and nitridation synthesis of Si_3N_4 inherently produces powder with >95% α-Si_3N_4 phase and small amount of β-SiC intimately dispersed in-situ as composite material. The reaction is moderately endothermic (1268 kJ/mol at 1427°C) with an activation energy of 457 ± 55 kJ/mol. Kinetically, the reaction is reported to be slow, requiring 4–5 h to complete. This is due to a thermodynamic upper temperature limit (T<1500°C at P>0.1 MPa) for Si_3N_4 synthesis. Silicon carbide (SiC) synthesis is favored at higher temperatures (T>1500°C) where the reaction rate is faster [Weimer et al., 1999].

2.4 Resorcinol-Formaldehyde (RF) Gel

2.4.1 Sol-Gel Processing

The sol-gel process is a wet-chemical technique for the fabrication of materials starting either from chemical solution or colloidal particles to produce an integrated network, which undergo hydrolysis and polycondensation reactions to form a colloid, and form sol according to Equations 2.4 to 2.6.

$$M\text{-}O\text{-}R + H_2O \ \rightarrow \ M\text{-}OH + R\text{-}OH \qquad \text{(hydrolysis)} \qquad (2.4)$$

$$M\text{-}OH + HO\text{-}M \ \rightarrow \ M\text{-}O\text{-}M + H_2O \qquad \text{(water condensation)} \qquad (2.5)$$

$$M\text{-}O\text{-}R + HO\text{-}M \ \rightarrow \ M\text{-}O\text{-}M + R\text{-}OH \qquad \text{(alcohol condensation)} \qquad (2.6)$$
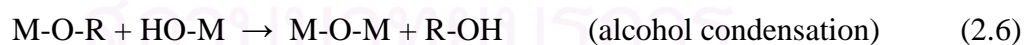
where M and R are metal atom and alkyl group, respectively. In general, the sol-gel process involves the transition of a system from liquid "sol" into solid "gel" phase. By applying the sol-gel process, it is possible to fabricate advanced materials in a wide variety of forms, e.g. ultra-fine or spherical shaped powders, thin film coatings, ceramic fibers, microporous inorganic membranes, monolithic ceramics and extremely porous aerogel materials.

2.4.2 Formation of RF Gel

RF gel is an interesting porous material with moderately high surface area and large mesopore volume. Carbon gel derived by pyrolysis of the RF gel is suitable for many applications such as column packing materials for high-performance liquid chromatography, electrode materials for electric double layer capacitors and materials for catalyst supports [Tamon et al., 1999].

The first resorcinol-formaldehyde (RF) gel was produced by Pekala via the sol-gel polycondensation of resorcinol (R) and formaldehyde (F) with sodium carbonate (C) as basic catalyst [Pekala, 1989]. The intermediates formed during the reaction further react to form a cross-linked polymer network. The two major reactions include: (a) the formation of hydroxymethyl ($-CH_2OH$) derivatives of resorcinol, and (b) the condensation of the hydroxymethyl derivatives to form methylene ($-CH_2-$) and methylene ether ($-CH_2OCH_2-$) bridged compounds [Ruben et al., 1992].

The sol-gel polymerization of metal alkoxides or certain multifunctional organic monomers leads to the formation of highly cross-linked, transparent gels. Porosity of the final products depends on the structure of their parent hydrogel, which is mostly formed during the sol-gel transition. A catalyst used in the sol-gel polycondensation usually plays the most important role for the formation of the porous structure of the hydrogel. The catalyst initially promotes the generation of resorcinol anions. These anions are subsequently transformed into substituted resorcinols, which form RF clusters through polycondensation. Then RF clusters react with each other and grow into colloidal particles, which finally form a RF hydrogel [Yamamoto et al., 2003].

(a) Addition Reaction

Condensation product

Cluster   **Colloidal particles**   **RF hydrogel**

(b) Condensation Reaction

Figure 2.6   Schematic diagram of the sol-gel polycondensation of a RF solution
(a) addition reaction (b) condensation reaction [Yamamoto et al., 2003].

2.4.3 Drying of Gel

Three kinds of drying processes are available to convert hydrogel to a solid RF gel.

2.4.3.1 Supercritical drying

Solvent can be removed from RF hydrogel under CO_2 supercritical conditions. Supercritical carbon dioxide (CO_2) can replace water in the gel structure, resulting in what is called RF aerogel. Since water is poorly soluble in CO_2, skeletons of the gel are preserved and highly porous organic gels can be obtained [Yamamoto et al., 2001]. Supercritical extraction with carbon dioxide yields RF aerogels, but the drying cost is extremely expensive.

2.4.3.2 Freeze drying

During freeze drying, the solvent inside the pores is removed by sublimation after the solvent is pre-frozen. Such removal of the solvent can avoid capillary force occurring in the conventional drying, which may cause the shrinkage of pore structure [Yamamoto et al., 2001].

2.4.3.3 Air drying

This conventional technique uses atmospheric convective drying to remove the solvent, without any preliminary treatment. Indeed, when synthesis conditions are adequate, the mechanical strength of the gel network is high enough to withstand capillary pressure, avoiding the collapse of the structure. By drying the gel by means of low temperature treatment (25-100°C), it is possible to obtain porous solid matrices called RF xerogels [Czakkel et al., 2005 and Leonard et al., 2007].

2.5 Classification of Pore Size

Pores are classified into three main groups according to the accessible size. According to IUPAC classification, pores can be divided into three categories depending on their sizes, namely micropores $\leq$ 2 nm, mesopores 2-50 nm and macropores $\geq$ 50 nm.

CHAPTER III

EXPERIMENTAL

3.1 Chemical Agents
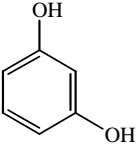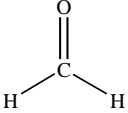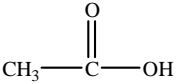
The list of chemical agents used in this research are shown in Table 3.1.

Table 3.1 List of chemical agents used in the research.

Chemical agents	Using for	Manufacturer / Grade
1. Resorcinol ($C_6H_4(OH)_2$)	Synthesis of Resorcinol-Formaldehyde (RF) solution	Fluka / 99.8%
2. Formaldehyde (HCOH)	Synthesis of Resorcinol-Formaldehyde (RF) solution	Ajax Fine Chemical / 37%
3. Sodium carbonate (Na_2CO_3)	Synthesis of Resorcinol-Formaldehyde (RF) solution	Ajax Fine Chemical / 99.8%
4. Distilled water (H_2O)	Synthesis of Resorcinol-Formaldehyde (RF) solution	
5. Acetic acid (CH_3COOH)	Synthesis of Resorcinol-Formaldehyde (RF) solution	Q&C / 99.8%
6. 3-amino propyl trimethoxysilane (APTMS) $(CH_3O)_3Si(CH_2)_3NH_2$	Synthesis of Silica /Resorcinol-Formaldehyde (RF) gel	Aldrich / 97%
7. 3-mercapto propyl trimethoxysilane (MPTMS) $(CH_3O)_3Si(CH_2)_3SH$	Synthesis of Silica /Resorcinol-Formaldehyde (RF) gel	Aldrich / 95%
8. Nitrogen (N_2)	Carbonization and Carbothermal-Nitridation	TIG / purity 99.999%
9. Hydrogen (H_2)	Carbothermal-Nitridation	TIG / purity 99.999%
10. Argon (Ar)	Carbothermal-Nitridation	TIG / industial

The chemical structure of the organic materials employed in this work is illustrated in Table 3.2

Table 3.2 Chemicals structure.

Chemical name	Designation	Chemical structure
3-Aminopropyltrimethoxysilane	APTMS	$H_2N-CH_2-CH_2-CH_2-Si(OCH_3)_3$
3-Mercaptopropyltrimethoxysilane	MPTMS	$HS-CH_2-CH_2-CH_2-Si(OCH_3)_3$
Resorcinol	R	
Formaldehyde	F	
Acetic acid	Ac	

3.2 Preparation of Silica/RF Gel

To form silica/RF gel, RF solution was first prepared from resorcinol (R), formaldehyde (F), distilled water (W) and sodium carbonate (C) at the R/F mole ratio of 0.5, R/W mole ratio of 0.15 and C/W ratio of 10 mol/m^3. Resorcinol was dissolved into distilled water and stirred until it dissolved completely. Next, the resorcinol solution was added by sodium carbonate (C) and formaldehyde solution. The solution was stirred at room temperature for 15 min. After that, the RF solution was aged without stirring at 30°C for 1 h. Then silica precursor was added to the RF solution under continuous stirring at room temperature to form silica/RF gel.

The silica/RF gel was aged at room temperature until the gel was completely set for 3 days. The obtained solid product was crushed into powder and dried in oven at 110°C for 16 h.

3.3 Preparation of Porous Silica/Carbon Composite

The dried silica/RF gel was converted into silica/carbon composite by pyrolysis in a step-wise fashion. The dried gel was heated under continuous flow of nitrogen (200 ml/min) at temperature of 250°C for 2 h and subsequently heated at 750°C for 4 h. The heating rate employed was fixed at 10°C/min. The product from this step is silica/carbon composite.
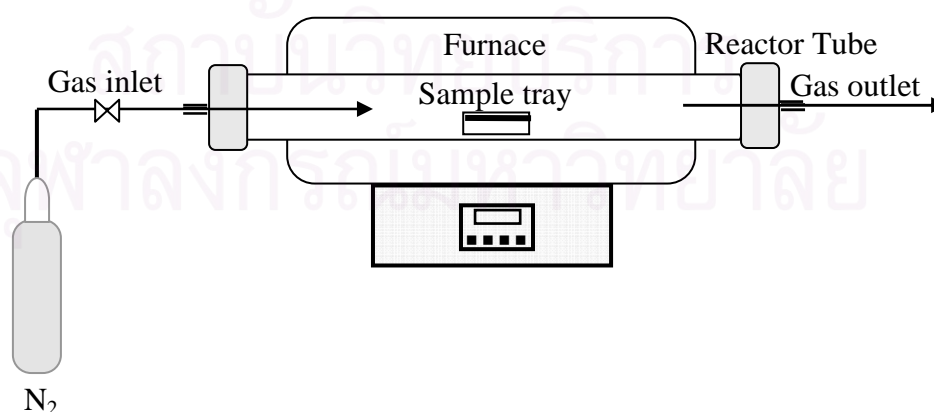
Figure 3.1   Schematic diagram of the tubular flow reactor used for the preparation
of silica/carbon composite.

3.4 Carbothermal Reduction and Nitridation

In the carbothermal reduction and nitridation process, the silica/carbon composite powder was put into an alumina tray (25 mm x15 mm x 5 mm deep) and placed in a horizontal tubular flow reactor. The schematic diagram of the reactor system is shown in Figure 3.2. In this process, the composite was heated to 1450°C at the rate of 10°C/min, under a flow of argon. After the system had reached 1450°C, the reaction was initiated by switching the gas stream from argon to mixture of 90% nitrogen and 10% hydrogen with total flow rate of 50 l/h. The reaction was held at constant temperature for 6 h. The obtained product was later calcined in a box furnace at 700°C for 10 h to remove excess carbon.
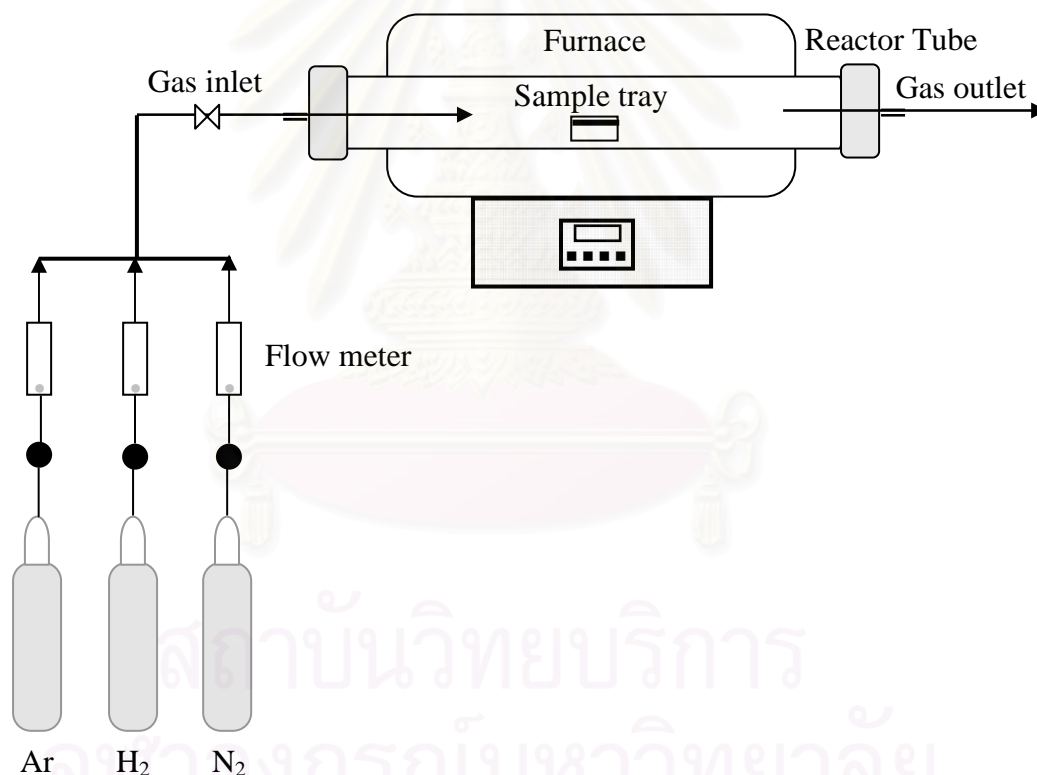
Figure 3.2 Schematic diagram of the tubular flow reactor used for the carbothermal reduction and nitridation.

3.5 Characterization of the Products

The obtained products were characterized by using various techniques, as following:

3.5.1 X-ray Diffraction Analysis (XRD)

Crystalline phases of the product were identified by using a Siemens D5000 X-ray diffractometer at the Center of Excellence on Catalysis and Catalytic Reaction Engineering, Chulalongkorn University. The measurement was carried out by using Ni-filtered CuKα radiation, operated in the 2θ range of 20-50° at the scan step of 0.04°.

3.5.2 Fourier-Transform Infrared Spectroscopy (FT-IR)

The functional groups in the samples were identified by using a Nicolet 6700 infrared spectrometer. The sample was mixed with KBr with sample-to-KBr ratio of 1:100 and formed into a thin pellet, before measurement. The spectra were recorded at wavenumber between 400 and 4000 cm^{-1} with resolution of 4 cm^{-1}. The number of scan for the measurement was 64.

3.5.3 Thermogravimetric Analysis (TGA)

The residual carbon content and thermal behavior of the samples were determined by using thermogravimetric analysis on a SDT Q600 instrument. The analysis was performed from temperature of 50 to 1,000°C under a heating rate of 10°C /min in 100 ml/min flow of either oxygen or nitrogen.

3.5.4 Scanning Electron Microscopy (SEM)

Morphology of the products was observed by using a scanning electron microscope (SEM) model Hitachi S-3400N SEM/WDX at a research laboratory collaborated between Mektec Manufacturing Corporation (Thailand) Ltd. and Chulalongkorn University.

3.5.6 Surface Area Measurement

The surface area, pore volume and pore size were measured by a Micromeritics ASAP 2020 using nitrogen as the adsorbate at the Center of Excellence on Catalysis and Catalytic Reaction Engineering laboratory, Chulalongkorn University. The operating conditions are as follows:

Degas temperature $200^{\circ}C$
Vacuum pressure < 10 mmHg

CHAPTER IV

RESULTS AND DISCUSSION

4.1 Effect of Aging Time for RF Solution

RF solution was prepared by sol–gel polycondensation according to reported procedures in literature [Tonanon et al., 2005], using resorcinol and formaldehyde as raw materials and Na_2CO_3 as catalyst. In the initial period, the sol-gel process slowly converts RF solution into nanoparticles suspended in liquid or sol. Then, the colloidal nanoparticles are linked together in three dimensional to form liquid-filled solid network or gel. This transformation from sol to gel can be initiated in several ways, but the most convenient approach is to change the pH of the reaction solution. The mechanism for the sol-gel process is shown in Figure 4.1.

(a)   (b)   (c)

Figure 4.1 Progress of the reaction of RF solution: (a) solution (b) colloid and (c) gel.

The formation of nanoparticles in the RF solution can be witnessed from light scattering behavior, i.e., a beam of light can be observed only when nanoparticles are already formed in the solution. The greater the number of the nanoparticle formed, the more obvious the scattered beam becomes. Figure 4.2 shows light scattering of RF solution after aging time of 1, 12 and 30 h. The initial solution is clear and colorless, but, after aging time of 12 h, the solution turns into pale yellow and pH of solution

decreases from 5 to 4. Colloid is formed in the solution as well, as it could be perceived from light scattering of laser beam. At the aging time of 30 h, the pH of solution decreases to 3 and the mixture becomes highly viscous, which indicates gel formation. The effect of aging time of RF solution is summarized in Table 4.1. Since the RF solutions aged for 1 and 30 h are signifiontly different in both physical and chemical properties, the aging time of 1 and 30 h were chosen in further investigation.
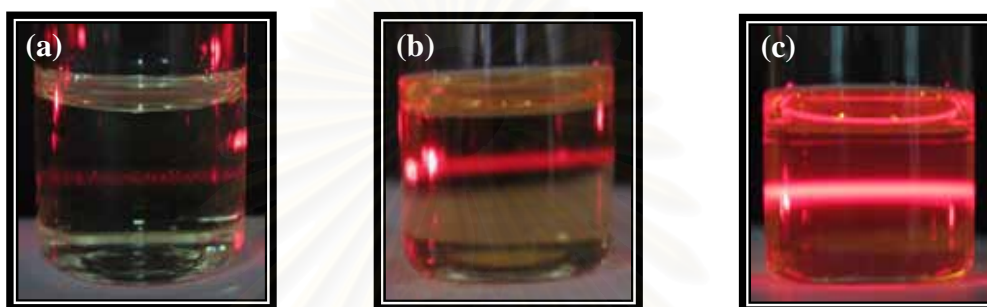
Figure 4.2   Light scattering of RF solution aged for various times: (a) 1 h (RF-1), (b) 12 h (RF-12) and (c) 30 h (RF-30).

Table 4.1 Effect of aging time of RF solution.

Sample	Aging time (h)	pH	Appearance
RF-1	1	5	Solution
RF-12	12	4	Colloid
RF-30	30	3	Nearly gel

Figure 4.3 shows the structural image of network of a RF gel. The RF solution formation has been associated with two reactions. The first addition reaction of resorcinol and formaldehyde leads to the formation of methylol groups (CH_2OH) at 2, 6 (ortho) and 4 (para) positions of phenolic. In the second condensation reaction, hydroxylmethyl derivative ($-CH_2OH$) is able to form covalent bridges between the resorcinol rings. The chain growth may result from two types of condensations: (i) condensation between two methylol resorcinols resulting in methylene ether ($-CH_2-O-$

CH$_2$-) bridges and (ii) further condensation of the methylol group with ortho and para position of resorcinols resulting in methylene (-CH$_2$-) bridges between resorcinol rings [Handique and Baruh, 2002]. The condensation product is transformed into RF clusters through polycondensation. Then RF clusters are reacted with each other and grow into colloidal particles, which finally produce RF hydrogel [Yamamoto et al., 2003].
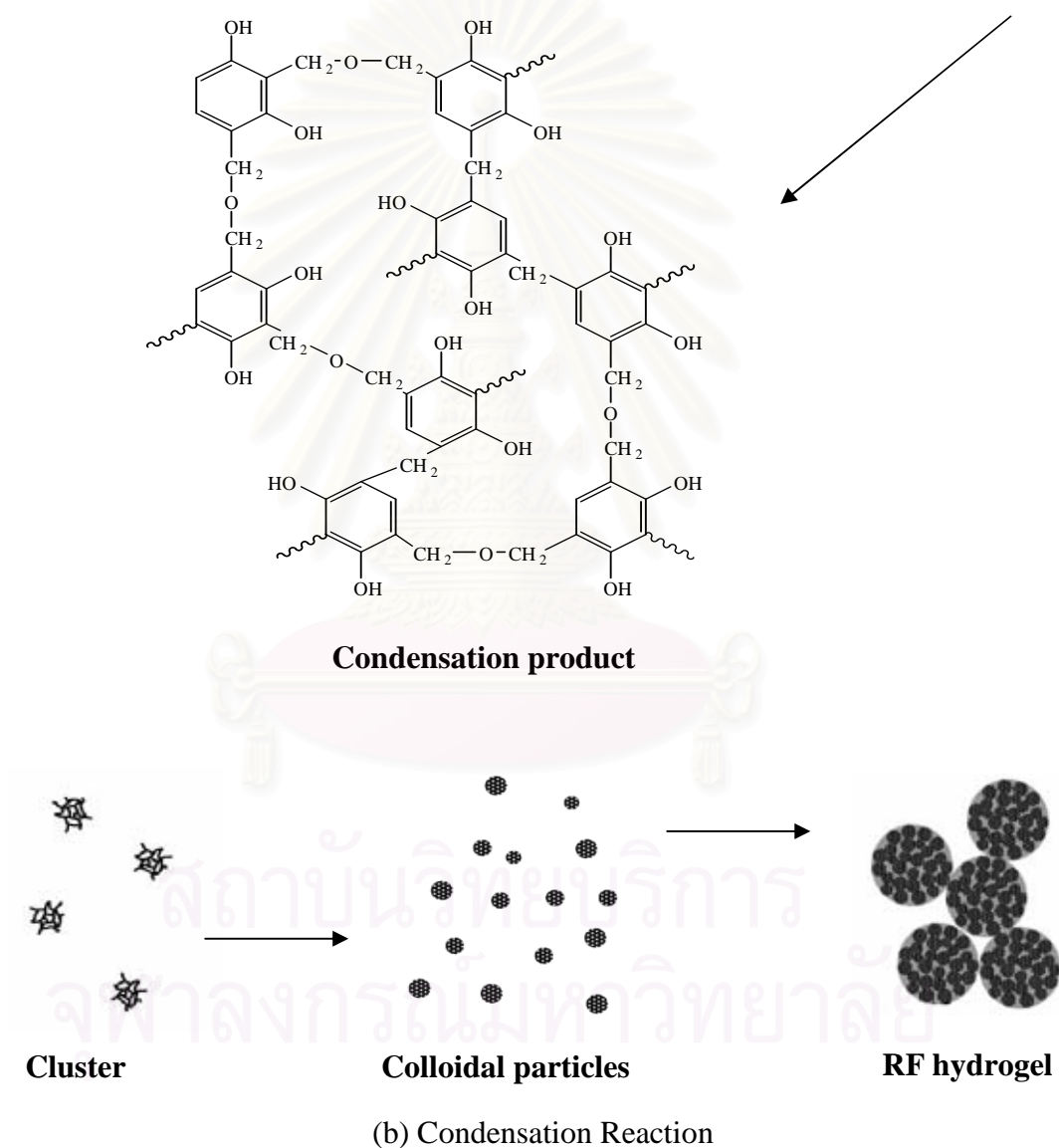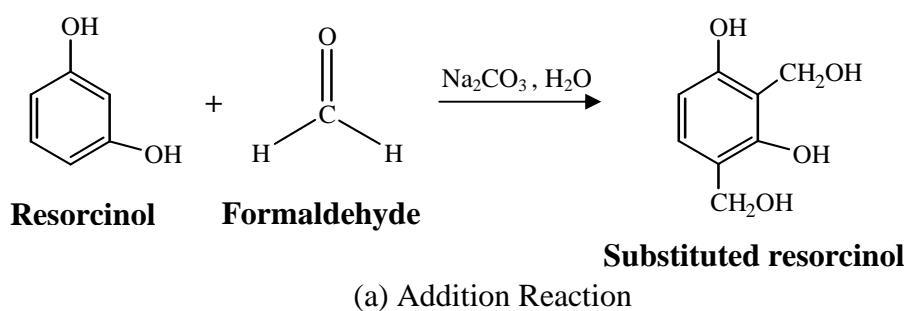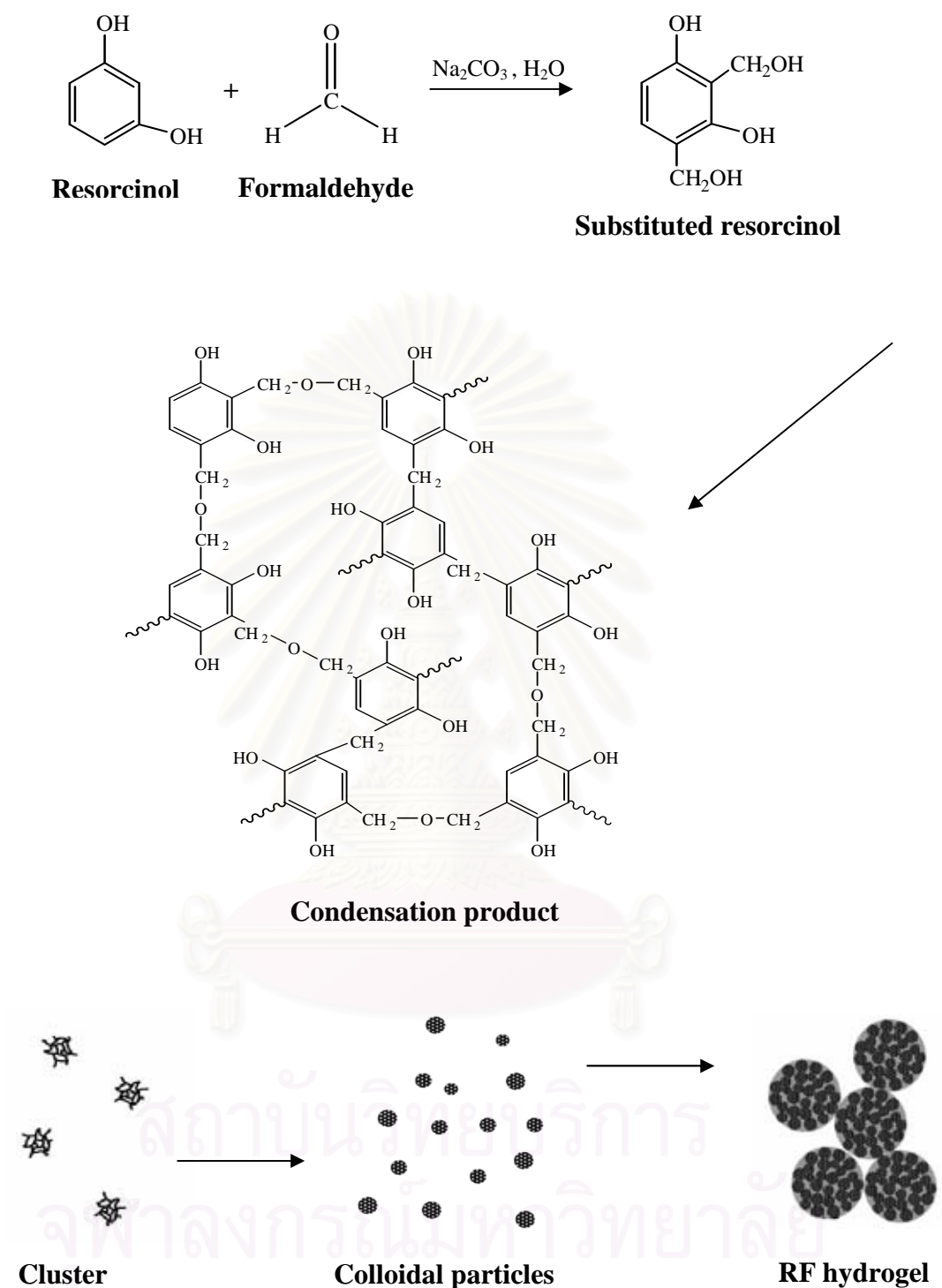
Figure 4.3 Schematic diagram of the sol-gel polycondensation of a RF solution [Yamamoto et al., 2003].

The principle reaction can be supported in part by the IR spectra of the RF solution as shown in Figure 4.4.

According to Figure 4.4, the characteristic peaks of resorcinol at 1607.9, 1509.1, 1295.2, and 976.3 cm^{-1} corresponding to the C=C aromatic ring, C-O stretch and 2,4- substituted benzene ring, increases with increasing aging time due to networking of resorcinol. Since formaldehyde aqueous solution was added into the resorcinol at the beginning of the reaction, the present of peaks at 2917.2, 1473.4, 1220.9 and 1092.0 cm^{-1} confirms the formation methylene (-CH$_2$) and methylene ether bridges (-CH$_2$-O-CH$_2$-) in the RF solution.
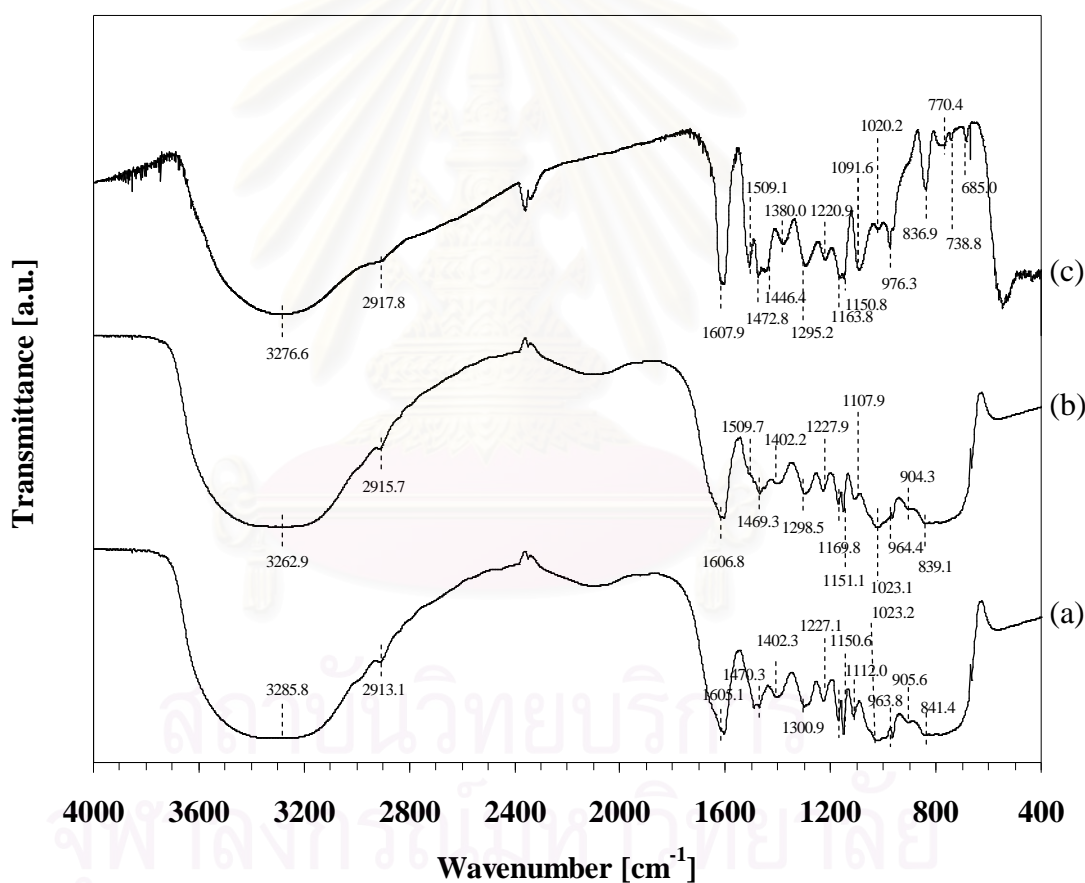
Figure 4.4 FT-IR spectra of RF solution aged for various time: (a) 1 h, (b) 12 h and (c) 30 h.

All peaks that have been proposed to associate with the functional groups of the RF solutions are shown in Table 4.2.

Table 4.2 Assignments of FTIR absorption bands of the RF solutions.

IR bands [cm^{-1}]			Functional groups
RF 1 h	RF 12 h	RF 30 h	
3285.8	3262.9	3276.6	OH stretching[1]
2913.1	2915.7	2917.2	in phase stretching vibration of -CH$_2$- alkane[1]
1605.1	1606.8	1607.0	C=C aromatic ring[1]
-	1509.7	1507.3	C=C aromatic ring[1]
1470.3	1469.3	1473.4	-CH$_2$- methylene bridge[1]
1402.3	1402.2	1380.3	OH in plane[1]
1300.9	1298.5	1295.6	C-O stretching[1]
1227.1	1227.9	1220.9	C-O-C stretching vibrations of methylene ether bridges between resorcinol molecules[2]
1170.4	1169.8	1163.9	CH aromatic, in-plane[1]
1150.6	1151.1	1149.1	C-O stretching[1]
1112.0	1107.9	1092.0	C-O-C stretching vibrations of methylene ether bridges between resorcinol molecules[2]
1023.2	1023.1	1019.6	aliphatic hydroxyl[1]
963.8	964.4	976.0	2, 4- substituted benzene ring[1]
905.6	904.3	-	C-H out of plane, isolated H[1]
841.4	839.1	836	C-H out of plane, para substituted[1]

[1] Poljansek and Krajnc, 2005 and [2] Liang et al., 2000

4.2 Effect of Reaction Temperature during the Sol-Gel Polycondensation of Silica/RF Gel

In this section, RF solution was prepared with the ratio of resorcinol-to–formaldehyde (R/F), resorcinol-to-water (R/W) and sodium carbonate-to-water (C/W) at 0.5 mol/mol, 0.15 mol/mol and 10 mol/m^3, respectively. The mixture was stirred for 15 min at controlled temperature of 30°C during gel formation. After aging, the RF solution was kept for 1 h. The silica precursor (APTMS) was added to the mixture with the ratio Si/C = 0.05. The mixture of RF solution and APTMS rapidly formed into gel by strongly exothermic reaction.

Figure 4.5 shows photographs of silica/RF gel formed at different reaction temperature. The gel was prepared by the sol-gel polycondensation of silica precursor (APTMS) and RF solution aged for 1 h. The reaction temperature was varied from 50, 30 and -10°C, of which the sample was denoted as RF-AP-50, RF-AP-30 and RF-AP-10, respectively. The reaction is strongly exothermic when it is conducted at 50 and 30°C, but the extent of the exothermic nature of the reaction decreases at -10°C. It can be seen from Figure 4.5 that the laser beam can not penetrate through all silica/RF gel samples because of the network within the silica/RF cluster.
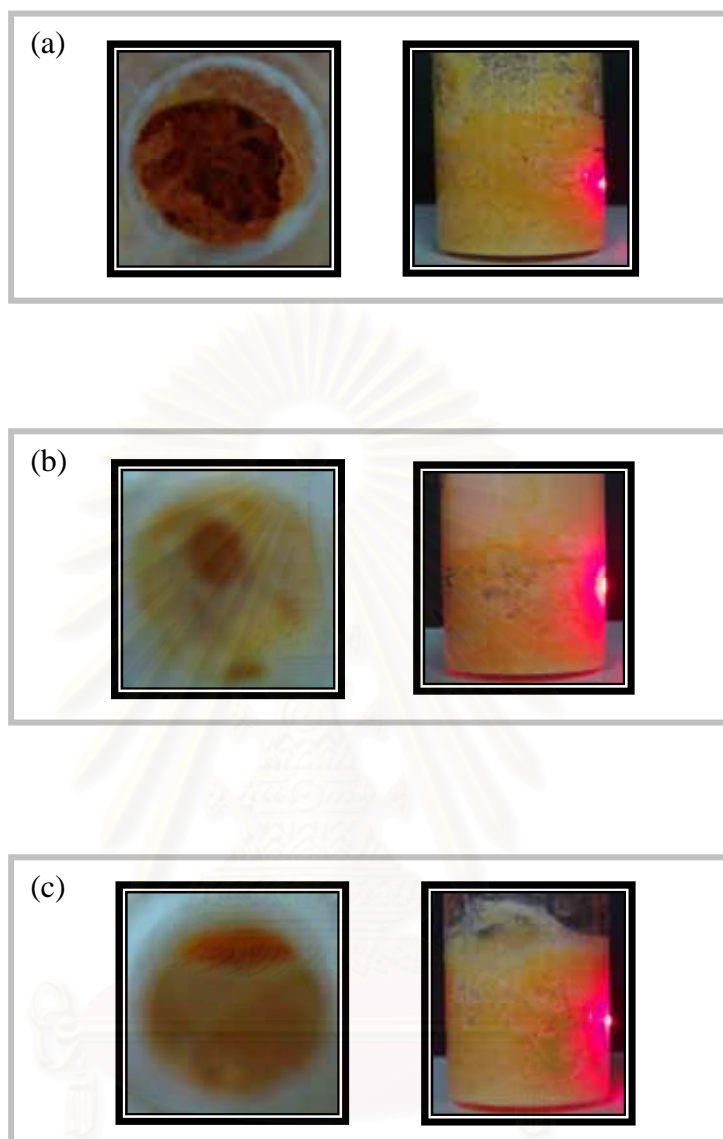
Figure 4.5 Silica/RF gel formed by the sol-gel polycondensation at: (a) 50°C, (b) 30°C and (c) -10°C.

Figure 4.6 shows FT-IR spectra of the gel, in which APTMS is incorporated into RF solution. Incorporation of trimethoxyl groups of APTMS into RF clusters is confirmed by Si-O-C and Si-O-Si symmetric deformation at 1110.5 cm^{-1} [Vejayakumaran et al., 2008 and Li et al., 2009]. The broad band ranging from 2940 – 3400 cm^{-1} can be attributed to hydroxyl (OH) stretching that overlaps with amino (NH) stretching of aminopropyl trimethoxysilane [Vejayakumaran et al., 2008]. The bands around 2945.6, 2885.5 and 1471.7 cm^{-1} are associated with methylene bridge(-CH$_2$-) [Ida and Matjaz, 2005], while the band at 1223.2 and 1107.6 cm^{-1} are corresponding to methylene ether bridge (-C-O-C-), all of which are connecting between two aromatic rings [Liang et al., 2000]. The absorption bands at 1616.2 and 1490.7 cm^{-1} are associating with C=C bonding with in aromatic ring [Ida and Matjaz, 2005]. All peaks that have been proposed to associate with the functional groups of the Silica/RF gel are shown in Table 4.3.
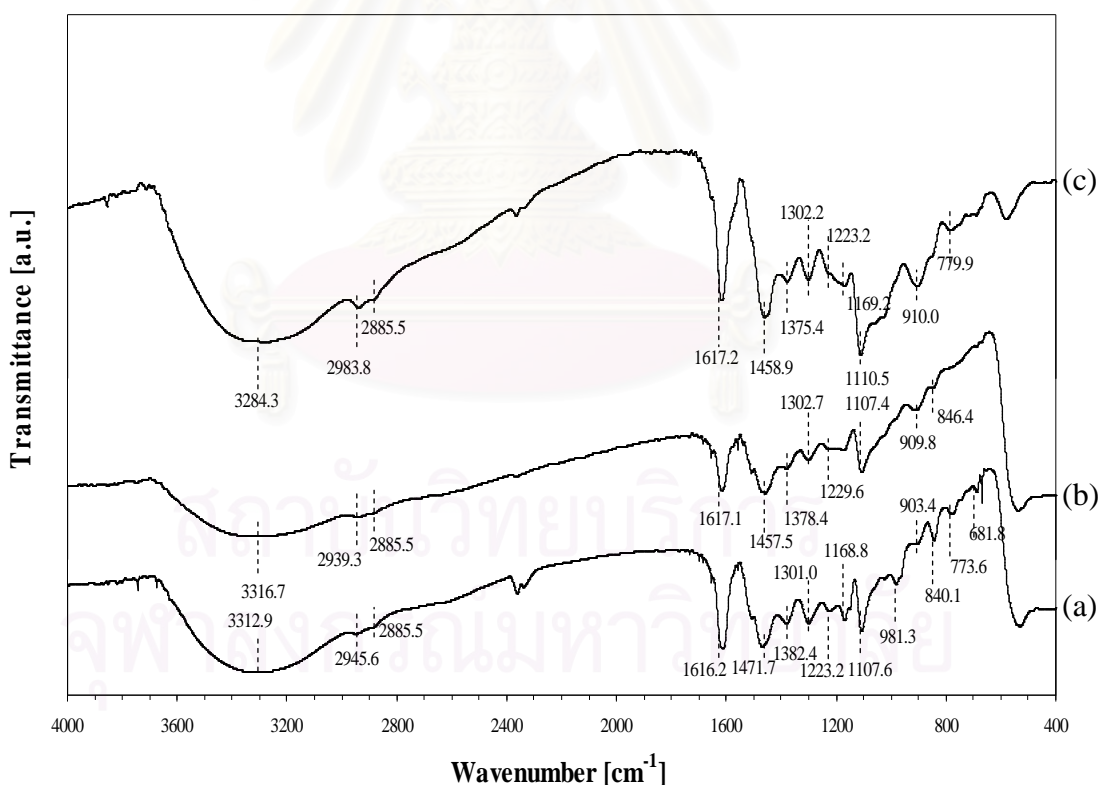
Figure 4.6 FT-IR spectra of silica/RF gel prepared at various temperatures: (a) 50°C, (b) 30°C and (c) -10°C.

Table 4.3 Assignments of FTIR absorption bands of the silica/RF gels.

IR bands [cm⁻¹]			Functional groups
At 50°C	At 30°C	At -10°C	
3312.9	3316.7	3284.3	OH stretching and NH_2 stretching[4]
2945.6	2939.3	2938.8	in phase stretching vibration of $-CH_2-$ alkane[3]
2885.5	2885.5	2885.5	$-CH_2-$ methylene bridge[3]
1616.2	1617.1	1617.2	C=C aromatic ring[3]
1490.7	-	-	C=C aromatic ring[3]
1471.7	1457.5	1458.9	$-CH_2-$ methylene bridge[3]
1382.4	1378.4	1375.4	OH in plane[3]
1301.0	1302.7	1302.2	C-O stretching[2]
1223.2	1229.6	1223.2	C-O-C stretching vibrations of methylene ether bridges between resorcinol molecules[1]
1168.8	1166.2	1169.2	CH aromatic, in-plane[3]
1144.1	-	-	C-O stretching[3]
1107.6	1107.4	1110.5	C-O-C stretching vibrations of methylene ether bridges between resorcinol molecules[1], Si-O-Si stretching[4] and Si-O-C stretching[5]
1023.2	-	1019.6	aliphatic hydroxyl[3]
981.3	-	-	-C-H[3]
903.4	909.3	910.0	-Si-OH[5]
840.1	846.4	-	-Si-O-H[6]
773.6	-	779.9	SiC stretching[5]

[1] Liang et al., 2000; [2] Fuente et al., 2003; [3] Ida and Matjaz, 2005

[4] Vejayakumaran et al., 2008; [5] Li et al., 2009 and [6] Hruby and Shanks, 2009

After the addition of APTMS into RF gel, the decrease in the broad FR-IR band for OH stretching centered at 3316.7 cm^{-1} and the formation of Si-O-Si bonding as witnessed from a band at 1117.4 cm^{-1} [Vejayakumaran et al., 2008], confirm the APTMS grafting reaction with RF clusters, as shown in Figure 4.7. Figure 4.8 shows mechanism for the incorporation of APTMS into RF clusters, which proposes the reaction between the hydroxyl groups on surface of RF clusters and the trimethoxyl group of APTMS.
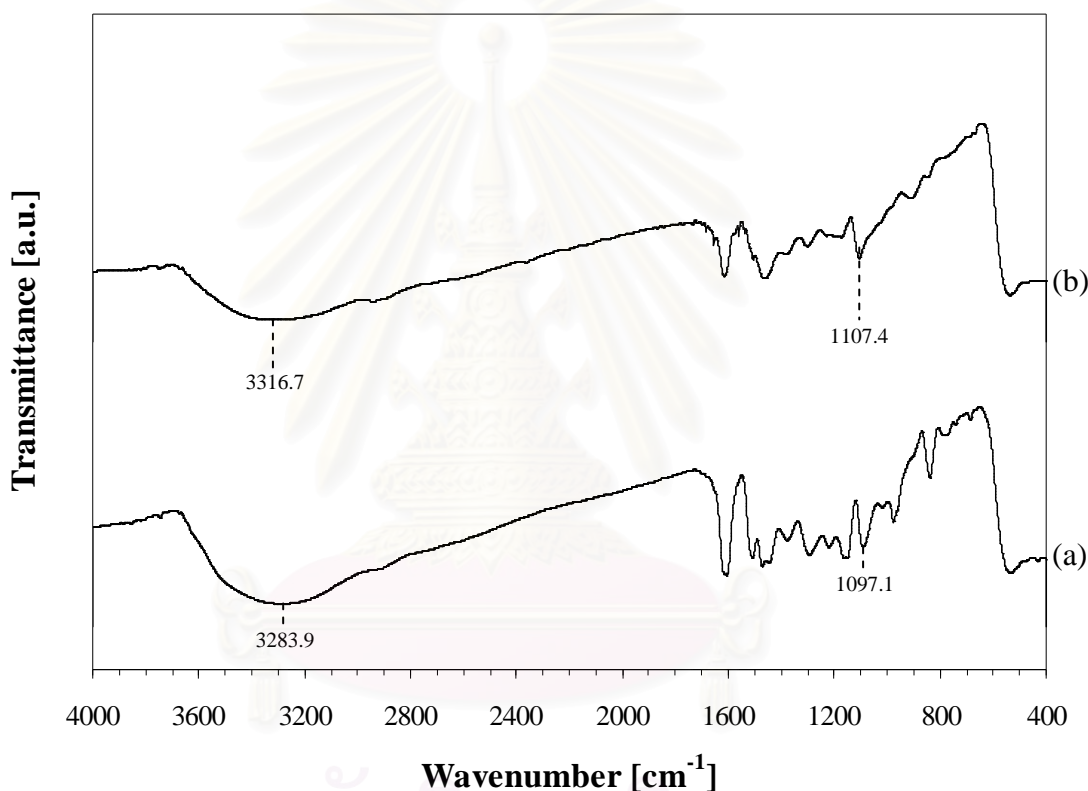
Figure 4.7   FT-IR spectra of: (a) RF gel and (b) Silica/RF gel.
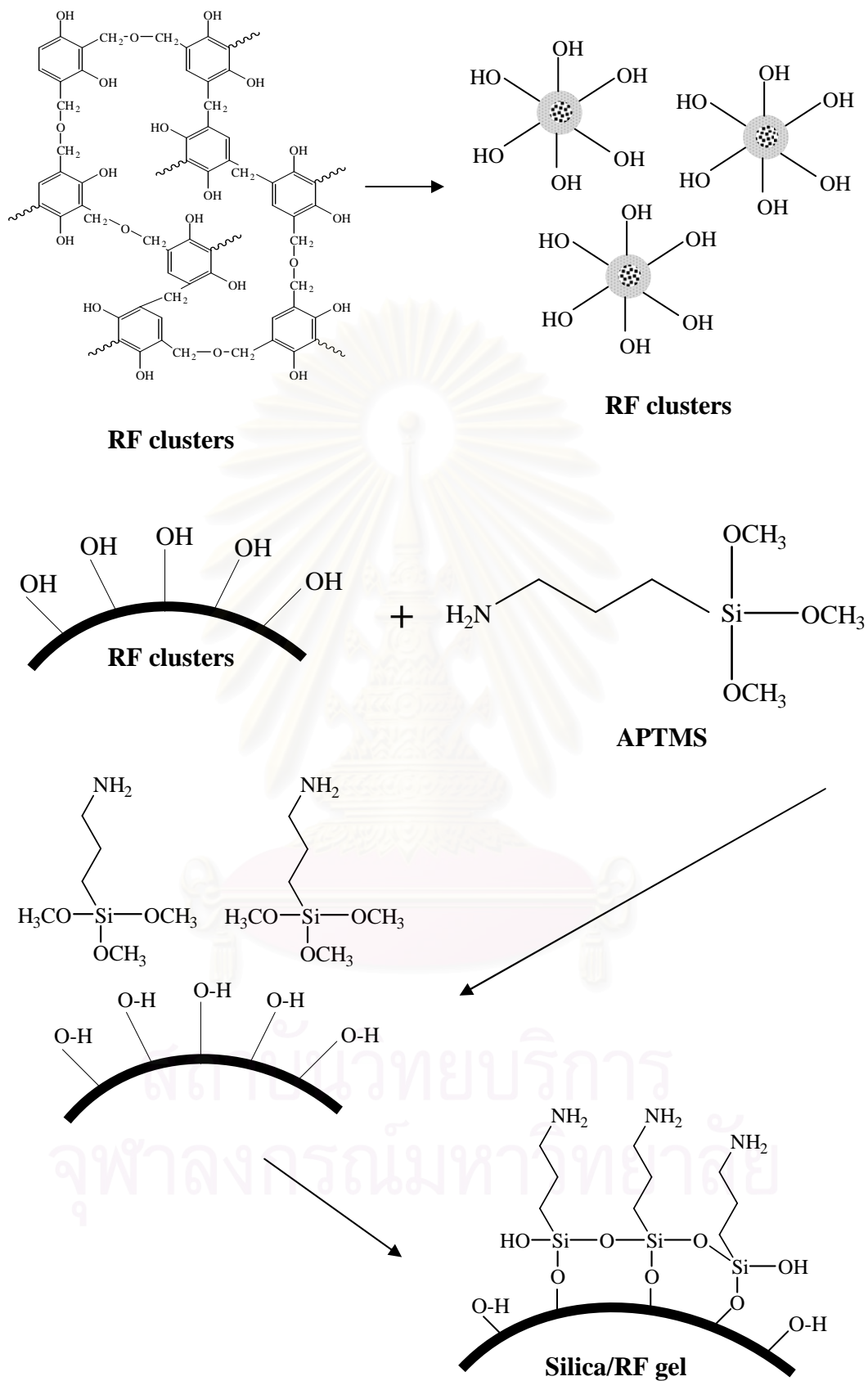
Figure 4.8 Idealized mechanism for the incorporation of APTMS into RF clusters.

4.3 Effect of Acetic Acid Addition on RF Solution

In this section, RF solution was prepared with the ratio of resorcinol-to–formaldehyde (R/F), resorcinol-to-water (R/W) and sodium carbonate-to-water (C/W) at 0.5 mol/mol, 0.15 mol/mol and 10 mol/m^3, respectively. The mixture was stirred for 15 min at controlled temperature of 30°C during gel formation. After aging the RF solution (e.g. kept for 1 or 30 h), 5 ml of acetic acid was added to the mixture.

Figure 4.9 shows light scattering of laser beam through RF mixture before and after the addition of acetic acid into the aged RF solution. It can be seen that the addition of acetic acid into the RF solution results in the decrease in laser beam scattering. It also makes the RF mixture faded in color. The effect of acetic acid is further investigated from FT-IR spectra shown in Figure 4.10.

Before adding acetic acid   After adding acetic acid

(a)

Before adding acetic acid   After adding acetic acid

(b)
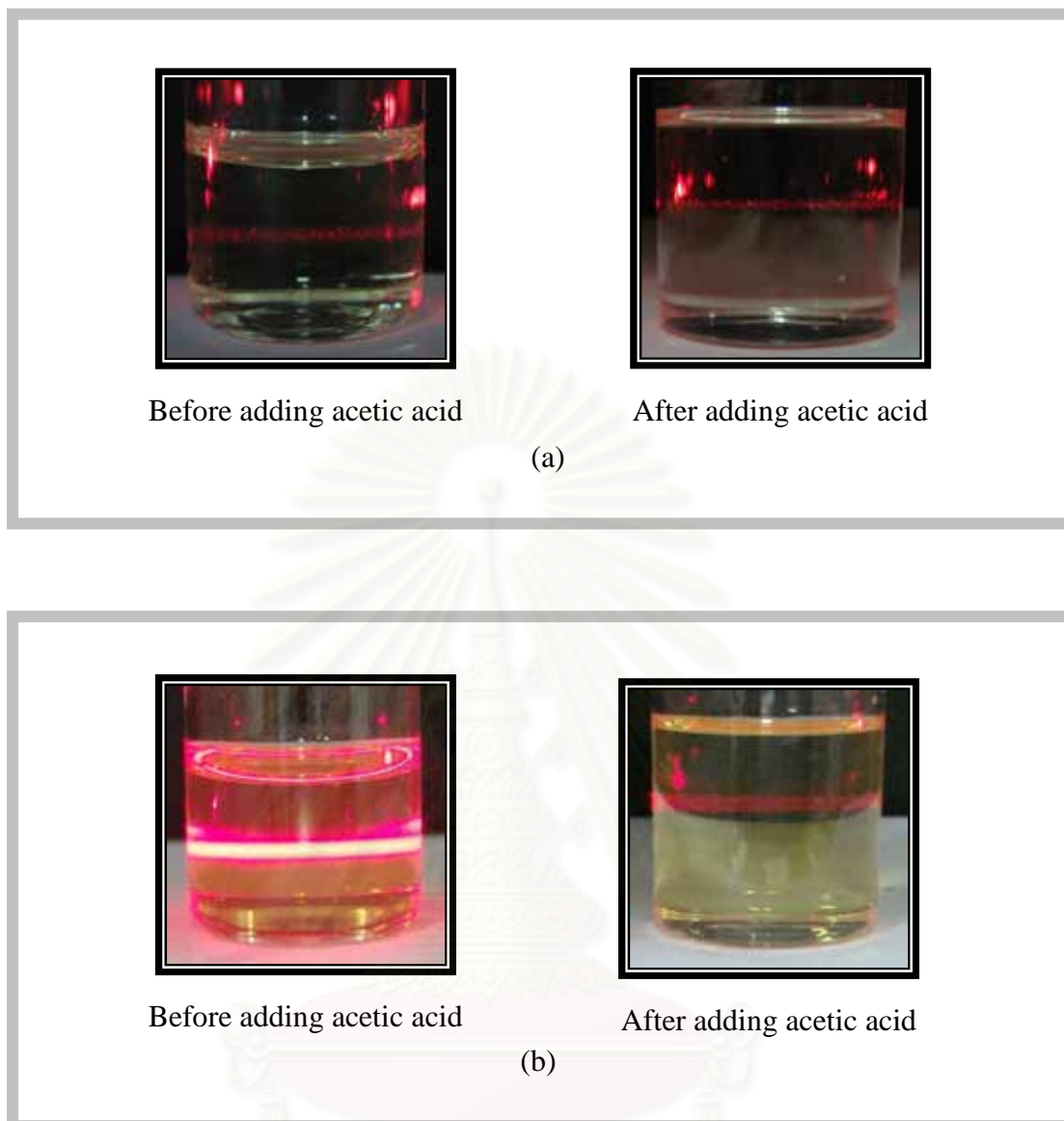
Figure 4.9 Light scattering of RF solution aged for 1 h (a) and 30 h (b), before and after adding acetic acid.

According to Figure 4.10, the bands around 2913.1, 1470.3, 1227.1 and 1112.0 cm^{-1}, which are assigned to the methylene bridge (-CH$_2$-) and methylene ether bridge (-CH$_2$-O-CH$_2$-) [Ida and Matjaz, 2005] can not be observed after the addition of acetic acid. On the contrary, the oxygenated functional group (C=O) is detected at 1708.3 cm^{-1} [Ida and Matjaz, 2005]. Moreover, the absorption bands at 3217.8 and 1011.3 cm^{-1} attributing to OH stretching and aliphatic hydroxyl group [Ida and Matjaz, 2005], respectively are observed. The bands around 1650.3 and 1508.4 cm^{-1} corresponding to C=C in aromatic ring [Ida and Matjaz, 2005], can still confirm the existence of the resorcinol group in the RF mixture. According to all signals has discussed above, it is suggested that the acetic acid has damaging effect on the network of RF clusters.
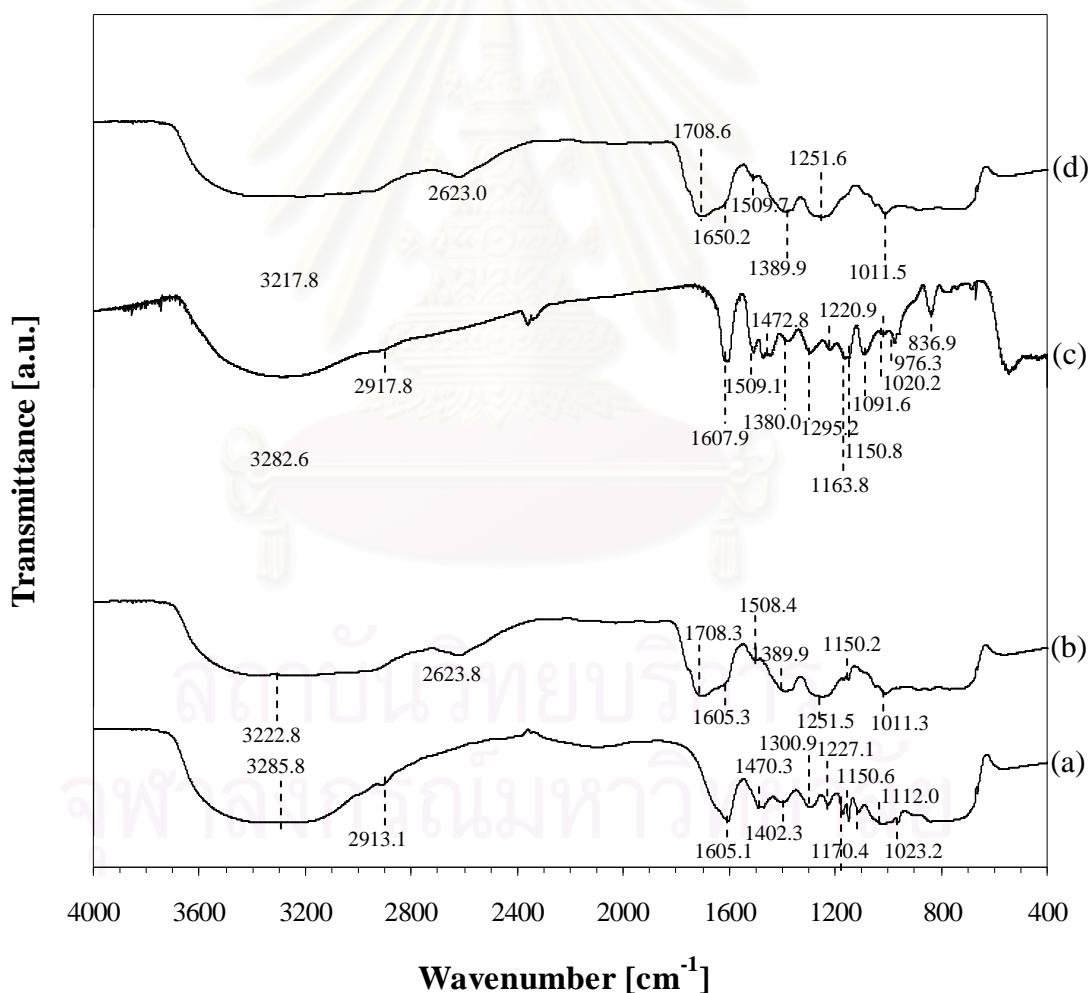
Figure 4.10 FT-IR spectra of RF-solution aged for 1 h, before (a) and after (b) adding acetic acid comparing with that of RF solution aged for 30 h, before (c) and after (d) adding acetic acid.

Figure 4.11 shows FT-IR spectra of the RF mixture after adding acetic acid and reforming into gel. Both spectra are similar to that of the RF gel before adding acetic acid. Details of the FT-IR absorption bands are listed in Table 4.4. As mentioned earlier, acetic acid damages methylene ($-CH_2-$) and methylene ether ($-CH_2-O-CH_2-$) bridges of the RF clusters, forming carboxyl group ($-COOH$) attaching to benzene ring. It is suggested that hydroxymethyl ($-CH_2OH$) is later replaced the carboxyl groups at 2, 4, 6 position of the benzene ring, which enables the formation of gel network. After, the transformation from solution to gel is completed, the crosslink between resorcinol and formaldehyde is restored (or partially restored). Methylene ($-CH_2-$) and methylene ether ($-CH_2-O-CH_2-$) bridges are established between two aromatic rings once again. The proposed mechanism is shown in Figure 4.12.
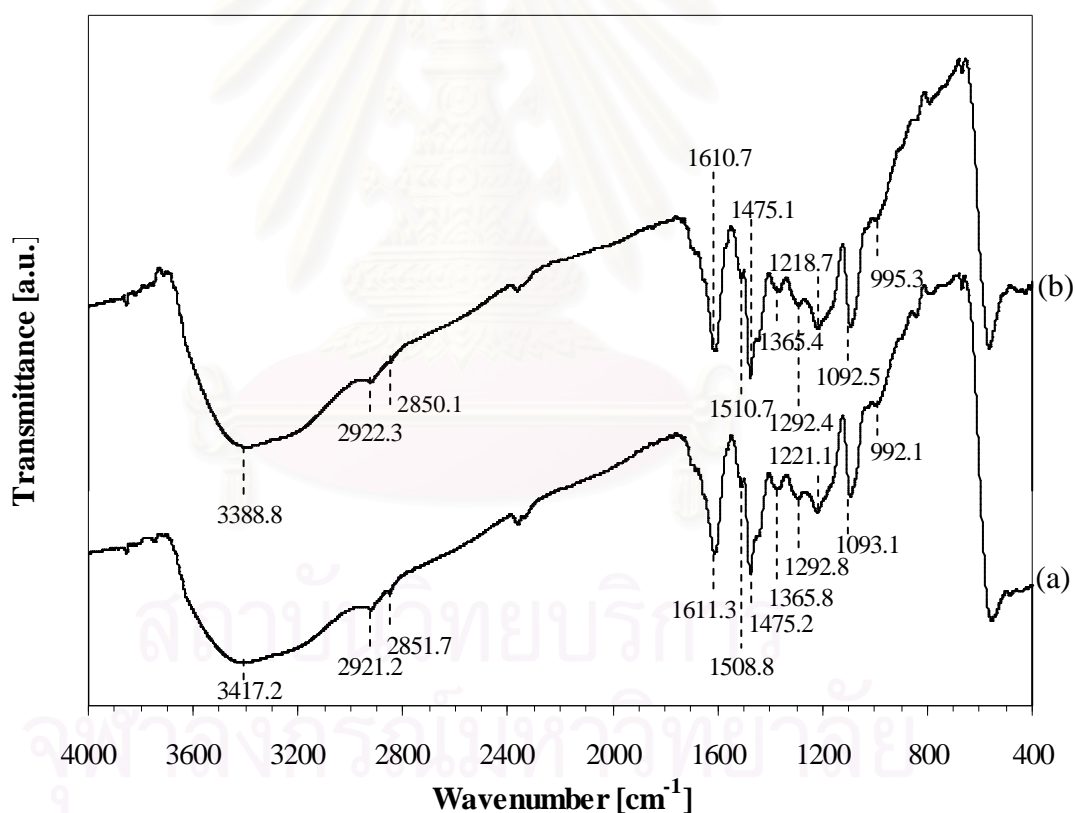
Figure 4.11 FT-IR spectra of RF-solution aged for 1 h (a) and 30 h (b), after adding acetic acid at gel and forming into gel again.

Table 4.4 Assignments of FTIR absorption bands of the RF gel reformed after acetic acid was added.

IR bands [cm^{-1}]		Functional groups
RF 1 h	**RF 30 h**	
3222.8	3217.3	OH stretching[2]
2921.2	2922.3	in phase stretching vibration of -CH$_2$- alkane[2]
2851.7	2850.1	-CH$_2$- methylene bridge[2]
1708.3	1708	C=O stretching from unreaction formaldehyde, carbonyl generated when furfural underwent a ring-opening reaction under acid condition [3].
1650.3	1650.2	C=C aromatic ring[2]
1508.4	1509.7	C=C aromatic ring[2]
1389.9	1389.9	OH in plane[2]
1251.5	1251.6	asymmetric stretch of phenolic (C-C-OH)[2]
1221.1	1218.7	C-O-C stretching vibrations of methylene ether bridges between resorcinol molecules[1]
1168.8	-	CH aromatic, in plane[2]
1150.2	-	C-O stretching[2]
-	1048.8	single bond C-O stretching vibrations of –CH$_2$OH group[2]
1011.3	1011.5	aliphatic hydroxyl[2]
963.0		2,4- substituted benzene ring[2]
885.0	884.8	C-H out of plane[2]
845.2	-	C-H out of plane[2]

[1] Liang et al., 2000; [2] Poljansek and Krajnc, 2005 and [3] Long et al., 2008
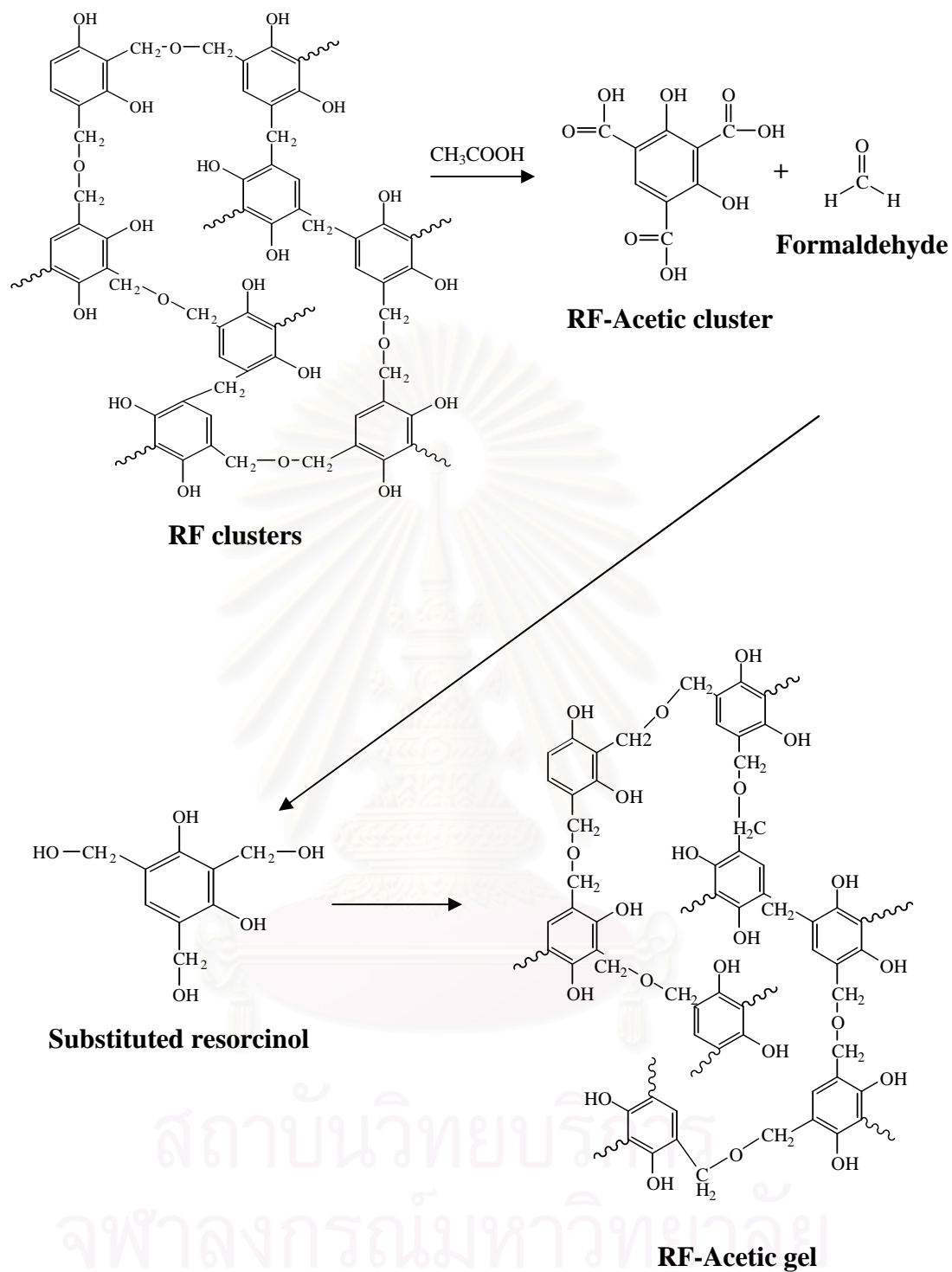
Figure 4.12 Proposed mechanism for the effect of acetic acid on RF gel.

4.4 Effect of Amount of Acetic Acid Added into Silica/RF Mixture

In this section, RF solution was prepared with the ratios of resorcinol-to-formaldehyde (R/F), resorcinol-to-water (R/W) and sodium carbonate-to-water (C/W) of 0.5 mol/mol, 0.15 mol/mol and 10 mol/m^3, respectively. The solution was stirred for 15 min before aging in the controlled temperature of 30°C for 1 or 30 h. After aging, acetic acid was added in the amount varied from 1, 3, 5, 7, 9 and 11 ml together with silica precursor (APTMS) (fixed Si/C = 0.05 mol/mol) with continuous stirring at -10°C, until gelation occurred. Then, the silica/RF gel was aged at 30°C for 3 days.

Table 4.5 and Figure 4.13 show the results of gelation time for silica/RF mixture. The gelation time is affected by increased amount of acetic acid. The RF solution aged for 1 h results in longer gelation time than the RF solution aged for 30 h because the hydrogel network is formed in greater extent along the increasing aging time of the RF solution via sol-gel polycondensation. When APTMS is added to the RF mixture that has been nearly completely gelled, the mixture solidifies rapidly (i.e. the gelation time for silica/RF mixture is extremely short). In order to increase gelation time for silica/RF gel, acetic acid can slow down the reaction between RF solution and APTMS, which consequently lead to homogenous gel. The result is shown in Figure 4.14.

Table 4.5 Synthesis conditions for silica/RF Mixture with the addition of acetic acid.

Sample ID	Aging time for RF solution (h)	Amount of acetic acid (ml)	APTMS (ml)	Gelation time
R1-1	1	1	1.36	10 min
R1-2	1	3	2.22	20 min
R1-3	1	5	3.07	25 min
R1-4	1	7	3.93	36 min
R1-5	1	9	4.78	1.30 h
R1-6	1	11	5.64	8 h
R30-1	30	1	1.36	3 sec
R30-2	30	3	2.22	4 sec
R30-3	30	5	3.07	3 min
R30-4	30	7	3.93	21 min
R30-5	30	9	4.78	1.28 h
R30-6	30	11	5.64	7.30 h
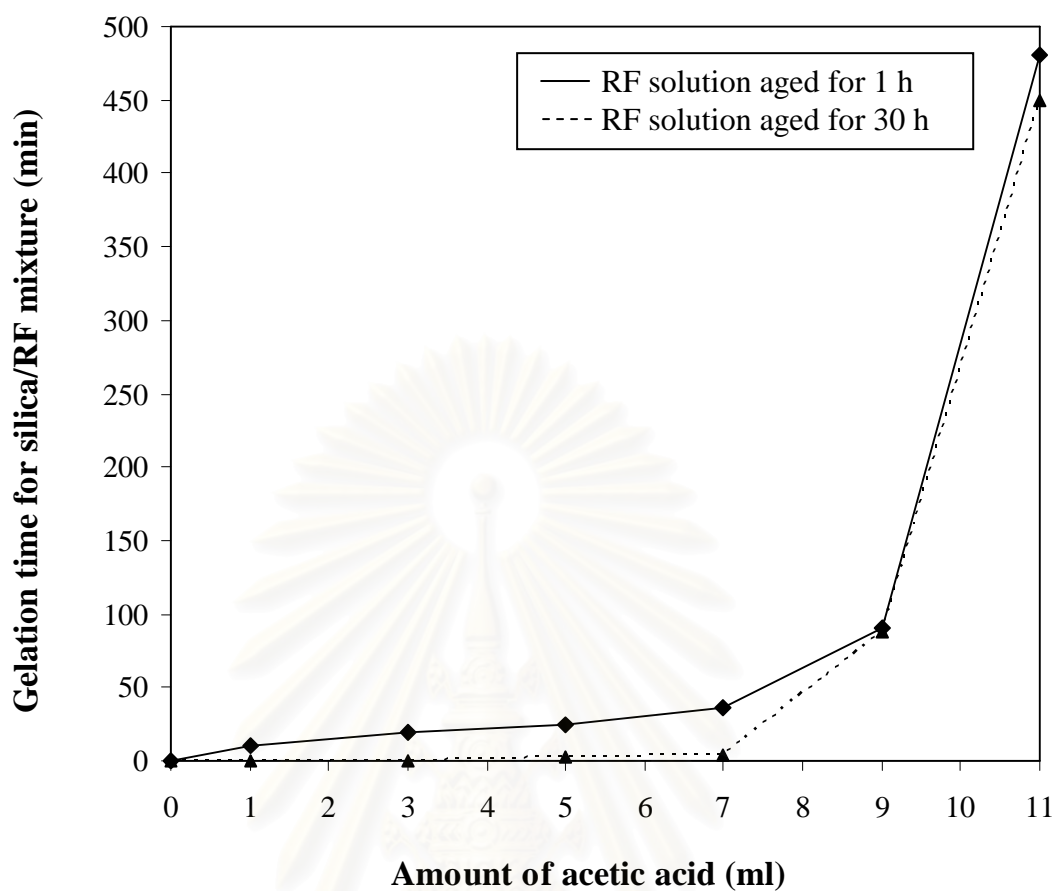
Figure 4.13   Relation ship between amount acetic acid added and gelation time of silica/RF mixture.
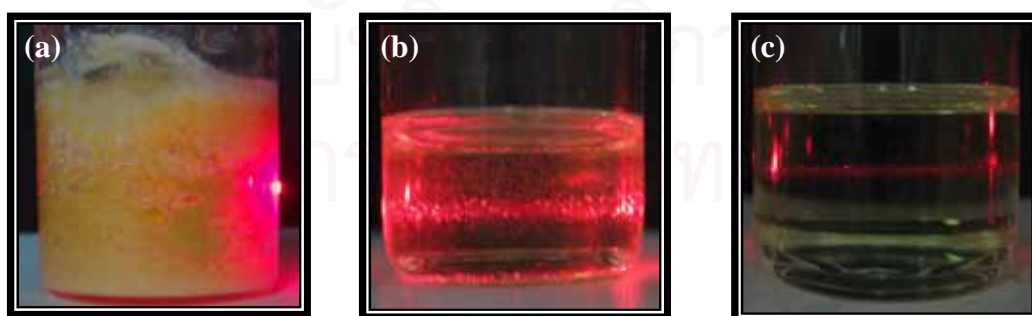
Figure 4.14   Light scattering of silica/RF mixture contain various amount of acetic acid: (a) 0 ml, (b) 1 ml and (c) 5 ml, after adding APTMS.

After aging of the silica/RF gel at room temperature for 3 days, the obtained solid product was crushed into powder and dried in oven at 110°C for 16 h. Then, the dried silica/RF gel was converted into silica/carbon composite by pyrolysis at 250°C for 2 h and 750°C for 4 h under continuous flow of nitrogen.

Table 4.6 shows BET surface area and pore diameter of pyrolysis sample with Si/C molar ratio of 0.05 at various amount of acetic acid. From the results, it is found that the surface area is decreased as more acetic acid is added. For the gel with small volume of acetic acid, silica/carbon composite is highly porous, in which the pore diameter is small. In contrast, if large volume of acetic acid is added, the pyrolyzed sample has low surface area and becomes nonporous. This can be explained by the mechanism that the low condensation reaction rate and long gelation time created a less cross-linked structure consisting of large nanoparticles that collapse during drying and pyrolysis. The result conforms with the report by Yamamoto et al., 2001, shown in Figure 4.15.

Table 4.6 Surface area and average pore diameter of silica/carbon composite after pyrolysis.

Sample	Surface area (m^2/g)	Average pore diameter (Å)
R1-1	291.4	76.3
R1-2	67.7	55.5
R1-3	23.1	486.8
R1-4	23.3	490.2
R1-5	6.5	no pore
R1-6	2.0	no pore

As the sol-gel polycondensation of silica/RF gel transition proceeds, colloidal particles can behave as Brownian particles as long as the mixture has not solidified. Then, the colloidal particles form a network structure which is still not percolated yet. Their dynamics are also governed by concentration fluctuation associated with the translational motion of the network. In Figure 4.15, it is suggested that size of the particles forming the cross-linked structure of silica/RF mixture tends to decrease with decreasing amount acetic acid. On the contrary, size of the particles tend to increase with increasing amount of acetic acid. Hence, increasing volume of acetic acid in the silica/RF solution results in increasing gelation time of silica/RF gel. The experiment conforms to the report by Yamamoto et al., (2001).
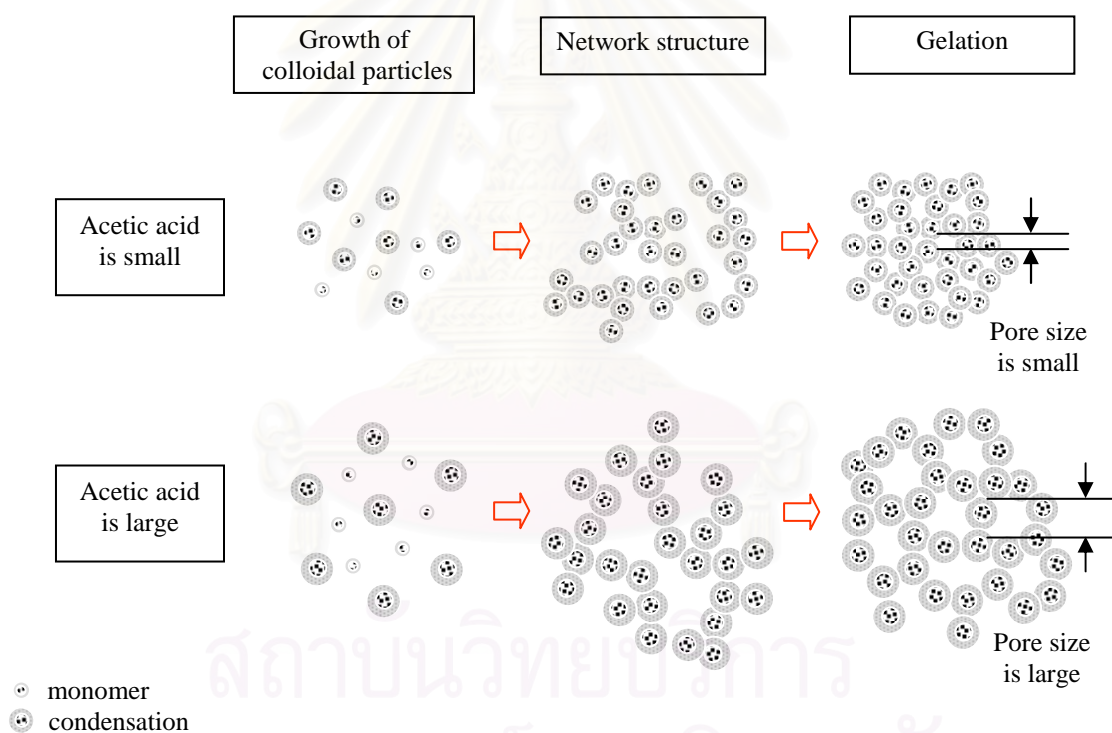
Figure 4.15 Images for structure formation during the sol-gel transition [Yamamoto et al., 2001].

4.5 Effect of Type of Silica Precursor

4.5.1 Effect of Silica Precursor without the presence of Acetic Acid

In this work, two types of silica precursor, i.e. APTMS and MPTMS were investigated. The RF solution was prepared by the same procedure described earlier. After aging the RF solution for 1 h, silica precursor (APTMS or MPTMS) was added into the RF solution under continuous stirring at -10°C (fixed Si/C = 0.05 mol/mol), until gelation occurred. Then, the silica/RF gel was aged at 30°C for 3 days.

Table 4.7 and Figure 4.16 show gelation time and photograph of silica/RF mixture after the silica precursor was added to the RF solution for 15 min, respectively. It can be observed that RF solution solidified almost as soon as APTMS was added to the solution. On the contrary, the silica/RF mixture with MPTMS as silica precursor form into gel after 22 h.

Table 4.7 Synthesis conditions of silica/RF gel using different type of silica precursor.

Type of silica precursor	Aging time for RF solution (h)	Amount of acetic acid (ml)	Silica Precursor (ml)	Gelation time
APTMS	1	-	0.94	1 sec
MPTMS	1	-	1.00	22 h
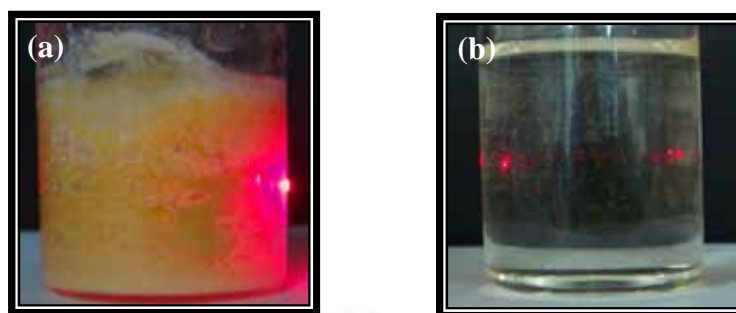
Figure 4.16   Light scattering of silica/RF mixture formed by using: APTMS (a) and MPTMS (b) as silica precursor.

Figure 4.17 shows FT-IR spectra of silica/RF gel, which uses APTMS or MPTMS as precursor of silica. Both samples exhibit absorption bands at 1110–1095 cm^{-1} indicating the presence of Si-O-Si, Si-O-C and C-O-C, at 950–910 cm^{-1} indicating the presence of Si-OH bonds [Li et al., 2009]. The peaks at 2860-2848 cm^{-1} associating with Si-O-CH$_3$ [Brito et al., 2002] can not be observed in either sample. These results indicate that both APTMS and MPTMS react to form silica/RF gel completely. The details for the absorption bands associated with functional groups of APTMS, MPTMS and silica/RF gel are shown in Table 4.8
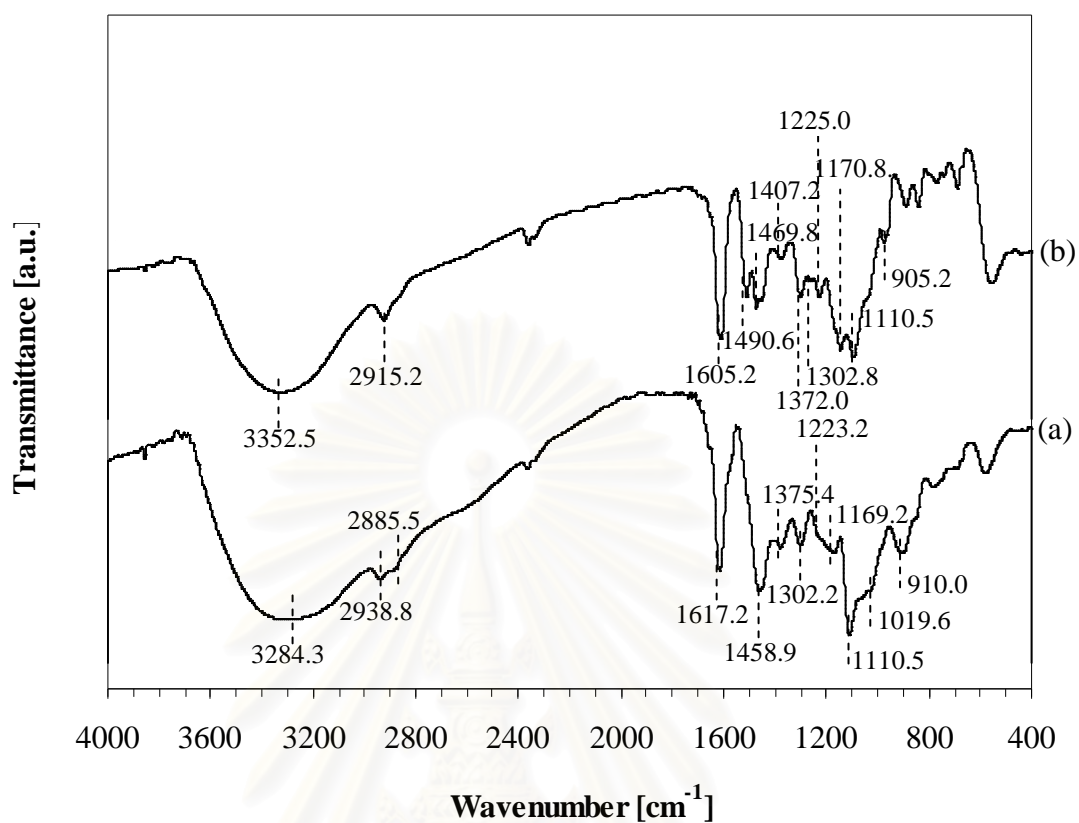
Figure 4.17 FT-IR spectra of silica/RF gel, which uses APTMS (a) and MPTMS (b) as precursor for silica.

Table 4.8 Assignments of FTIR absorption bands of the silica/RF gels using either APTMS or MPTMS as precursor of silica.

IR bands [cm^{-1}]		Functional groups
APTMS	MPTMS	
3284.3	3352.5	NH$_2$, OH stretch[4]
2938.8	2926.9	in phase stretching vibration of -CH$_2$- alkane
2885.5	-	-CH$_2$- methylene bridge[3]
-	2848.4	-SiOCH$_3$ stretching[7]
1617.2	1605.2	C=C aromatic ring[3]
-	1490.6	C=C aromatic ring[3]
1458.9	1469.8	-CH$_2$- methylene bridge[3]
-	1407.2	OH in plane[3]
1375.4	1372.0	C-O stretching[2]
1302.2	1302.8	C-O stretching[2]
1223.2	1225.0	C-O-C stretching vibrations of methylene ether bridges between resorcinol molecules[1]
1169.2	1170.8	CH aromatic, in-plane[3]
1110.5	1110.5	C-O-C stretching vibrations of methylene ether bridges between resorcinol molecules[1], Si-O-Si stretching and Si-O-C stretching[4,5]
-	1058.0	-SiOCH$_3$ stretching[7]
1019.6	1014.2	aliphatic hydroxyl[3]
-	963.9	C-H out of plane[3]
910.0	905.2	-Si-OH[5]

[1] Liang et al., 2000; [2] Fuente et al., 2003; [3] Ida and Matjaz, 2005;

[4] Vejayakumaran et al., 2008; [5] Li et al., 2009; [6] Hruby and Shanks, 2009; and

[7] Brito et al., 2002

Since the gelation of the silica/RF mixture using APTMS as silica precursor is rapid, we can not study the structure formation during the period of gelation. On the other hand, long gelation time achieved by MPTMS enables us to study structure formation of the silica/RF gel. Figure 4.18 shows FT-IR spectra of silica/RF gel mixture that uses MPTMS as silica precursor, after aging for various periods of time. It should be noted that the mixture turns into gel (by visual observation) after 1 day of aging. The silica/RF solution in Figure 4.18(a) shows the evidences for the stretching of $-SiOCH_3$ at 2860-2848 and 1058 cm^{-1}, and Si-OH at 905.2 cm^{-1}. After aging for 10 h, the absorption spectra for the stretching of $-SiOCH_3$ and C-C-OH at 2860-2848, 1058 and 1257.7 cm^{-1} [Brito et al., 2002] are decreased, but the signals attributing for Si-O-Si, Si-O-C and Si-OH stretching at 1110.9 and 904.0 cm^{-1}, respectively are detected. These results indicate that the trimethoxyl groups of MPTMS is being adsorbed on (or reacted with) the OH functional group of RF clusters. After the silica/RF solution completely transforms to gel after 3 days, according to Figure 4.18(d), the band at 2848.4, 1058.0 and 1023.0 cm^{-1}, corresponding to the $-SiOCH_3$ and C-C-OH bonding are disappeared.
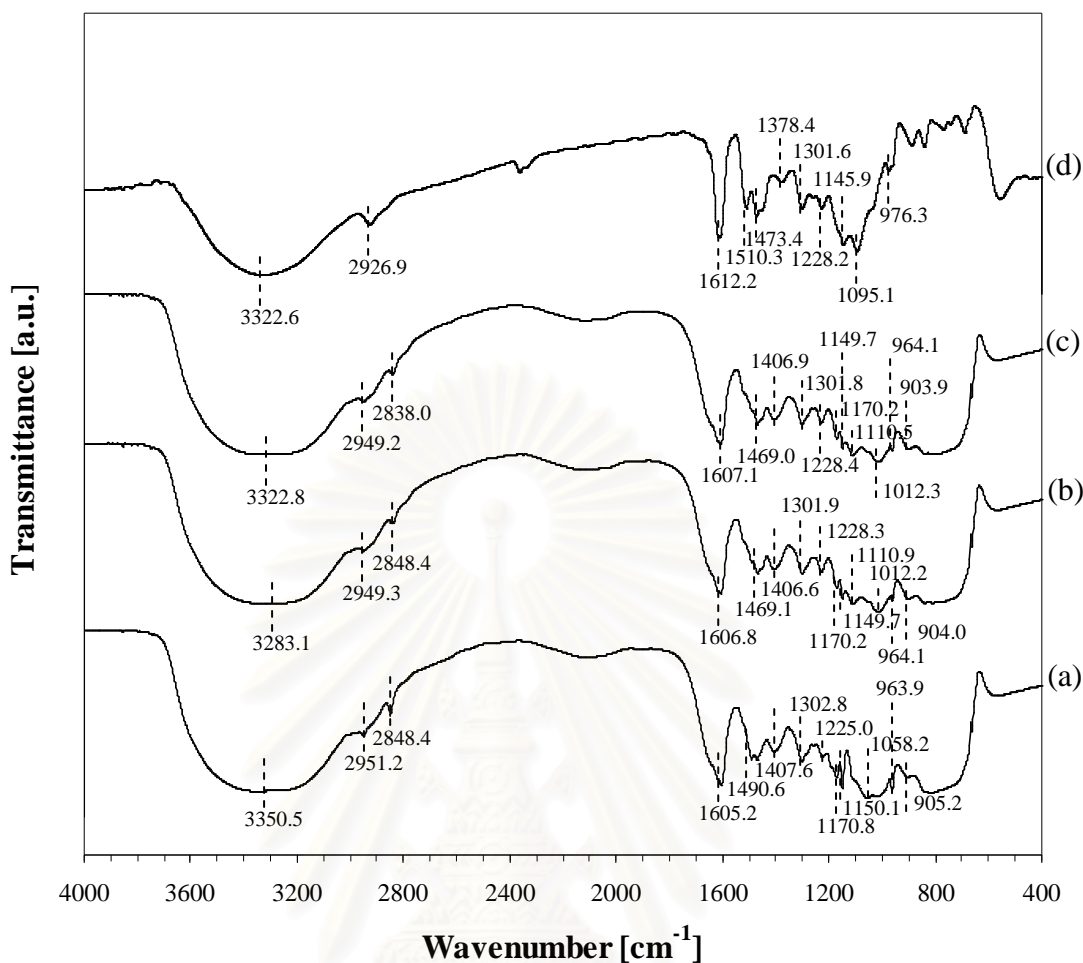
Figure 4.18 FT-IR spectra of silica/RF mixture that uses MPTMS as precursor for silica, after aging for: (a) 0 h, (b) 10 h, (c) 1 day and (d) 3 days.

Figure 4.19 shows mechanism for the incorporation of MPTMS into RF clusters, which indicates the reaction between the hydroxyl (OH) groups on the surface of RF clusters and the trimethoxyl silane ($-SiOCH_3$) groups of MPTMS. This is in agreement with the FT-IR bands corresponding to OH stretching at 3312.9 cm^{-1} and trimethoxyl silane ($-SiOCH_3$) at 2848.4 and 1058.0 cm^{-1}. Then, the crosslinking by trimethoxyl silane ($-SiOCH_3$) of two molecules results in the formation of Si-O-Si bonding as observed from the FT-IR band at 1110.5 cm^{-1} [Fiolli et al., 2008; Hruby and Shanks, 2009; Ida and Matjaz, 2005 and Brito et al., 2002].
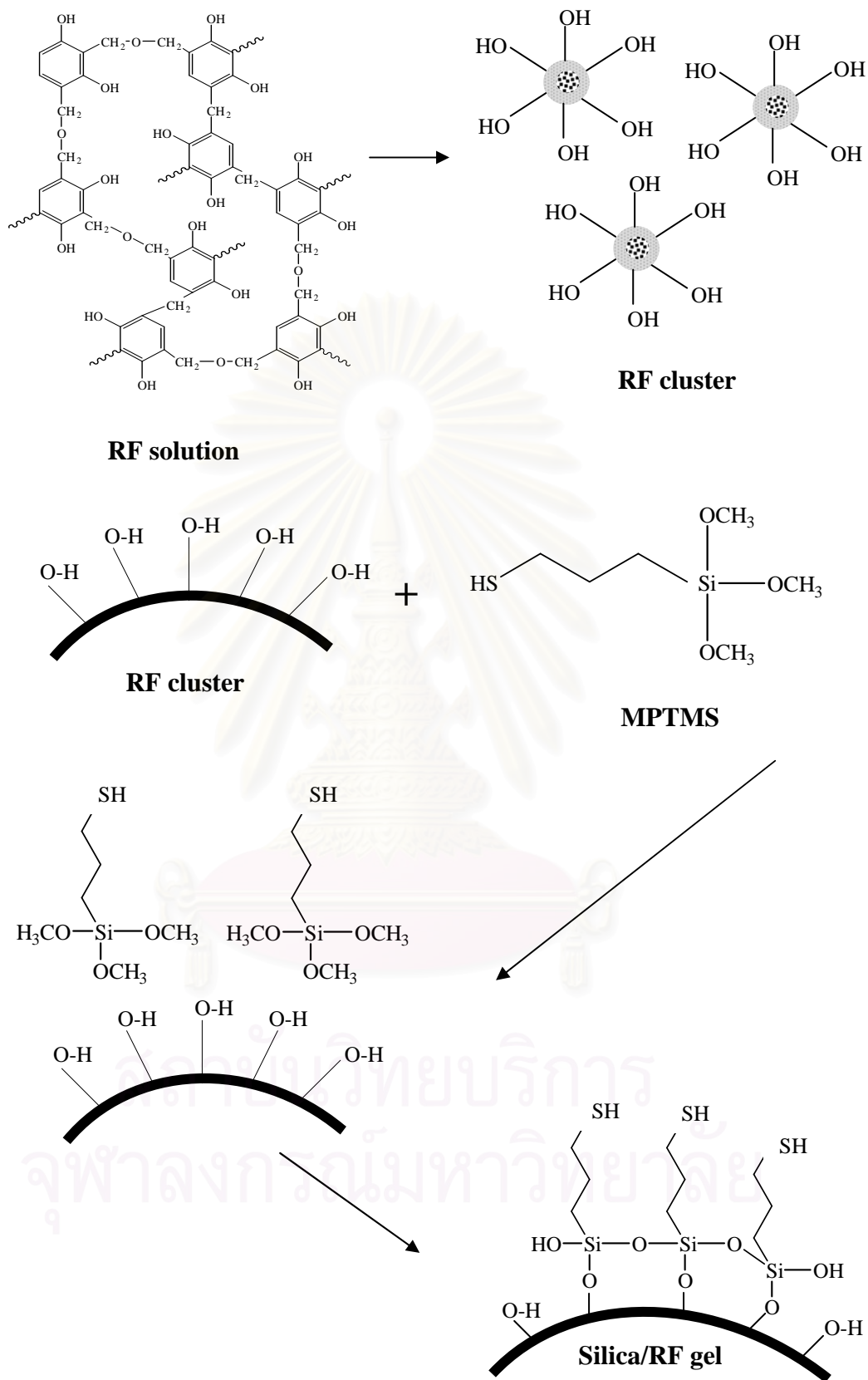
Figure 4.19 Idealized mechanism for the incorporated MPTMS into RF clusters.

4.5.2 Effect of Silica Precursor with the Presence of Acetic Acid

In this part, the effect of acetic acid on the silica/RF gel formed with either APTMS or MPTMS was investigated. Acetic acid was added in to the aged RF solution before adding silica precursor (APTMS or MPTMS) under continuous stirring at -10°C. The silica/RF gel was aged at 30°C for 3 days. Details of the synthesis condition are shown in Table 4.9.

Table 4.9 Synthesis conditions of silica/RF solution at various kinds of silica precursor.

Sample	Aging time for RF solution (h)	Amount of acetic acid (ml)	Silica precursor (ml)	Gelation time
RF-Ac1-APTMS	1	1	1.36	10 min
RF-Ac1-MPTMS	1	1	1.47	72 h

Comparing to the results shown in Table 4.7, it can be seen that addition of acetic acid prolongs the gelation time of the silica/RF mixture, regardless of the type of silica precursor. Nevertheless, it is shown that MPTMS is less reactive than APTMS.

According to Figure 4.20 and Table 4.9, which show photograph of silica/RF mixture and gelation time, respectively, it can be observed that RF solution added with APTMS forms into gel within 10 min. On the other hand, the silica/RF solution which uses MPTMS as silica precursor, forms into gel at 72 h.
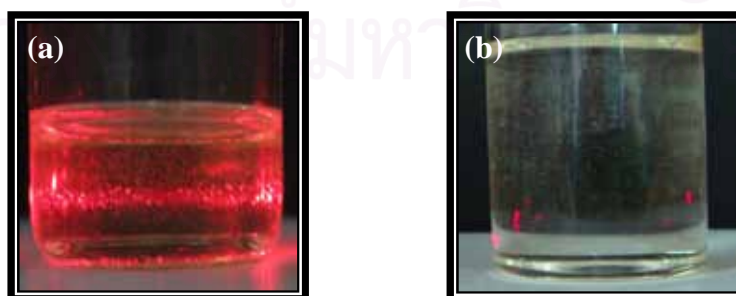
Figure 4.20 Light scattering of silica/RF solution added acetic acid at various kinds of silica precursor are used: (a) APTMS and (b) MPTMS.

The FT-IR signal from silica/RF gel that uses APTMS as silica precursor (Figure 4.21(a)) can be attributed to stretching of $-SiOCH_3$, Si-O-Si, Si-O-C and Si-OH at 2834.8, 1113.5 and 908.0 cm^{-1}, respectively. The oxygenated functional group (C=O) generated and C=O stretching of formaldehyde appears at 1704.5 cm^{-1}. After aging for 1 day, the silica/RF mixture started turning into gel. The FT-IR spectrum in Figure 4.21(b) shows that the absorption band attributed to $-SiOCH_3$ at 2834.8 cm^{-1} is disappearing. Then, after 3 days, the silica/RF mixture transformed to gel completely. The FT-IR signal at 1704.5 cm^{-1} corresponding to C=O stretching of formaldehyde disappears (see Figure 4.21(c)). The results suggest the crosslinking between two resorcinol molecules by formaldehyde.
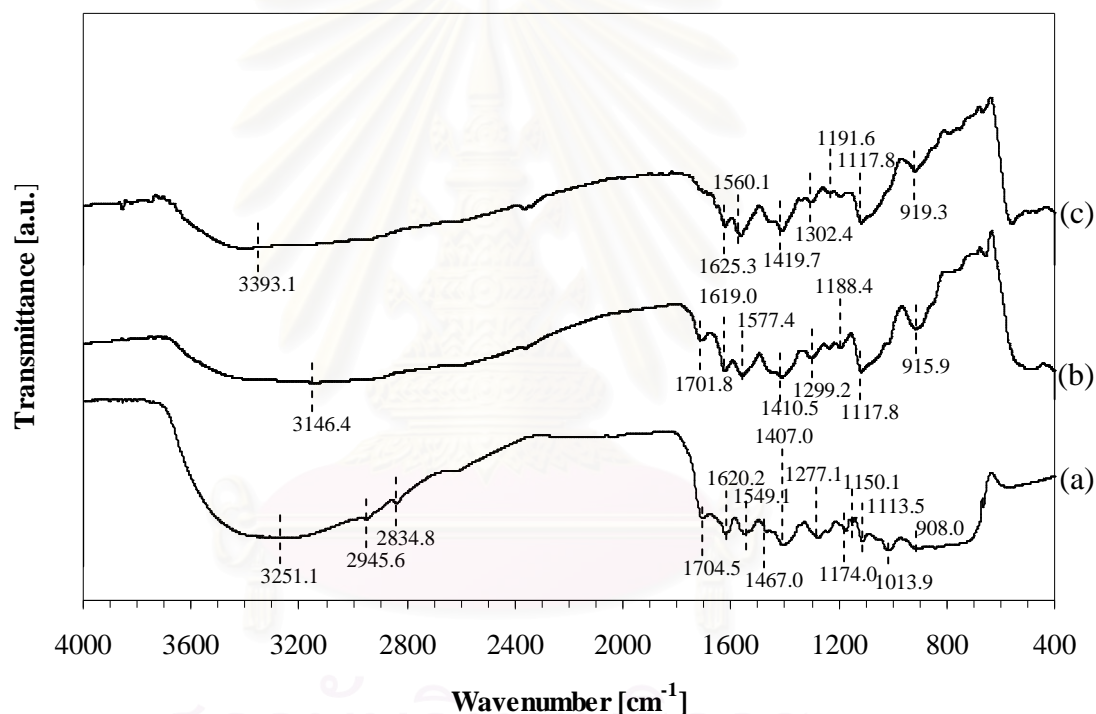
Figure 4.21 FT-IR spectra of silica/RF gel, which was formed by adding APTMS after the addition of acetic acid and aged for: (a) 0 h, (b) 1 day and (c) 3 days.

The FT-IR signal from silica/RF gel that uses MPTMS as silica precursor (Figure 4.22(a)) can be attributed to stretching of –SiOCH$_3$, Si-O-Si, Si-O-C and Si-OH at 2839.3, 1108.5 and 905.3 cm^{-1}, respectively. The oxygenated functional group (C=O) generated and C=O stretching of formaldehyde appears at 1708.2 cm^{-1}. After aging for 1 day, the silica/RF mixture started turning into gel. The FT-IR spectrum in Figure 4.22(b) shows that the absorption band attributed to –SiOCH$_3$ at 2839.3 cm^{-1} is disappearing. Then, after 3 days, the silica/RF mixture transformed to gel completely. The FT-IR signal at 1708.2 cm^{-1} corresponding to C=O stretching of formaldehyde disappears (see Figure 4.22(c)). The results suggest the crosslinking between two resorcinol molecules by formaldehyde.
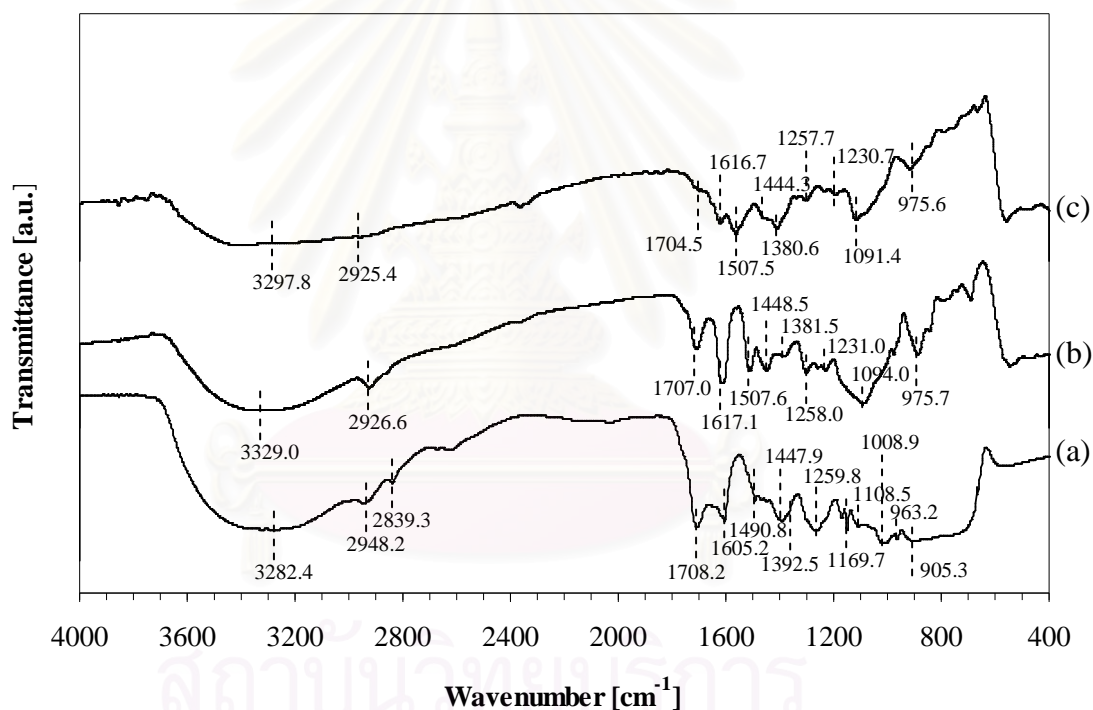
Figure 4.22 FT-IR spectra of silica/RF gel, which was formed by adding MPTMS after the addition of acetic acid and aged for: (a) 0 h, (b) 1 day and (c) 3 days.

All FT-IR bands that have been proposed to associate with the functional groups of silica/RF gel formed by using APTMS and MPTMS as precursor of silica, are shown in Table 4.10 and 4.11, respectively.

Table 4.10 Assignments of FTIR absorption bands of the silica/RF gel, which was formed by adding APTMS in the presence of acetic acid.

IR bands [cm⁻¹]			Functional groups
Aged for 0 h	Aged 1 day	Aged for 3 days	
3251.1	3146.4	3393.1	NH$_2$, OH stretch [4]
2945.6	-	-	in phase stretching vibration of -CH$_2$- alkane[3]
2834.8	-	-	-SiOCH$_3$ stretching[7]
1704.5	1710.8	-	C=O stretching[3]
1620.2	1619.0	1625.3	C=C aromatic ring[3]
1549.1	1557.4	1560.1	C=C aromatic ring[3]
1467.0	-	-	-CH$_2$- methylene bridge[3]
1407.0	1410.5	1419.7	OH in plane[3]
1277.1	1299.2	1302.4	C-O stretching[2]
1174.0	1188.4	1191.6	CH aromatic, in-plane[3]
1150.1	-	-	C-O stretching[2]
1113.5	1117.8	1117.8	C-O-C stretching vibrations of methylene ether bridges between resorcinol molecules[1], Si-O-Si stretching and Si-O-C stretching[4,5]
908.0	915.9	919.3	Si-OH stretching[5,6]

[1] Liang et al., 2000; [2] Fuente et al., 2003; [3] Ida and Matjaz, 2005;
[4] Vejayakumaran et al., 2008; [5] Li et al., 2009; [6] Hruby and Shanks, 2009 and
[7] Brito et al., 2002

Table 4.11 Assignments of FTIR absorption bands of the silica/RF gel, which was formed by adding MPTMS in the presence of acetic acid.

IR bands [cm^{-1}]			Functional groups
Aged for 0 h	Aged 1 day	Aged for 3 days	
3282.4	3329.0	3297.8	OH stretch[4]
2948.2	2926.6	2925.4	in phase stretching vibration of -CH$_2$- alkane[3]
2839.3	-	-	-SiOCH$_3$ stretching[7]
1708.2	1707.0	1704.5-	C=O stretching[8]
1605.2	1617.1	1616.7	C=C aromatic ring[3]
1490.8	1507.6	1507.5	C=C aromatic ring[3]
1447.9	1448.5	1444.3	-CH$_2$- methylene bridge[3]
1392.5	1381.5	1380.6	OH in plane[3]
1259.8	1258.0	1257.7	C-C-OH[3]
1169.7	1231.0	1230.7	CH aromatic, in-plane[3]
1108.5	1094.0	1091.4	C-O-C stretching vibrations of methylene ether bridges between resorcinol molecules[1], Si-O-Si stretching and Si-O-C stretching[4,5]
1008.9	-	-	aliphatic hydroxyl[3]
963.2	975.7	975.6	C-H out of plane[3]
905.3	-	-	Si-OH[5]

[1] Liang et al., 2000; [2] Fuente et al., 2003; [3] Ida and Matjaz, 2005; [4] Vejayakumaran et al., 2008; [5] Li et al., 2009; [6] Hruby and Shanks, 2009; [7] Brito et al., 2002 and [8] Long et al., 2008

4.6 Effect of Aging Temperature for Silica/RF Gel

In this part, the effect of aging temperature for silica/RF gel is investigated. The silica/RF mixture was prepared by using APTMS as a precursor for silica (Si/C = 0.05 mol/mol). Acetic acid was also added to the RF solution, which had seen aged for 1 h. The aging of the silica/RF gel was conducted at 30, 50, 70°C for 3 days, of which the samples are denoted as R1-13, R1-15 and R1-17, respectively.

The obtained solid product was crushed into powder and dried in oven at 110°C for 16 h. After that the dried silica/RF gel was converted into silica/carbon composite by pyrolysis at 250°C for 2 h and 750°C for 4 h under continuous flow of nitrogen.

The influence of the aging temperature on the obtained silica/carbon composite is illustrated in Table 4.12. Increasing the temperature leads to significant reduction in surface area of the silica/carbon gel, which may relate to the problem in the formation of crosslinking polymer network in silica/RF gel. High temperature affects mobility of both molecules and clusters and may influence the rate of condensation. That is one of the most important step in gel formation.

Table 4.12 Surface area and average pore diameter of silica/carbon composite synthesized from silica/RF gel aged at various temperatures.

Sample	Aging temperature for silica/RF gel (°C)	Surface area (m^2/g)	Average pore diameter (Å)
R1-13	30	291.4	76.3
R1-15	50	283.6	56.4
R1-17	70	188.8	29.9

4.7 Results from the Carbothermal Reduction and Nitridation

In the carbothermal reduction and nitridation process, the silica/carbon composite was heated to 1450°C for 6 h under flow nitrogen and hydrogen. The obtained product was further calcined at 700°C for 10 h to remove excess carbon.

Figure 4.23 shows XRD analysis results of products after pyrolysis, nitridation and subsequently calcination of silica/RF gel prepared at different reaction temperature. It is formed that all calcined products are α-silicon carbide.
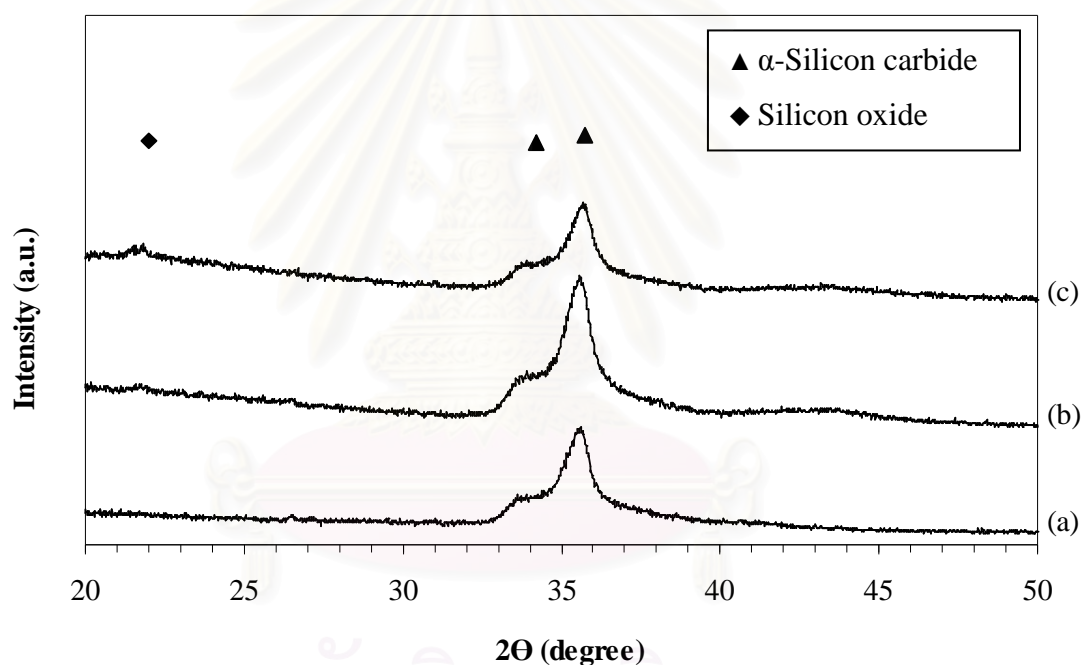
Figure 4.23   XRD patterns of products from the nitridation and subsequent calcination of pyrolyzed silica/RF gel synthesized at various temperatures: (a) 50°C, (b) 30°C and (c) -10°C using APTMS as silica precursor.

Table 4.13 shows BET surface area of silica/carbon composite after each step of the process (i.e. pyrolysis, carbothermal reduction and nitridation, and calcination). The resulting surface area of the product obtained after pyrolysis (e.g. 291.5 m^2/g for RF-AP-10) and after nitridation (e.g. 520.6 m^2/g for RF-AP-10) is increased because the reaction progresses toward the formation of α-silicon carbide. Surface area is decreased after calcination because product after either pyrolysis or nitridation still contains high content of carbon, which is a major source for porosity. The calcination remove the residual carbon and therefore results in dramatic drop in the surface area. Nevertheless, the results confirm that porous silicon carbide can be synthesized according to the process proposed in this research.

Table 4.13 Surface area of silica/carbon composite after different stage of reaction. The composite was prepared from silica/RF gel formed at various temperature.

Sample ID	Temperature for the synthesis of silica/RF gel (°C)	Surface area (m^2/g)		
		Pyrolysis	Nitridation	Calcination
RF-AP-50	50	360.2	1,294.1	70.0
RF-AP-30	30	325.8	1,781.8	54.5
RF-AP-10	-10	291.5	520.6	71.9
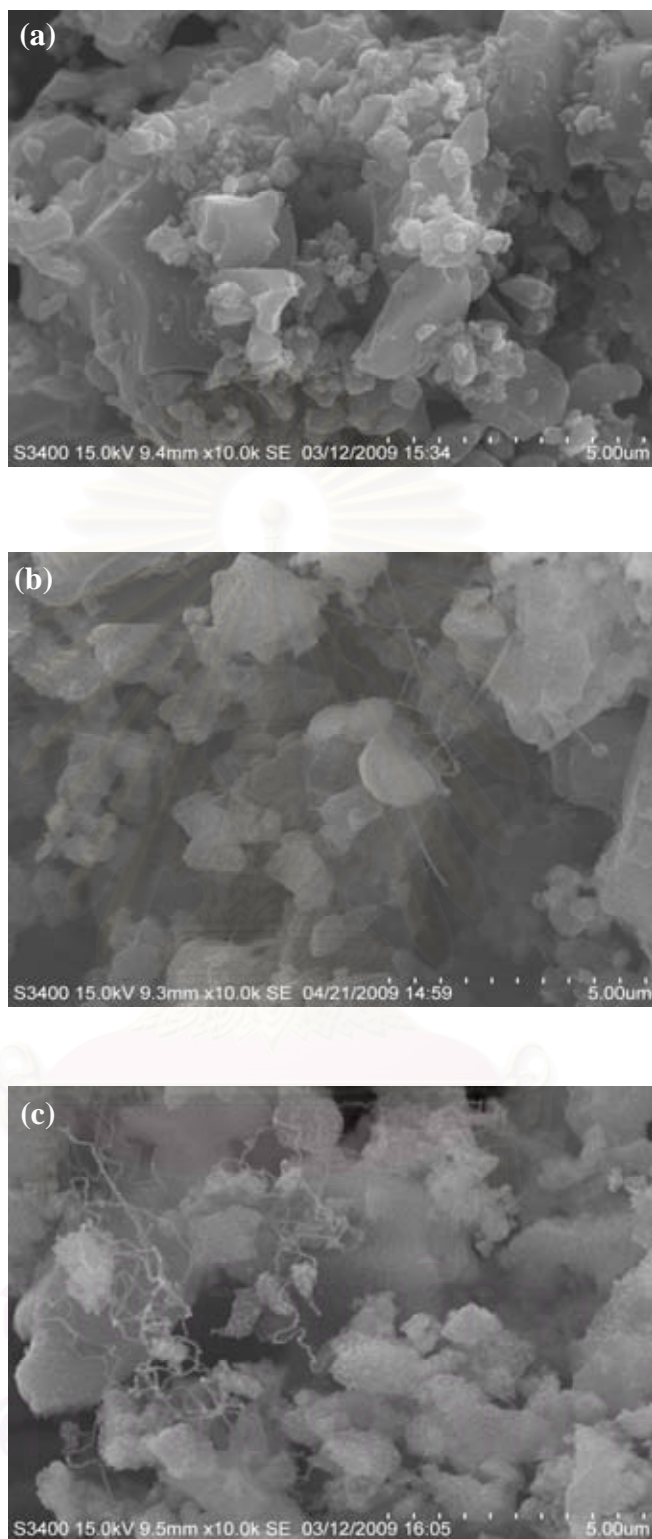
Figure 4.24   SEM micrographs of silica/carbon composite of RF-AP-10: (a) after pyrolysis, (b) after nitridation (c) after calcination.

Figure 4.25 is XRD analysis results of products from the nitridation and subsequent calcination of silica/carbon composite. The composites that were synthesized from RF solution aged for 1 h α-silicon nitride/silicon carbide composite. In contrast, aging of the RF solution for 30 h results in α-silicon carbide after pyrolysis, nitridation and calcination.
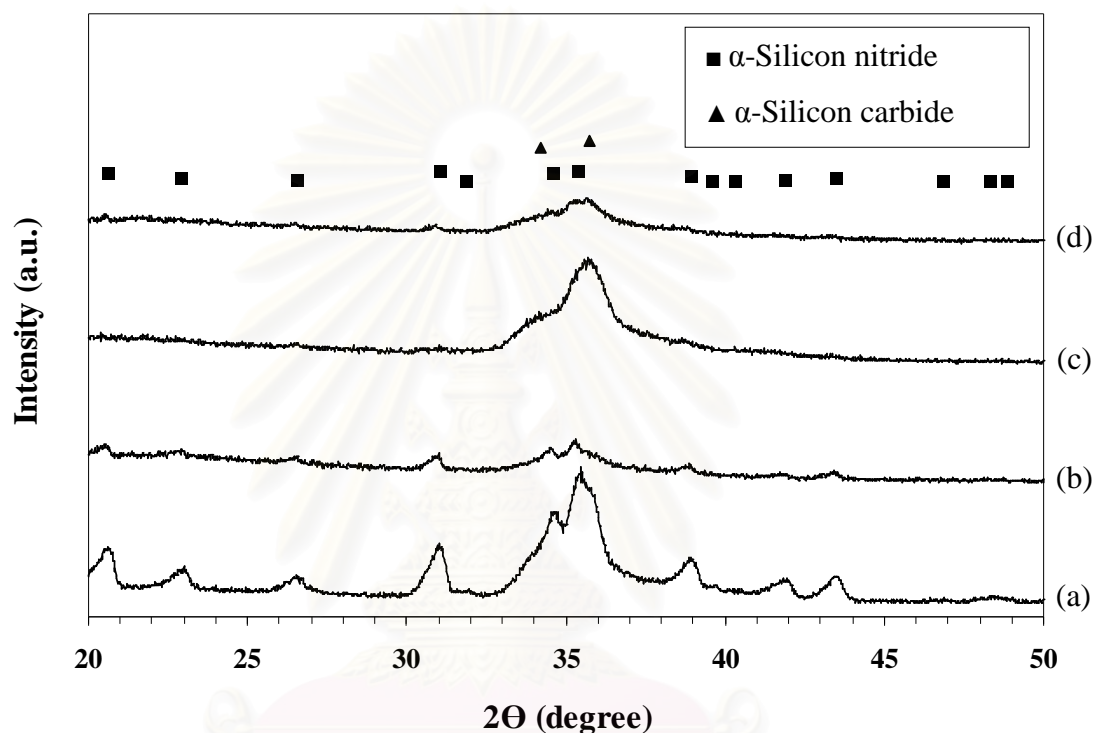
Figure 4.25 XRD patterns of products from the nitridation and subsequent calcination of pyrolyzed silica/RF gel synthesized using APTMS with an addition of acetic acid (a) R1-1, (b) R1-3, (c) R30-1 and (d) R30-3.

Table 4.14 shows the specific surface area of the samples analyzed in Figure 4.25 after each preparation step. It indicates that all products synthesized are highly porous silicon nitride or silicon carbide. Amount of acetic acid added significantly affects the surface area of the final product, since the porosity of the product is controlled by the dispersion of silica clusters in the carbonized RF gel. It should be noted that the surface area of the product is dramatically increased after the nitridation process. This should be the results from the activation of the carbon by hydrogen fed into the reactor to assist the nitridation. This residual carbon was completely removed by the calcination process so that the surface area of the calcined product is decreased.

Table 4.14 Specific surface area of the product after each preparation step.

Sample	Surface area (m^2/g)		
	Pyrolysis	Nitridation	Calcination
R1-1	291.4	288.5	54.5
R1-3	23.1	115.8	193.4
R30-1	300.7	625.7	67.0
R30-3	56.6	n.a.	142.9

Figure 4.26 and 4.27 show SEM micrographs of the product after different preparation steps. It can be seen that morphology of the silica/RF gel after pyrolysis is clusters. After the carbothermal reduction and nitridation, nanostructure is formed within the porous carbon. The removal of the residual carbon by the calcination produces porous silicon nitride or silicon carbide in ether fiber or pellet form.

R1-1   R1-3
(a)

R1-1   R1-3
(b)
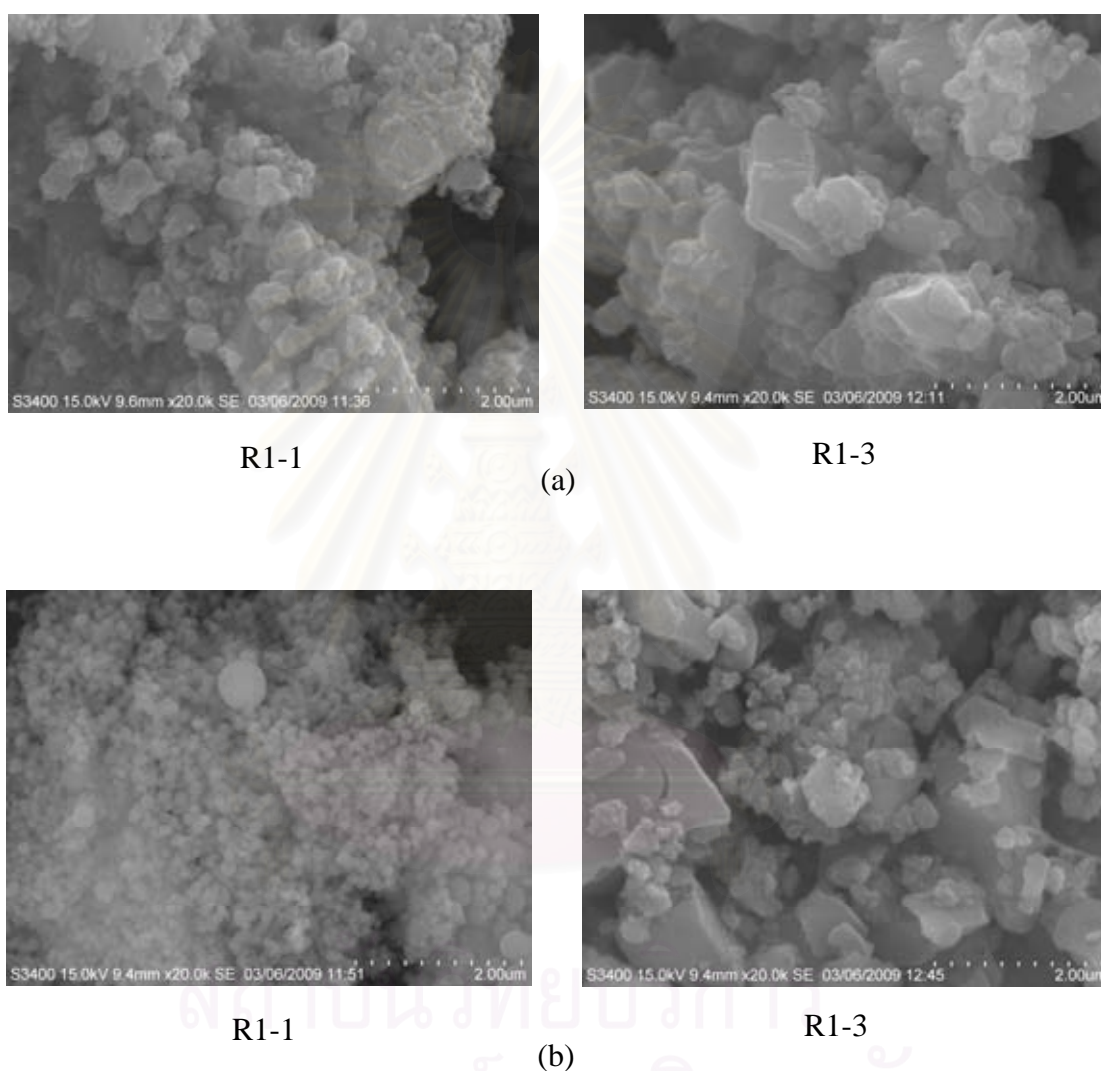
Figure 4.26   SEM micrographs of silica/RF gel formed by using APTMS with an
                addition of acetic acid in various amount at the RF aging time 1 h:
                (a) after pyrolysis and (b) after calcination.

R30-1

(a)

R30-3

R30-1

(b)

R30-3
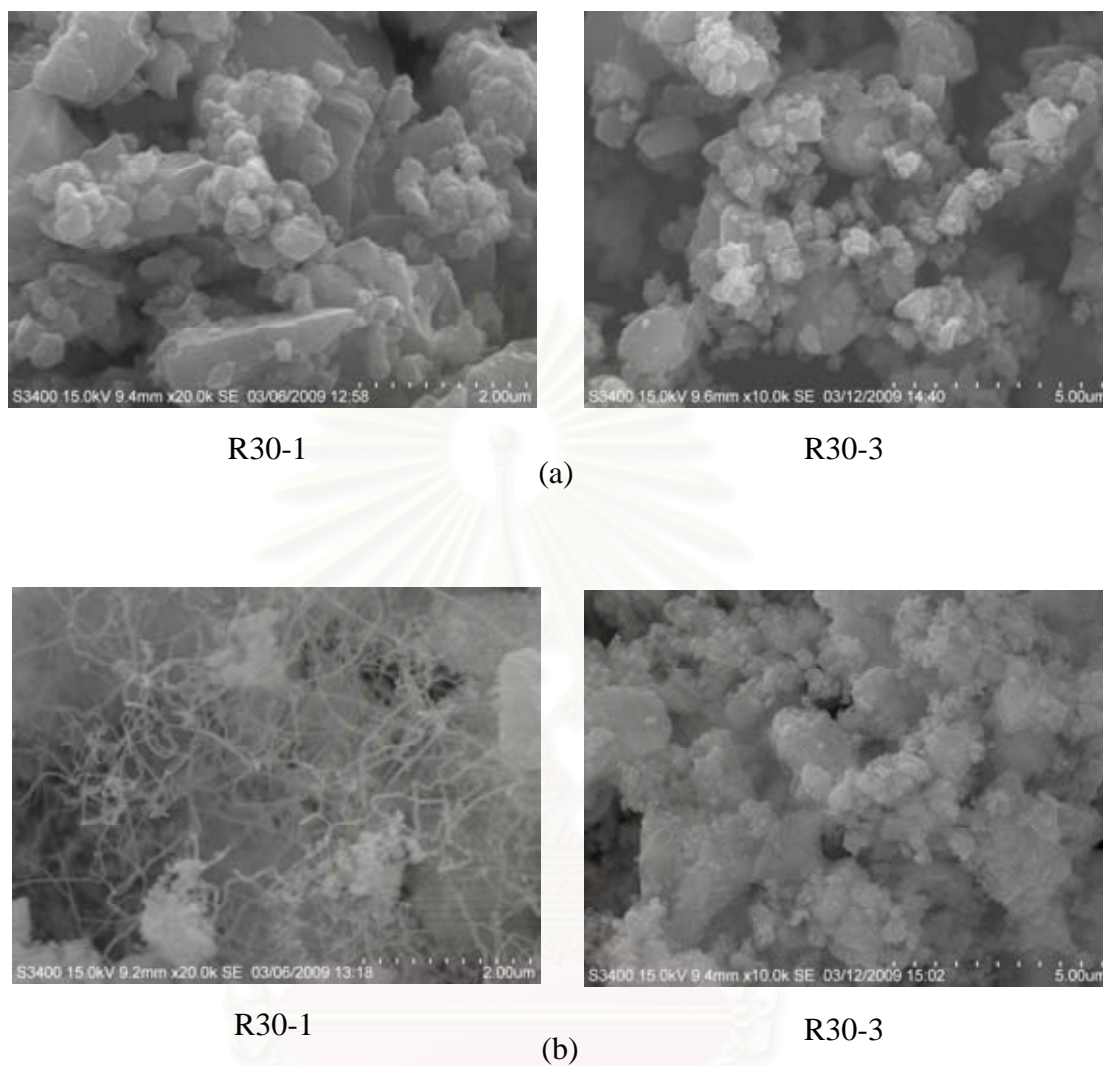
Figure 4.27 SEM micrographs of silica/RF gel formed by using APTMS with an addition of acetic acid in various amount at the RF aging time 30 h: (a) after pyrolys and (b) after calcination.

Figure 4.28 shows results from X-ray diffraction analysis of products after calcination step. The sample was prepared by using either APTMS or MPTMS as precursor for silica. Nevertheless, both samples appear to be α-silicon carbide. Table 4.15 shows surface area of these samples after each preparation step. It should be noted that the surface area of the product is dramatically increased after the nitridation process. This should be the results from the activation of the carbon by hydrogen fed into the reactor to assist the nitridation, as mentioned earlier. This residual carbon was completely removed by the calcination process so that the surface area of the calcined product is decreased.
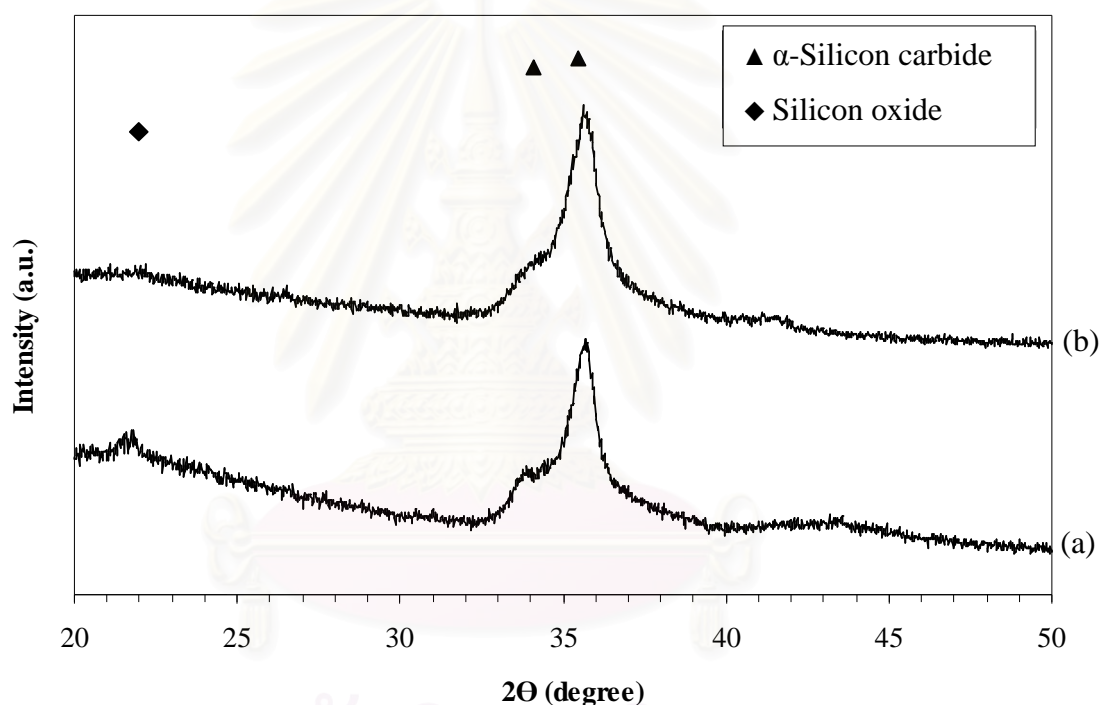
Figure 4.28　XRD patterns of products after calcination when (a) APTMS [RF-AP-10] and (b) MPTMS [RF-MP-10] were used as precursor for silica.

Table 4.15 Surface area of silica/carbon composite after each preparation step. The composite was prepared by using either APTMS or MPTMS as precursor for silica.

Sample	Surface area (m^2/g)		
	Pyrolysis	Nitridation	Calcination
RF-APTMS	291.5	520.6	71.9
RF-MPTMS	383.0	1069.1	73.5

Figure 4.29 shows results from X-ray diffraction analysis of products after calcination step. The sample prepared by using APTMS as precursor for silica appears to be α-silicon nitride/silicon carbide composite, but the sample prepared by using MPTMS as precursor for silica appears to be α-silicon carbide.
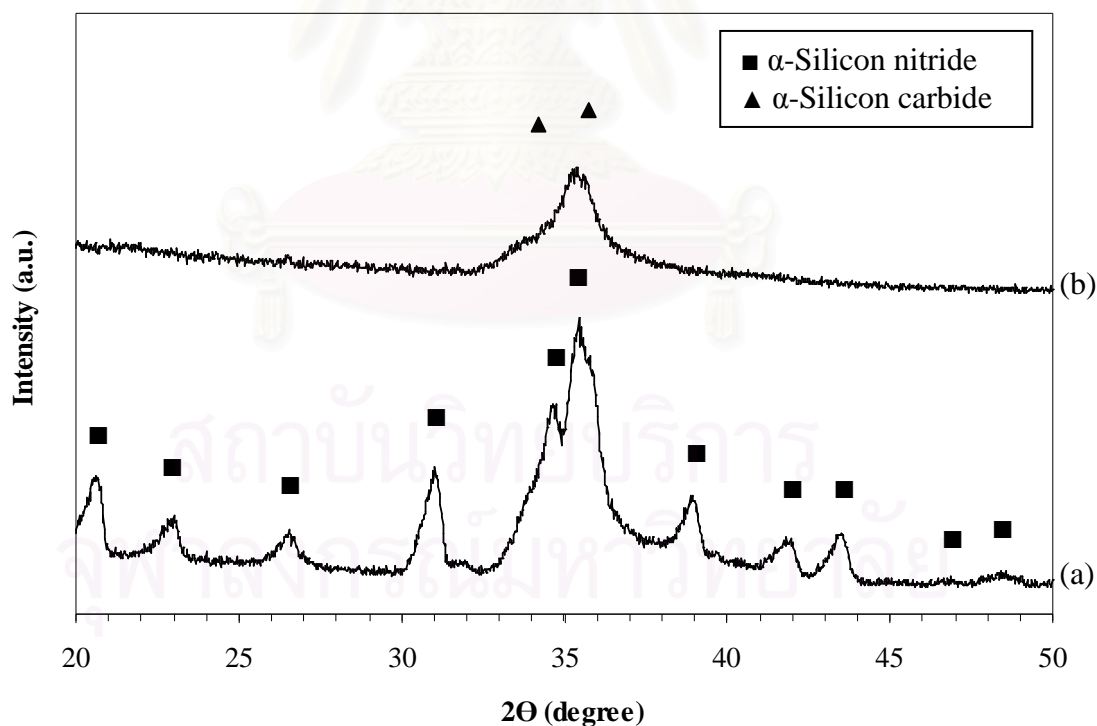
Figure 4.29 XRD patterns of products after calcination when (a) APTMS [RF-Ac1-AP-10] and (b) MPTMS [RF-Ac1-MP-10] were used as precursor of silica with the addition of acetic acid.

Table 4.16 shows surface area of these samples after each preparation step. This should be the results from the activation of the carbon by hydrogen fed into the reactor to assist the nitridation, as mentioned earlier. This residual carbon was completely removed by the calcination process so that the surface area of the calcined product is decreased.

Table 4.16 Surface area of silica/carbon composite after each preparation step. The composite was prepared by using either APTMS or MPTMS as precursor for silica with the addition of acetic acid.

Sample	Surface area (m^2/g)		
	Pyrolysis	Nitridation	Calcination
RF-Ac1-APTMS	291.4	288.5	54.5
RF-Ac1-MPTMS	380.4	1186.5	157.8

Table 4.17 shows surface area of the samples analyzed in Figure 4.30 after each preparation step. The result can be observed that increasing aging temperature of silica/RF gels decreases surface area after pyrolysis step, because of rapid condensation of silica/RF gel structure. The data shown in Table 4.12 also indicate that the pyrolyzed structure contains smaller pores as the aging temperature is increased.

Table 4.17 Surface area of silica/carbon composite after each preparation step. The composite was prepared from silica/RF gel aged at different temperature.

Sample	Surface area (m^2/g)		
	Pyrolysis	Nitridation	Calcination
R1-13	291.4	288.5	54.5
R1-15	283.7	816.9	161.5
R1-17	188.8	768.5	208.2

The results shown in Figure 4.30 are X-ray diffraction analysis results of the final products after calcination. The final product from R1-13 (Figure 4.30(a)) remains α-silicon nitride/silicon carbide composite, whereas R1-15 (Figure 4.30(b)) and R1-17 (Figure 4.30(c)) exhibit crystalline structure of α-silicon carbide.
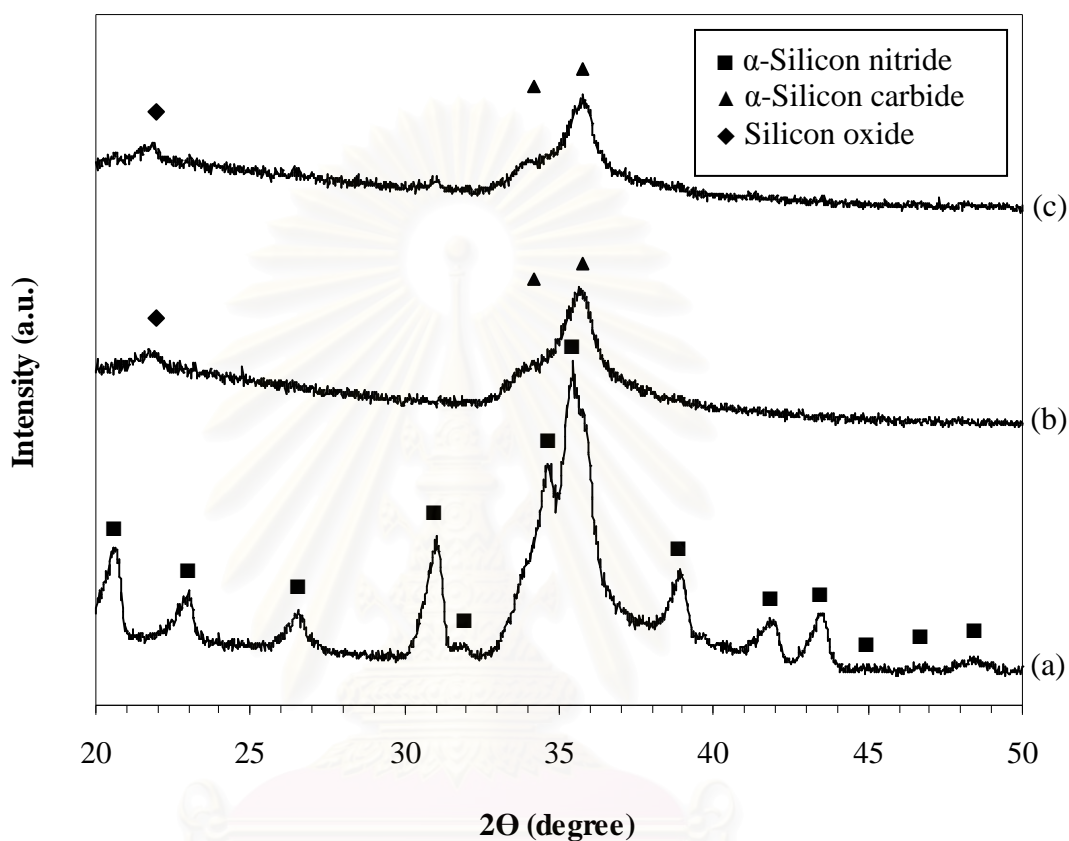
Figure 4.30 XRD patterns of products from calcination of silica/carbon composite synthesized from silica/RF gel aged at various temperatures: (a) 30°C [R1-13], (b) 50°C [R1-15] and 70°C [R1-17].

CHAPTER V

CONCLUSIONS AND RECOMMENDATION

5.1 Conclusions

This work studies the incorporation of silica into RF clusters via the sol-gel polycondensation. The result shows that the reaction between silica precursor and RF solution is rapid. The addition of acetic acid into RF mixture damages structure of RF clusters, which can slow down the reaction between silica precursor and RF solution. However, re-formation of the silica/RF gel results in changes in chemical structure that affect phase of the product from the subsequent carbothermal reduction and nitridation process.

5.2 Recommendations for Future Work

In this study effects of various factors, such as aging time for RF solution, reaction temperature during the sol-gel polycondensation of silica/RF gel, acetic acid addition on RF solution, amount of acetic acid added into silica/RF solution, type of silica precursor, aging temperature for silica/RF gel, on the synthesis of silicon nitride and silicon carbide via the carbothermal reduction and nitridation of silica/RF composite have been investigated. Some recommendations for future work are listed as follows: (i) relationship between chemical structure of silica/RF gel and phases of the final product should be investigated in details, (ii) thermodynamic calculation of the carbothermal reduction and nitridation process should be investigated.

REFERENCES

Brito, R., Rodriguez, V. A., Figueroa, and Caberar, C. R. 2002. Adsorption of 3-mercaptopropyltrimethoxysilane and 3-aminopropyltrimethoxysilane at platinum electrodes. Journal of Electronalytical Chemistry 520: 47-52.

Czakkel, O., Marthi, K., Geissler, E., and Laszlo, K. 2005. Influence of Drying on the Morphology of Resorcinol–Formaldehyde-Based Carbon Gels. Microporous and Mesoporous Materials 86: 124-133.

Ding, S., Zeng, Y. P., and Jiang, D. 2008. In-situ reaction bonding of porous SiC ceramics. Materials Characterization 59: 140-143.

Dingcai, W., Ruowen, F., Zhuodi, S., and Zhiquan, Y. 2004. Low-density organic and carbon aerogels from the sol-gel polymerization of phenol with formaldehyde. Journal of Non-Crystalline Solids 351: 915-921.

Fuente, E., Menendez, J. A., Diez, M. A., Suarez, D., and Montes, M. A. 2003. Infrared Spectroscopy of Carbon Materials: A Quantum Chemical Study of Model Compounds. Journal Physics Chemistry 107: 6350-6359.

Ghanem, H., Popovska, N., and Gerhard, H. 2007. Processing of biomorphic Si_3N_4 ceramics by CVI-R technique with $SiCl_4/H_2/N_2$ system. Journal of the European Ceramic Society 27: 2119–2125.

Handique, J. G., and Baruah, J. B. 2002. Polyphenolic compounds: an overview. Reactive & Functional Polymers 52: 163-188.

Hruby, S. L., and Shanks, B. H. 2009. Acid-base cooperativity in condensation reactions with functionalized mesoporous silica catalysts. Journal of Catalysis 263: 181-188.

Jinwang, L., and Ralf, R. 2007. Carbothermal Reaction of Silica–Phenol Resin Hybrid Gels to Produce Silicon Nitride/Silicon Carbide Nanocomposite Powders. Journal American Ceramic Society 90: 3786–3792.

Job, N., Panariello F., Marien, J., Crine, M., Pirard, J. P., and Leonard, A. 2006. Synthesis optimization of organic xerogels produced from convective air-drying of resorcinol–formaldehyde gels. Journal of Non-Crystalline Solids 352: 24–34.

Kawai, C., and Yamakawa, A. 1998. Crystal Growth of Silicon Nitridefe Whiskers Thuogh a VLS Mechanism Using SiO_2-Al_2O_3-Y_2O_3 Oxides as Liquid Phase. Ceramic International 24: 136-138.

Leonard, A., Blacher, S., Crine, M., and Jomaa W. 2008. Evolution of mechanical properties and final textural propertiesof resorcinol–formaldehyde xerogels during ambient air drying. Journal of Non-Crystalline Solids 354: 831–838.

Li, Y. S., Ba, A., and Mahmood, M.S. 2009. Infrared and Raman spectra of triacetoxyvinylsilane, aqueous sol-gel and xerogel. Spectrochimica Acta Part A 72: 605-509.

Liang, C. H., and Sha, G. Y., and Guo, S. C. 2000. Resorcinol-Formaldehyde Aerogels Prepared by Supercritical Acetone Drying. Journal of Non-Crystalline Solids 271: 167-170.

Long, D. H., Zhang, J., Yang, J. H., Hu, Z. J., Li, T. Q., Cheng, G., Zhang, R., and Ling, L. C. 2008. Preparation and microstructure control of carbon aerogels produced using m-cresol mediated sol-gel polymerization of phenol and furfural. New Carbon Materials 23(2): 165-170.

Matovic, B., Saponjic, A., Devecerski, A., and Miljkovic, M. 2007. Fabrication of SiC by carbothermal-reduction reactions of diatomaceous earth. Journal of Materials Science 42: 5448–5451.

Pekala, R. W. 1989. Organic Aerogels from the Polycondensation of Resorcinol with Formaldehyde. Journal of Materials Science 24: 3221-3227.

Poljansek, I., and Krajnc, M. 2005. Characterization of Phenol-Formaldehyde Prepolymer Resins by In Line FT-IR Spectroscopy. Acta Chim Slov 52: 238-244.

Ruben, G. C., Pekala R. W., Tillotson T. M., and Hrubesh, L. W. 1992. Imaging aerogels at the molecular level. Journal of Materials Science 27: 4341-4349.

Shields, V. B. Applications of Silicon Carbide for High Temperature Electronics and Sensors. Jet Propulsion Laboratory, California Institute of Technology, MS 303-308, 4800 Oak Grove Drive, Pasadena, California 91109, USA

Tamon, H., and Ishizaka, H. 1998. Porous characterization of carbon aerogels. Carbon 36: 1397-1409.

Tamon, H., Ishizaka, H., Yamamoto, T., and Suzuki T. 1999. Preparation of mesoporous carbon by freeze drying. Carbon 37: 2049–2055.

Turkdogan, E. T., Bills, P. M., and Tippett, V. A. 1996. Silicon Nitrides: Some Physico-Chemical Properties. Journal of Apply Chemistry 16: 413-420.

Vejayakumaran, P., Rahman, L. A., Sipaut, C. S., Ismail, J., and Chee, C. K. 2008. Structural and thermal characterizations of silica nanoparticles grafted with pendant maleimide and epoxide groups. Journal of Colloid and Interface Science 328: 81-91.

Weimer, A. W., and Bordia, R. K. 1999. Processing and properties of nanophase SiC/Si$_3$N$_4$ composites. Composites: Part B 30: 647–655.

Yamamoto, T., Yoshida, T., Suzuki, T., Mukai, S. R., and Tamon, H. 2001. Dynamic and Static Light Scattering Study on the Sol-Gel Transition of Resorcinol-Formaldehyde Aqueous solution. <u>Journal of Colloid and Interface Science</u> 245: 391-396.

Yamamoto, T., Nishimura, T., Suzuki, T., and Tamon, H. 2001. Control of mesoporosity of carbon gels prepared by sol-gel polycondensation and freeze drying. <u>Journal of Non-Crystalline Solids</u> 288: 46-55.

Yamamoto, T., Mukai, S. R., Endo A., Nakaiwa, M., and Tamon, H. 2003. Interpretation of structure formation during the sol-gel transition of a resorcinol-formaldehyde solution by population balance. <u>Journal of Colloid and Interface Science</u> 264: 532-537.

Yang, J. F., Shan, S. Y., Janssen, R., Schneider, G., Ohji, T., and Kanzaki, S. 2005. Synthesis of Fibrous β-Si_3N_4 Structured Porous Ceramics Using Carbothermal Nitridation of Silica. <u>Acta Materialia</u> 53: 2981-2990.

Zhang, W., Wang, H., and Jin, Z. 2005. Gel casting and properties of porous silicon carbide/silicon nitride composite ceramics. <u>Materials Letters</u> 59: 250–256.

Ziegler, G., Heinrich, J., and Wotting, G. 1987. Review Relationships between processing, microstructure and properties of dense and reaction-bonded silicon nitride. <u>Journal of Materials Science</u> 22: 3041-3086.

APPENDIX

APPENDIX A

PICTURES OF RF SOLUTION
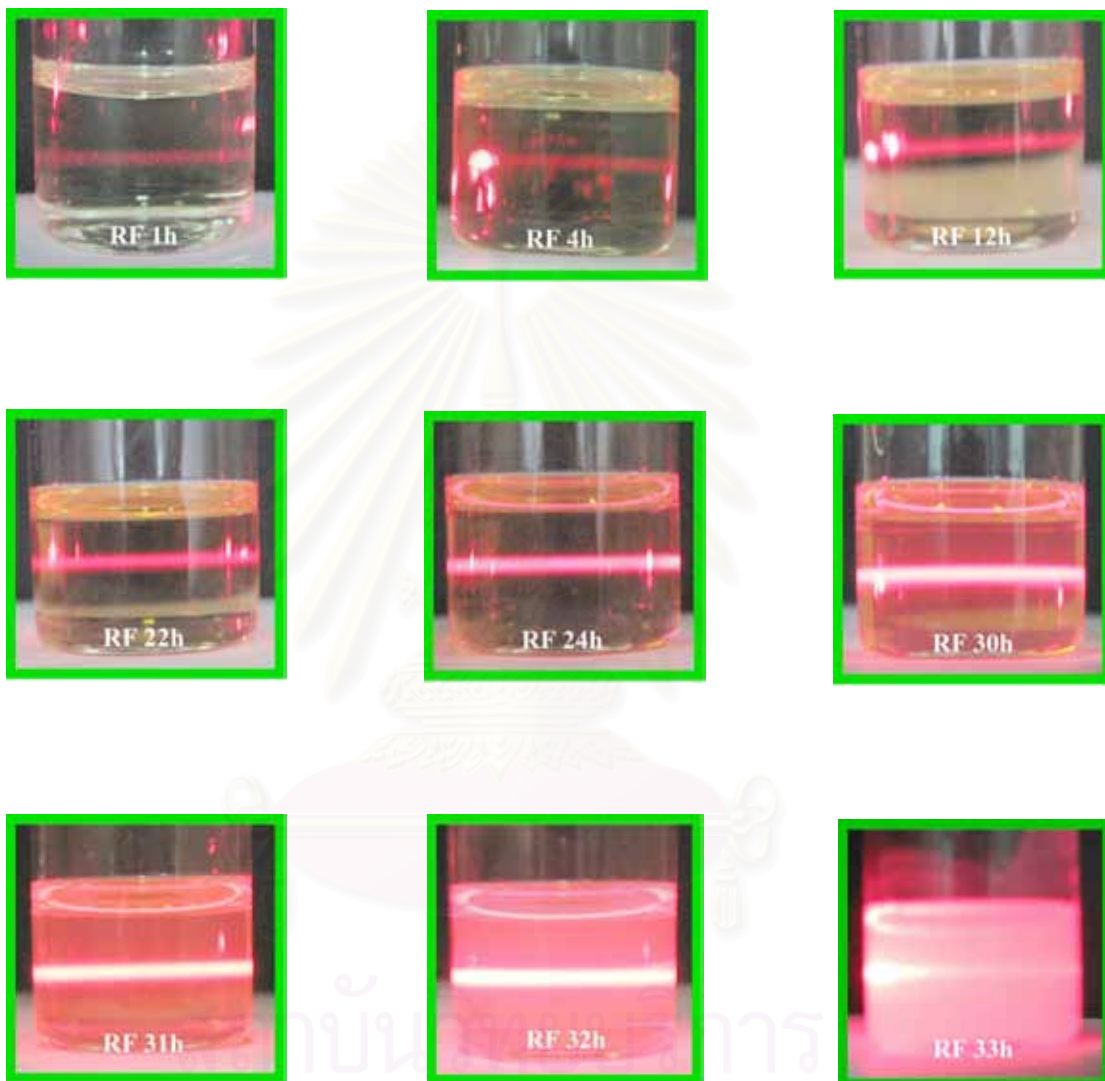
Figure A.1   Scatter Light scattering of RF solution aged for various times.

APPENDIX B

DATA OF PORE DIAMETER AND PORE VOLUME

Table B.1   Data of pore diameter and pore volume of the silica/carbon composite after pyrolysis, prepared from silica/RF gel formed at 50°C.

Pore Diameter (Å)	Pore Volume (cm³/g)
710.4	0.020
434.7	0.020
298.5	0.011
208.5	0.006
135.9	0.003
87.3	0.004
53.3	0.010
34.2	0.032
21.9	0.108

Table B.2   Data of pore diameter and pore volume of the product after the carbothermal reduction and nitridation process, prepared from silica/RF gel formed at 50°C.

Pore Diameter (Å)	Pore Volume (cm³/g)
703.6	0.047
431.9	0.054
296.6	0.057
235.5	0.012
138.6	0.054
92.5	0.110
53.7	0.320
34.2	1.459
21.9	1.806

Table B.3 Data of pore diameter and pore volume of the product after calcination, prepared from silica/RF gel formed at 50°C.

Pore Diameter (Å)	Pore Volume (cm³/g)
716.5	0.083
440.6	0.277
299.6	0.277
234.2	0.165
135.5	0.060
84.1	0.017
47.8	0.022
30.7	0.038
18.6	0.089

Table B.4 Data of pore diameter and pore volume of the silica/carbon composite after pyrolysis, prepared from silica/RF gel formed at 30°C.

Pore Diameter (Å)	Pore Volume (cm³/g)
715.3	0.016
434.6	0.016
297.4	0.011
207.7	0.009
148.3	0.003
88.4	0.001
51.1	0.004
34.0	0.015
21.9	0.064

Table B.5   Data of pore diameter and pore volume of the product after the carbothermal reduction and nitridation process, prepared from silica/RF gel formed at 30°C.

Pore Diameter (Å)	Pore Volume (cm³/g)
710.5	0.108
435.8	0.171
299.3	0.335
236.2	0.504
153.1	0.526
94.3	0.514
53.8	0.621
34.3	1.749
21.9	2.119

Table B.6   Data of pore diameter and pore volume of the product after calcination, prepared from silica/RF gel formed at 30°C.

Pore Diameter (Å)	Pore Volume (cm³/g)
716.3	0.036
446.9	0.142
302.2	0.161
235.0	0.149
150.5	0.101
86.4	0.071
48.8	0.036
30.5	0.027
18.5	0.047

Table B.7 Data of pore diameter and pore volume of the product after the carbothermal reduction and nitridation process, prepared from silica/RF gel formed at -10°C.

Pore Diameter (Å)	Pore Volume (cm³/g)
708.9	0.038
435.3	0.065
298.9	0.059
209.3	0.051
149.6	0.061
95.6	0.119
54.9	0.379
35.4	1.059
23.0	0.865

Table B.8 Data of pore diameter and pore volume of the product after calcination, prepared from silica/RF gel formed at -10°C.

Pore Diameter (Å)	Pore Volume (cm³/g)
717.3	0.023
452.2	0.151
304.5	0.137
237.2	0.112
151.0	0.054
86.7	0.064
51.3	0.119
32.0	0.110
19.7	0.078

Table B.9 Data of pore diameter and pore volume of the sample ID R1-1 after pyrolysis.

Pore Diameter (Å)	Pore Volume (cm³/g)
727.0	0.049
444.0	0.095
301.7	0.063
208.8	0.034
135.9	0.023
87.3	0.025
53.3	0.012
33.0	0.037
21.8	0.081

Table B.10 Data of pore diameter and pore volume of the sample ID R1-1 after the carbothermal reduction and nitridation process.

Pore Diameter (Å)	Pore Volume (cm³/g)
709.6	0.084
436.9	0.200
299.4	0.281
236.0	0.354
152.1	0.319
93.2	0.305
52.7	0.453
33.1	0.313
19.9	0.314

Table B.11 Data of pore diameter and pore volume of the sample ID R1-1 after calcination.

Pore Diameter (Å)	Pore Volume (cm³/g)
722.2	0.052
450.9	0.207
306.6	0.291
235.9	0.338
149.7	0.250
86.0	0.075
48.4	0.010
30.1	0.005
19.0	0.042

Table B.12 Data of pore diameter and pore volume of the sample ID R1-3 after pyrolysis.

Pore Diameter (Å)	Pore Volume (cm³/g)
723.7	0.015
436.9	0.019
296.3	0.010
205.2	0.006
132.7	0.003
32.9	0.001
21.8	0.017

Table B.13 Data of pore diameter and pore volume of the sample ID R1-3 after the carbothermal reduction and nitridation process.

Pore Diameter (Å)	Pore Volume (cm³/g)
710.4	0.042
434.5	0.091
297.2	0.153
232.6	0.252
150.7	0.424
89.7	0.442
49.5	0.220
29.0	0.022
17.8	0.046

Table B.14 Data of pore diameter and pore volume of the sample ID R1-3 after calcination.

Pore Diameter (Å)	Pore Volume (cm³/g)
706.6	0.034
436.2	0.073
298.1	0.111
233.9	0.178
151.0	0.229
91.3	0.208
51.1	0.234
31.6	0.360
19.2	0.167

Table B.15 Data of pore diameter and pore volume of the sample ID R30-1 after the carbothermal reduction and nitridation process.

Pore Diameter (Å)	Pore Volume (cm³/g)
705.0	0.034
438.0	0.163
300.4	0.268
235.2	0.399
151.6	0.328
93.6	0.491
52.3	0.643
33.0	1.191
20.6	0.736

Table B.16 Data of pore diameter and pore volume of the sample ID R30-1 after calcination.

Pore Diameter (Å)	Pore Volume (cm³/g)
708.4	0.061
441.0	0.276
299.8	0.294
233.5	0.213
149.1	0.059
84.4	0.019
47.0	0.017
29.9	0.036
17.8	0.082

Table B.17 Data of pore diameter and pore volume of the silica/carbon composite after pyrolysis, prepared by using MPTMS as precursor for silica.

Pore Diameter (Å)	Pore Volume (cm³/g)
719.3	0.020
459.0	0.187
324.5	0.451
236.4	0.489
150.1	0.267
88.9	0.084
51.3	0.026
32.9	0.034
21.8	0.074

Table B.18 Data of pore diameter and pore volume of the product after the carbothermal reduction and nitridation process, prepared by using MPTMS as precursor for silica.

Pore Diameter (Å)	Pore Volume (cm³/g)
701.7	0.024
445.5	0.243
314.7	0.799
237.6	1.148
152.9	1.007
95.2	0.734
52.1	0.647
33.3	1.281
21.8	1.264

Table B.19 Data of pore diameter and pore volume of the product after calcination, prepared by using MPTMS as precursor for silica.

Pore Diameter (Å)	Pore Volume (cm³/g)
700.8	0.003
449.2	0.422
306.1	0.462
235.0	0.346
149.1	0.114
84.5	0.044
47.1	0.031
28.9	0.034

Table B.20 Data of pore diameter and pore volume of the silica/carbon composite after pyrolysis, prepared by using MPTMS as precursor for silica with the addition of acetic acid.

Pore Diameter (Å)	Pore Volume (cm³/g)
717.9	0.031
459.2	0.245
321.2	0.492
238.9	0.672
150.7	0.346
89.0	0.084
51.2	0.022
32.9	0.034
21.8	0.081

Table B.21 Data of pore diameter and pore volume of the product after the carbothermal reduction and nitridation process, prepared by using MPTMS as precursor for silica with the addition of acetic acid.

Pore Diameter (Å)	Pore Volume (cm³/g)
1013.6	1.192
613.0	1.179
397.0	1.031
252.8	0.790
152.8	0.749
94.1	0.682
53.6	0.678
34.2	0.917
21.9	1.320

Table B.22 Data of pore diameter and pore volume of the product after calcination, prepared by using MPTMS as precursor for silica with the addition of acetic acid.

Pore Diameter (Å)	Pore Volume (cm³/g)
704.7	0.157
441.6	0.972
299.6	0.956
232.8	0.529
134.3	0.109
82.8	0.076
46.6	0.106
28.4	0.072

Table B.23 Data of pore diameter and pore volume of the product after the carbothermal reduction and nitridation process, prepared from silica/RF gel aged at 50°C.

Pore Diameter (Å)	Pore Volume (cm³/g)
713.0	0.041
437.5	0.090
301.4	0.228
236.7	0.493
153.9	0.465
94.6	0.419
53.8	0.309
33.3	0.742
21.8	0.866

Table B.24 Data of pore diameter and pore volume of the product after calcination, prepared from silica/RF gel aged at 50°C.

Pore Diameter (Å)	Pore Volume (cm³/g)
1060.4	0.227
413.2	0.163
250.6	0.136
151.2	0.156
92.6	0.250
52.0	0.330
32.6	0.167
20.3	0.098

Table B.25 Data of pore diameter and pore volume of the product after the carbothermal reduction and nitridation process, prepared from silica/RF gel aged at 70°C.

Pore Diameter (Å)	Pore Volume (cm³/g)
714.5	0.033
439.0	0.073
301.2	0.137
237.0	0.294
154.3	0.337
94.0	0.325
53.8	0.311
34.5	0.764
21.9	0.809

Table B.26 Data of pore diameter and pore volume of the product after calcination, prepared from silica/RF gel aged at 70°C.

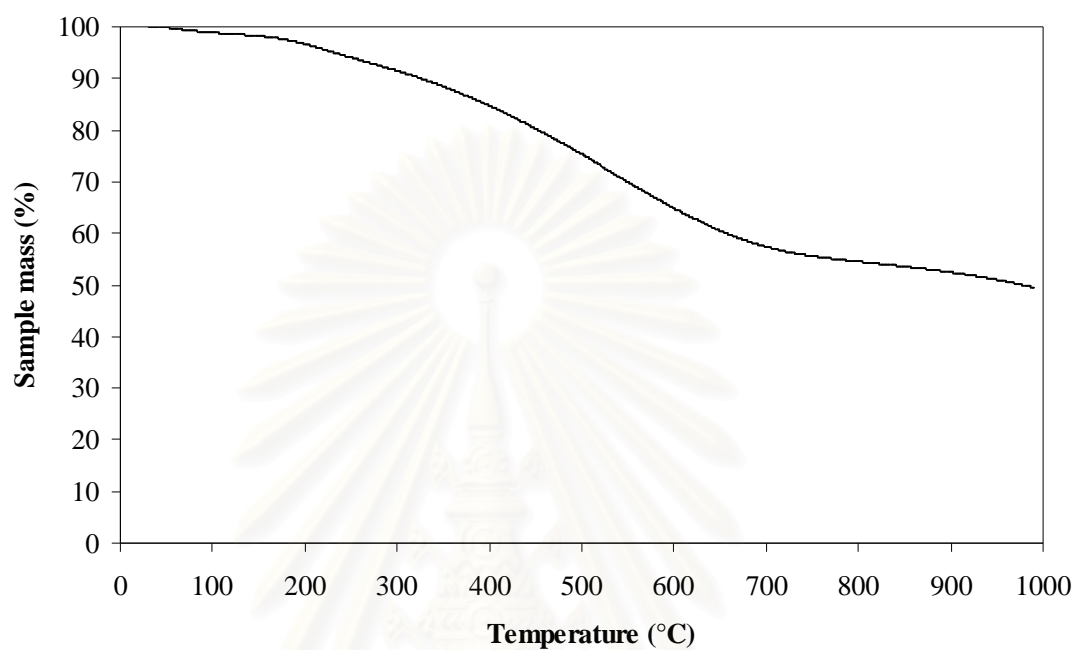| Pore Diameter (Å)	Pore Volume (cm³/g)
714.2	0.038
445.2	0.168
302.0	0.185
234.5	0.190
148.5	0.135
85.6	0.237
49.8	0.491
30.5	0.415
18.2	0.089

APPENDIX C

DATA OF TGA ANALYSIS

Figure C.1 TGA analysis in nitrogen atmosphere of silica/RF gel converts to silica/carbon composite, was prepared from silica/RF gel formed at -10°C.

สถาบันวิทยบริการ

จุฬาลงกรณ์มหาวิทยาลัย

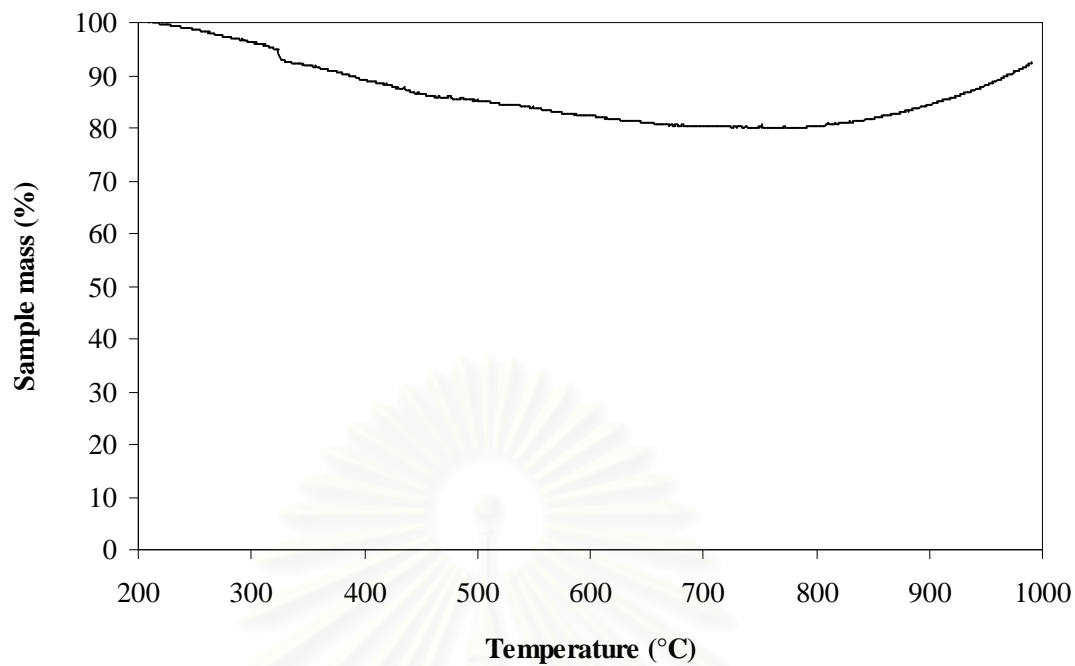**Figure C.2** TGA analysis in oxygen atmosphere of the final products after calcination, was prepared from silica/RF gel formed at -10°C.

Figure C.3 TGA analysis in oxygen atmosphere of final products after calcination with the sample ID R1-1.

Figure C.4 TGA analysis in oxygen atmosphere of final products after calcination
with the sample ID R1-3.

Figure C.5 TGA analysis in oxygen atmosphere of final products after calcination
with the sample ID R30-1.

Figure C.6 TGA analysis in oxygen atmosphere of final products after calcination with the sample ID R30-3.
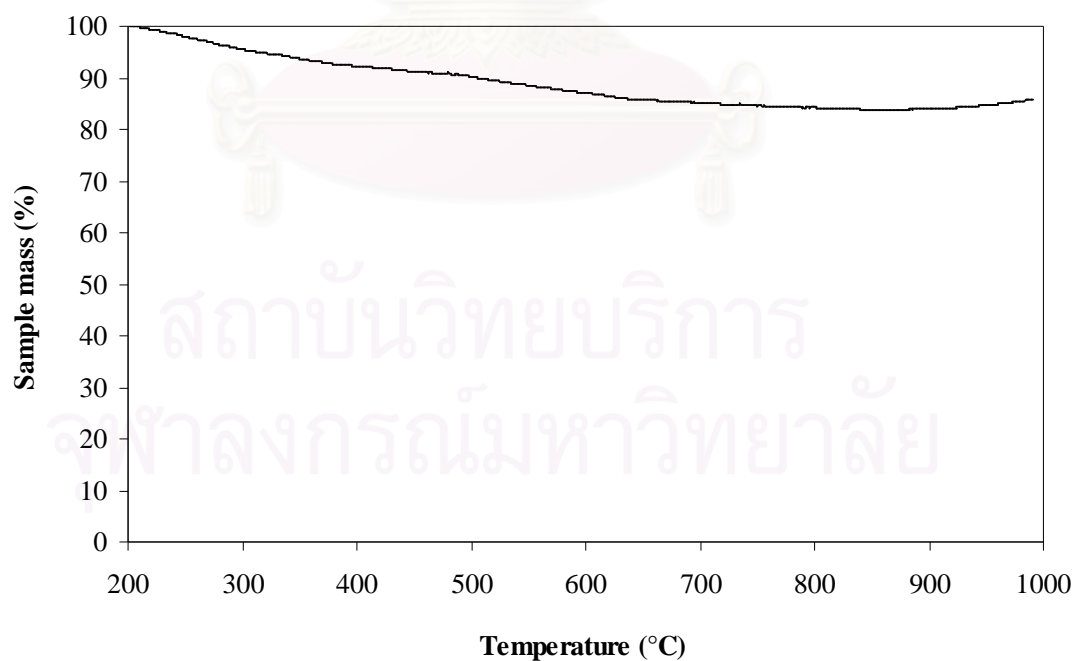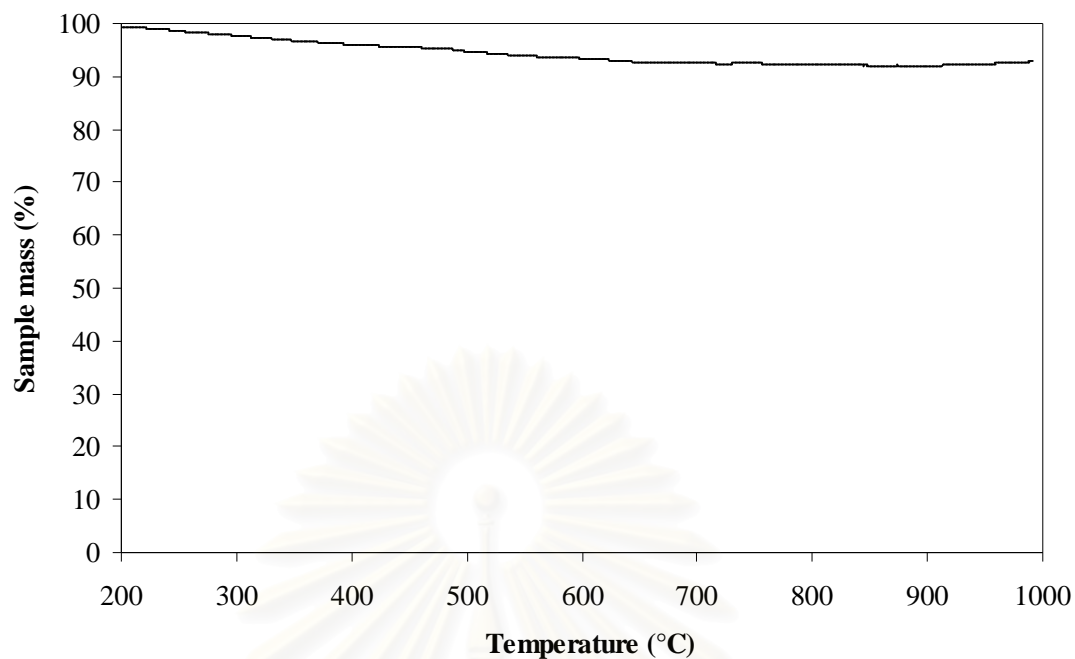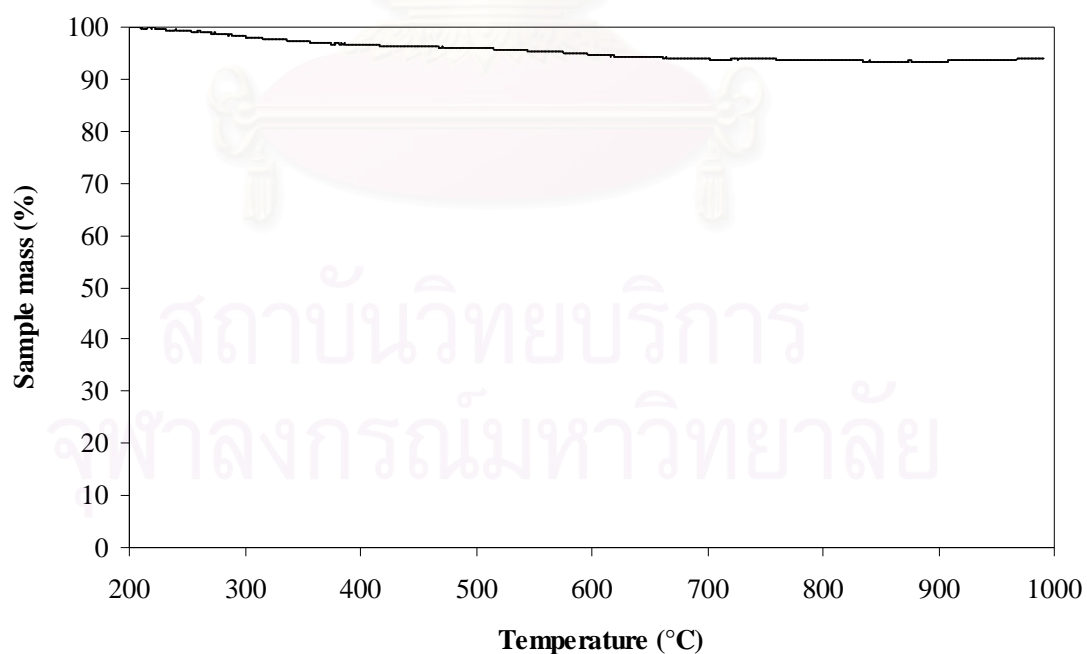

Figure C.7 TGA analysis in oxygen atmosphere of final products after calcination with the sample ID R1-17.
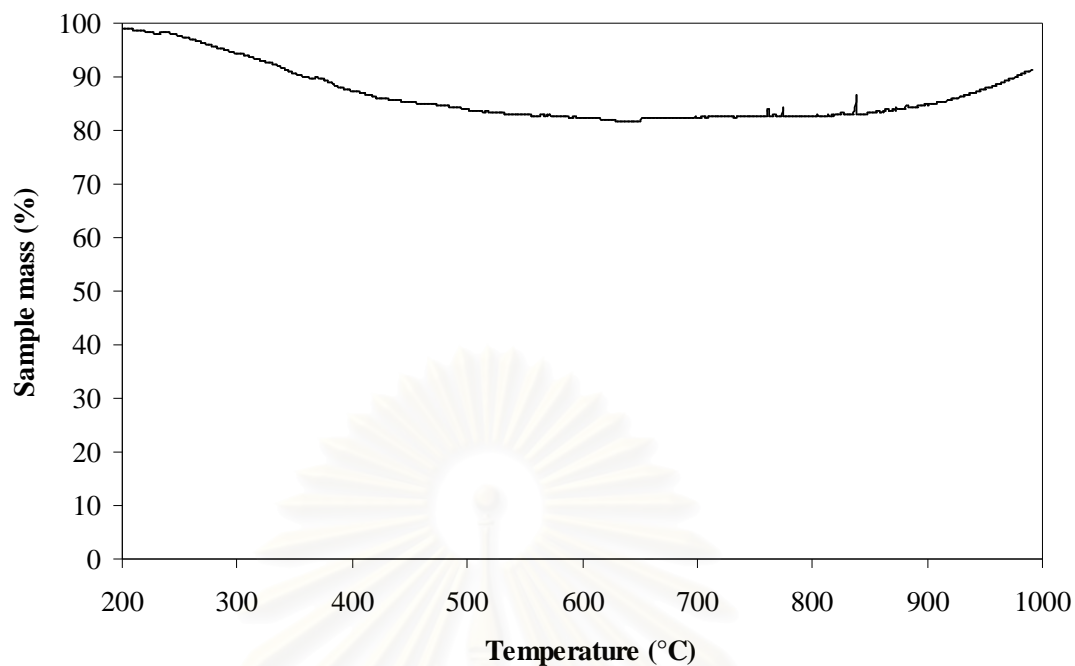
Figure C.8 TGA analysis in oxygen atmosphere of final products after calcination
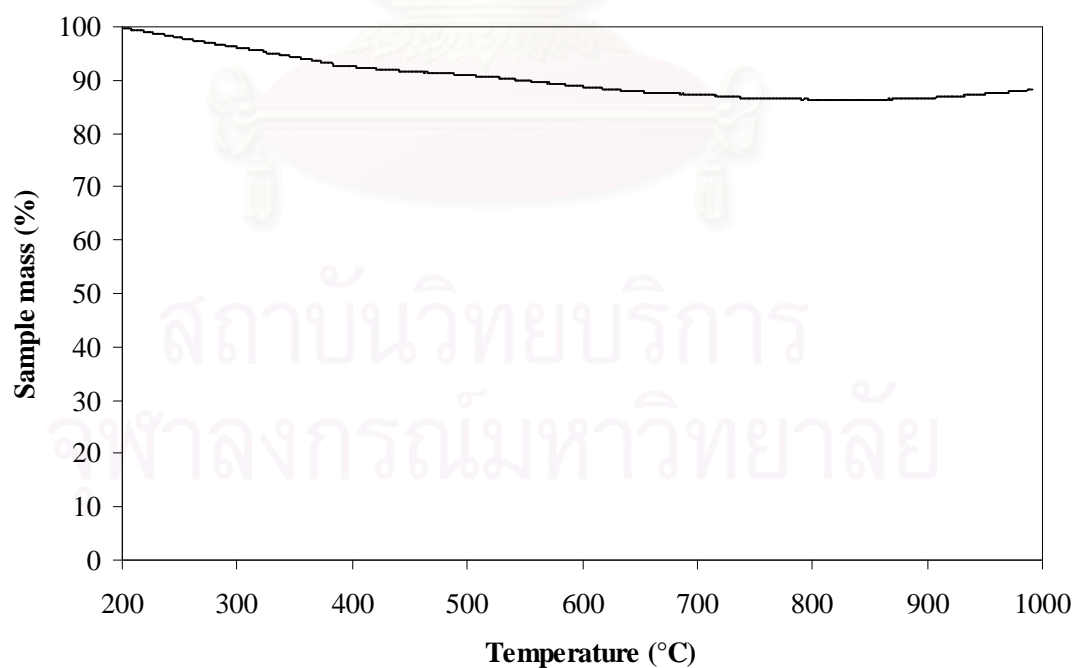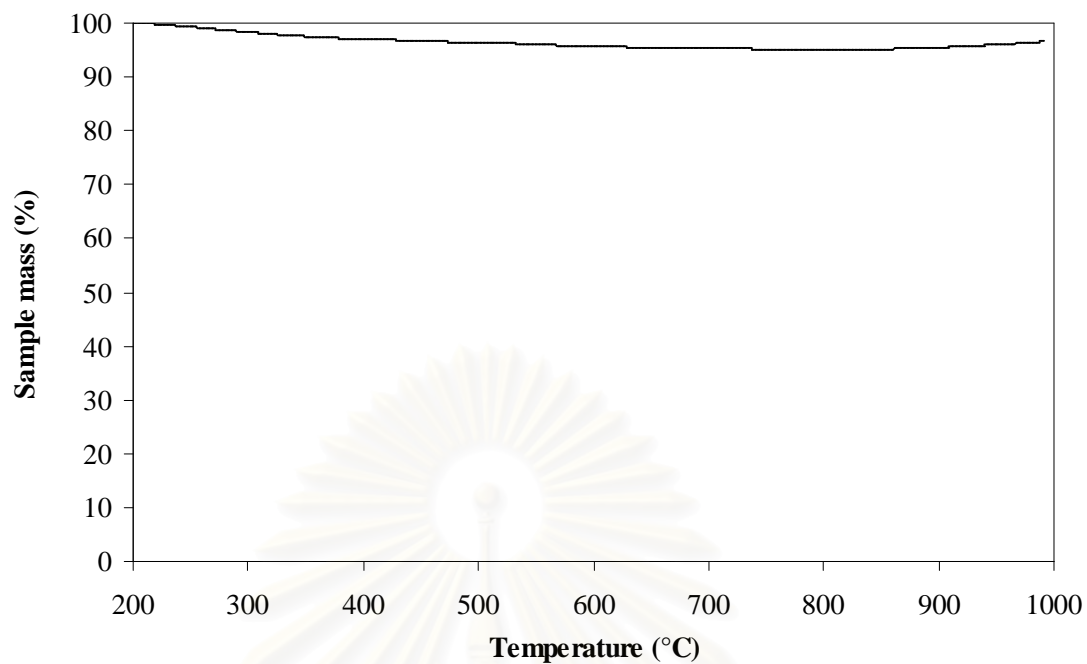of silica/RF gel formed by using MPTMS as silica precursor.
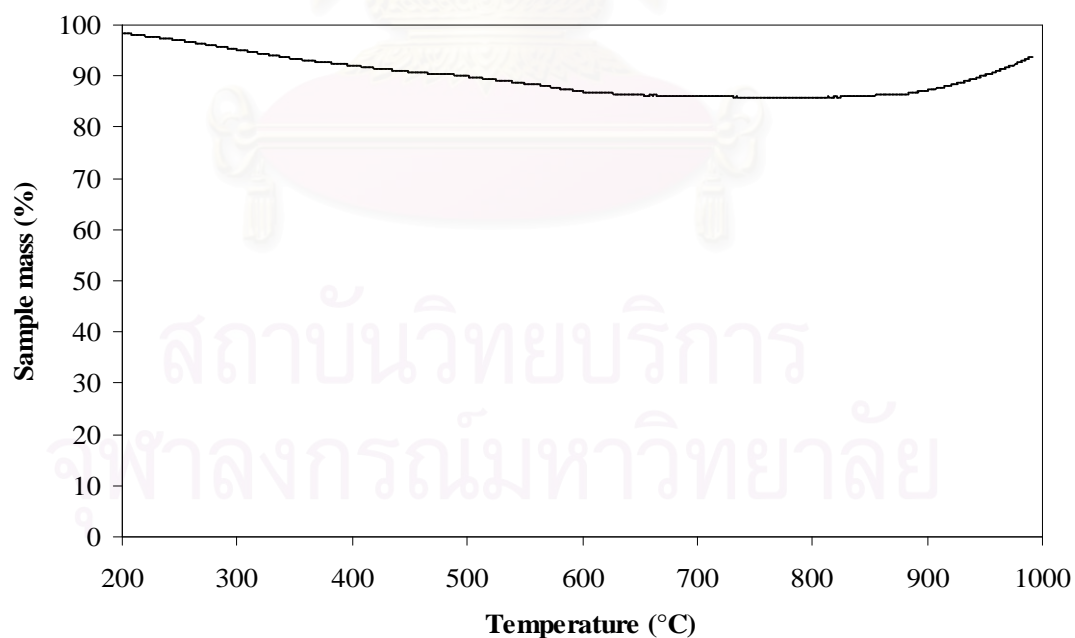
Figure C.9 TGA analysis in oxygen atmosphere of final products after calcination
of silica/RF gel formed by using MPTMS as silica precursor with the
addition of acetic acid.

APPENDIX D

LIST OF PUBLICATION

Charinya Poumuang, Nattaporn Tonanon and Varong Pavarajarn, "Effect of Silica Precursor on Si_3N_4/SiC Composite Synthesis via the Carbothermal Reduction and Nitridation of Carbonized Silica/RF Gel Composite", the 5th Thailand Materials Science and Technology Conference, Bangkok, Thailand, September 16-19, 2008.

Effect of Silica Precursor on Si_3N_4/SiC Composite Synthesis via the Carbothermal Reduction and Nitridation of Carbonized Silica/RF Gel Composite

Charinya Poumuang, Nattaporn Tonanon and Varong Pavarajarn[*]

Department of Chemical Engineering, Chulalongkorn University, Bangkok 10330

*Corresponding author: Phone 0-2218-6890, Fax 0-2218-6877, E-mail: fchvpv@eng.chula.ac.th

Abstract

Porous silicon nitride (Si_3N_4)/silicon carbide (SiC) composite can be synthesized via the carbothermal reduction and nitridation of carbonized composite of silica and resorcinol/formaldehyde (RF) gel. It was found that type of silica precursor used in the preparation of silica/RF gel significantly affected phase of the obtained product. However, it was not a critical factor influencing the porosity of the product.

1. Introduction

Porous Si_3N_4/SiC has been attracting great interest for engineering applications, such as gas filter, separation membranes and catalyst supports because of its high strength at high temperatures, good thermal stress resistance due to the low coefficient of thermal expansion, relatively good resistance to oxidation compared to other high-temperature and corrosion resistance structural materials[1-2]. Although sintering techniques have been proposed to fabricate porous Si_3N_4/SiC ceramics, the direct synthesis via the carbothermal reduction and nitridation of carbonized silica/RF gel composite has proved to be a simple and effective approach to produce mesoporous Si_3N_4 and Si_3N_4/SiC composite.[1] The technique is consisted of 3 main steps, i.e. formation of silica/RF gel, carbonization of silica/RF gel to form silica/carbon composite, and the carbothermal reduction and nitridation of the composite.

This work focuses on the effective incorporation of silica into the RF gel during the first step, as well as the study on the effect of silica precursor on the subsequent formation of Si_3N_4 and/or SiC.

2. Materials and Methods

To form the silica/RF gel, a solution was first prepared from resorcinol (R), formaldehyde (F) and water (W) at the R/F mole ratio of 0.5, R/W mole ratio of 0.15 and C/W ratio of 10 mol/m^3. The mixture was stirred at room temperature for 15 min, using magnetic stirrer, after which it was aged without stirring for 30 h at 30°C[4]. Then, the precursor for silica, i.e. amino propyl trimethoxysilane (APTMS) and tetraethyl orthosilicate (TEOS), in the amount that yield Si/C molar ratio in the final gel composite of 0.05 was slowly added to the RF solution under continuous stirring. After aging at room temperature for predetermined period of time, water was removed from the composite by means of solvent exchange with *t*-butanol. The obtained solid product was crushed into powder and dried in oven at 110°C for 16 h.

Next, the dried silica/RF gel was converted into silica/carbon composite by pyrolysis in a step-wise fashion. The dried gel was heated under continuous flow of nitrogen (200 mL/min) at temperature of 250°C for 2 h and subsequently heated at 750°C for 4 h. The heating rate employed was fixed at 10°C/min.

Then, the carbothermal reduction and nitridation process was conducted to convert the composite obtained from the pyrolysis step into Si_3N_4. In this process, the composite was heated to 1450°C at the rate of 10°C/min, under a flow of argon. After the system had reached 1450°C, the reaction was initiated by switching the gas stream from argon to mixture of 90% nitrogen and 10% hydrogen with a flow rate of 50 L/h. The nitridation was held at constant temperature for 6 h. The obtained product was later calcined in a box furnace at 700°C for 10 h to remove excess carbon.

The products were characterized by X-ray diffraction (XRD) analysis, Fourier transform infrared spectroscopy

(FTIR) and surface area determination via nitrogen absorption (BET).

3. Results and Discussion

In this work, two silica precursors, i.e. APTMS and TEOS were investigated. The silica precursor was added to the RF gel after the co-polymerization of resorcinol-formaldehyde was almost completed. However, it was observed that the addition of APTMS to the RF solution resulted in almost spontaneous gellation and solidification. It has been suggested that the addition of APTMS to the RF mixture does not simply immobilize APTMS to the RF structure, but it initiates the reaction to form other silicon-containing species within the RF gel.[1] The reaction is exothermic and becomes violent if APTMS is added to the RF solution rapidly. On the contrary, addition of TEOS did not result in spontaneous gel formation.

One of the major factors affecting the gellation of the RF gel was pH. The pH of the bare RF gel was about 3, after aging for 30 h. Since APTMS was more basic than TEOS (pH 8 vs. 5), the reaction between APTMS and the RF gel mixture was more violent. On the other hand, if the pH of TEOS was adjusted with ammonia prior to the addition into the RF gel, it was found that the mixture quickly became highly viscous and finally solidified in the similar manner as that observed when APTMS was used. This behavior agrees with the previous report in literature.[2]

Figure 1 shows Fourier Transform Infrared (FTIR) spectra of the silica/RF composite synthesized with APTMS and TEOS, before and after pyrolysis. It is shown that, for both samples, the absorption corresponding to the stretching vibration of aromatic ring at 1614 cm^{-1}, the absorption bands at 2942, 2874, and 1479 cm^{-1} for CH$_2$ stretching and the absorption bands at 1558 cm^{-1} for NH disappeared after pyrolysis. It is indicated that carbonization of the RF gel, which has been recognized to result in porous carbon structure, takes place during the pyrolysis. On the other hand, the absorption bands at 1090 and 800 cm^{-1} ascribing to Si-O-Si bond intensify, which suggests the formation of silica

within the pyrolyzed samples. It should be noted that although the FTIR spectra for the carbonized samples synthesized with APTMS and TEOS were similar, the intensity of the signals for Si-O-Si bond in the sample fabricated with TEOS were higher than that prepared with APTMS.
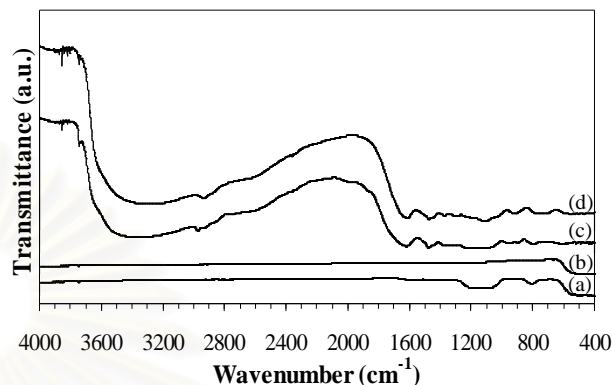

Fig. 1. FTIR spectra of: (a) TEOS/carbon gel after pyrolysis, (b) APTMS/carbon gel after pyrolysis, (c) TEOS/RF gel before pyrolysis, (d) APTMS/RF gel before pyrolysis.

The results from the X-ray diffraction (XRD) analysis revealed that the products after pyrolysis were indeed amorphous. However, the final products after the carbothermal reduction process and the calcination to remove excess carbon were crystalline, as shown in Figure 2. It was found that the sample prepared with APTMS was mainly Si$_3$N$_4$, while the sample prepared with TEOS was Si$_3$N$_4$/SiC composite, with SiC as the predominant phase. It was suggested that the greater amount of silica formed from TEOS could undergo solid state reaction with carbon to form SiC, according to the following equation.

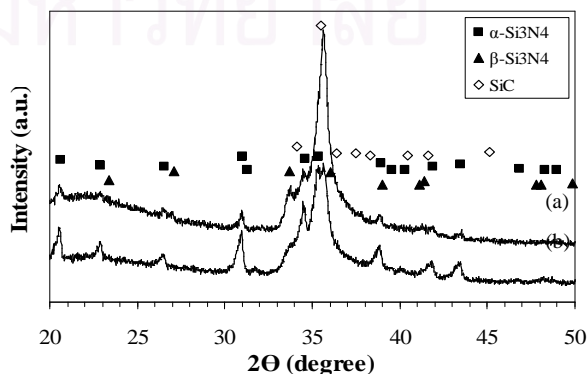$$SiO_2\ (s) + 3C\ (s) \rightarrow SiC\ (s) + 2CO\ (g) \qquad (1)$$

Fig. 2. XRD patterns for the final products prepared with APTMS (a) and TEOS (b), after calcination.

Table 1 summarizes the specific surface area of the samples after each preparation step. It indicates that all products synthesized are highly porous Si_3N_4/SiC composite. Type of the silica precursor does not significantly affect the surface area of the final product. Instead the porosity of the product was controlled by the dispersion of silica clusters in the carbonized RF gel. It should be noted that the surface area of the product was dramatically increased after the nitridation process. This should be the results from the activation of the carbon by hydrogen fed into the reactor to assist the nitridation. This residual carbon was completely removed by the calcination process so that the surface area of the calcined product was decreased.

Table 1. Specific surface area of the product after each preparation step.

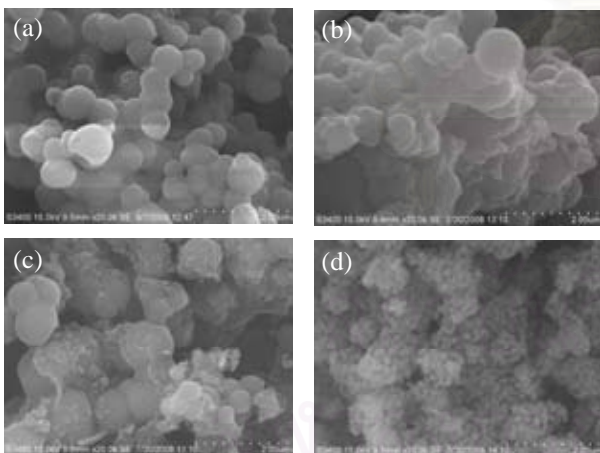| Silica Precursor	$S_{BET}(m^2/g)$		
	Pyrolysis	Nitridation	Calcination
APTMS	130.03	474.83	85.85
TEOS	282.18	488.93	98.04

Fig. 3.SEM micrographs of (a) Silica/RF gel, (b) Silica/Carbon composite, (c) nitrided product, and (d) product after calcination, for the products prepared with RF/APTMS composite.

Figure 3 shows SEM micrographs of the product after different preparation steps. It can be seen that morphology of the silica/RF gel before pyrolysis of is clusters. After the carbothermal reduction and nitridation, Si_3N_4 nanostructure is formed within the porous carbon. The removal of the residual carbon by the calcination produces porous Si_3N_4/SiC composite.

4. Conclusion

Porous silicon nitride/silicon carbide composite can be synthesized via the carbothermal reduction and nitridation of carbonized silica/RF gel composite. The porous structure of the product was formed according to the structure of the carbonized RF gel. However, the phase of the product was determined by type of the silica precursor employ.

References

[1] K. Luyjew, N. Tananon, and V. Pavarajarn, "Mesoporous Silicon Nitride Synthesis via the Carbothermal Reduction and Nitridation of Carbonized Silica/RF Gel Composite," J. Am. Ceram. Soc.,91(4): 1365-1368 (2008).

[2] G. Ziegler, J. Heinrich and G. Wotting, "Review Relationships between processing, microstructure and properties of dense and reaction-bonded silicon nitride," J. Mater. Sci. 22, 3041-3086 (1987).

[3] H. Tamon, T. Kitamura, and M. Okazaki, "Preparation of Silica Aerogel TEOS," J. Colloid Inter. Sci. 197, 353-359 (1998).

[4] A. Siyasukh, P. Maneeprom, S. Larpkiattaworn, N. Tonanon, W. Tanthapanichakoon, H. Tamon and T. Charinpanitkul, "Preparation of a carbon monolith with hierarchical porous structure by ultrasonic irradiation followed by carbonization, physical and chemical activation," Carbon. 46, 1309–1315 (2008).

VITA

Miss. Charinya Poumuang was born on 27th August, 1985, in Lopburi, Thailand. She received the Bachelor's Degree of Engineering with a major in Chemical Engineering from Srinakharinwirot University, Bangkok, Thailand in March 2007. She entered the Master of Engineering in Chemical Engineering at Chulalongkorn University, Bangkok, Thailand in May 2007.